THE VALIDATION OF THE VARIABLES (EVAPORATION AND SOIL MOISTURE) IN HYDROMETEOROLOGICAL MODELS

Report to the
Water Research Commission

by

M.G. Mengistu[1], C.S. Everson[1], N.C. Moyo[2], and M.J. Savage[2]

[1] Centre for Water Resources Research (CWRR), School of Agricultural, Earth and Environmental Sciences, University of KwaZulu-Natal, Pietermaritzburg, South Africa
[2] Agrometeorology, School of Agricultural, Earth and Environmental Sciences, University of KwaZulu-Natal, Pietermaritzburg, South Africa

WRC Report No. 2066/1/13
ISBN 978-1-4312-0514-1

March 2014

Obtainable from
Water Research Commission
Private Bag X03
Gezina, 0031

orders@wrc.org.za or download from www.wrc.org.za

EXECUTIVE SUMMARY

1. BACKGROUND AND MOTIVATION

The vulnerability of Southern African countries such as South Africa to climate and environmental change is likely to increase as demands on resources continue to rise in conjunction with rapidly growing populations. The implementation of effective and sustainable water resources management strategies is then imperative, to meet these increasingly growing demands for water. In addition, water resources management, crop modelling, and irrigation scheduling all require accurate, spatially distributed, daily estimates of soil moisture (*SM*) and total evaporation (*ET*) from catchment to national scale. However, there is a lack of basic understanding of the spatial and temporal variability of hydrological parameters which is the main concern and challenge for water resource managers. This will only be feasible through remote sensing technologies and it is therefore essential to further the development and integration of space-based technologies within already existing national disaster management plans.

ET and *SM* have only been available at isolated sites until recently, when the work carried out during two WRC research projects (Pegram *et al*., 2010; Sinclair and Pegram 2013) developed a detailed spatial product of real time estimates of *SM* and *ET*. The model has shown great promise, but still requires further development by the UKZN team, as errors in the input data streams are hampering the quality of the product. During the Reference Group meeting of K5/1683 (Pegram *et al*., 2010) held in May 2009, the need to provide an independent validation of the model was recognised. The purpose of this project is to provide a spatially explicit validation procedure for the 1 km grid of *SM* and *ET* produced by the SAHG UKZN and other hydrological models.

2. PROJECT OBJECTIVES

The aims of the project were:

- Provide data for the continued support of Soil moisture modelling of South Africa using a hydrologically consistent Land Surface Model (follow-on project proposed from K5/1683).
- Provide accurate field and satellite estimates of *ET* and *SM* for the calibration of Hydrometeorological models.
- Evaluate the spatial variability of *SM* at catchment scale.

3. STUDY AREA

Field measurements were carried out at Baynesfield Estate in KwaZulu-Natal, South Africa. Baynesfield climate is classified as sub-humid with dry and cool winters and warm and rainy summers. The mean monthly air temperature ranges from a maximum of 21.1^{o}C in January to a minimum of 13.3^{o}C in June with mean annual precipitation of 844 mm. The predominant wind direction is easterly. The research area has a variety of crops grown on a large scale. The predominant crops grown at the study site are maize, soybean, sugarcane, and avocados. Two sites (maize and soybean sites) were selected within Baynesfield for this study.

4. METHODOLOGY

Total evaporation (*ET*) was estimated using the eddy covariance method at the maize and soybean sites. An EC150 open path gas analyser and a 3D sonic anemometer (Campbell Scientific Inc., Logan, Utah, USA), an Applied Technologies, Inc. (ATI) Sonic Anemometer ("Sx" style probe), and an extended Open Path Eddy Covariance (OPEC) system (Campbell Scientific Inc., Logan, Utah, USA) were used as an eddy covariance system to measure fluxes of water vapour and carbon dioxide.

Root zone soil moisture contents were also monitored for the two sites using CS616 and Hydra Probe II soil moisture sensors. Three CS616 Campbell Scientific probes were used for volumetric soil moisture measurement. The CS616 probes were installed at 0.1, 0.5 and 1.0 m depths below the soil surface. Three Hydra Probe II soil moisture sensors (Stevens Water Monitoring Systems, Inc., Portland, Oregon, USA) were also used to measure soil moisture in the soybean field. The Hydra Probe II soil moisture sensors were also installed at 0.1, 0.5 and 1.0 m depths below the soil surface.

The Surface Energy Balance System (SEBS) remote sensing model was used to derive spatial *ET* and *SM* estimates from satellite data. Moderate Resolution Imaging Spectroradiometer (MODIS) TERRA, Landsat 7 ETM+ and Landsat 8 images were used in SEBS for *ET* and *SM* maps.

5. RESULTS AND DISCUSSION

First Validation Experiment

Energy flux measurements were carried out from 9 March to 28 May 2012 (Day of year 68 to 148) at the maize site. Daily *ET* from the maize crop ranged from 0.25 to 5.3 mm. Total evaporation was higher for March 2012 compared to April and May 2012 due to the higher solar radiation and higher air temperatures that occurred during this month. Energy flux measurements were also carried out from 3 March to 17 April 2012 (Day of year 62 to 107) at the soybean site. Daily *ET* from the soybean crop varied between 0.50 and 5.0 mm. As expected, based on the results for the maize crop, total evaporation was higher for March 2012 compared to April 2012.

Fractional volumetric soil water content (*SM*) values varied between 0.35 and 0.44 (m^3 m^{-3}) during the measurement period at the maize site. Soil moisture decreased with the increase in depth. *SM* was the highest for the 0.1 m depth and lowest for the 1.0 m depth below the soil surface. For the soybean site *SM* values varied between 0.20 and 0.38 during the measurement period. Soil moisture at the 0.1 m depth fluctuated most compared to the two deeper measurements. *SM* was highest at the 0.5 m depth for most of the measurement days.

Second Validation Experiment

Energy flux and soil moisture measurements were carried out from November 2012 to May 2013. Daily *ET* of the soybean crop ranged from 0.5 to 6.7 mm. Total evaporation was highest for January and February 2013. Daily *ET* estimates from the soybean crop decreased to less than 3 mm for most of the days in March and April 2013. Daily *ET* from the maize crop varied between 0.5 and 5.0 mm. As for the soybean crop, total evaporation was highest for January and February 2013, and decreased to less than 3 mm in March and April 2013.

At the soybean site, *SM* values varied between 0.25 and 0.55 during the measurement period. Soil moisture increased with the increase in depth and was the highest for the 1.0 m depth and lowest for the 0.1 m depth below the soil surface. For the maize site *SM* values varied between 0.20 and 0.38. Soil moisture at the 0.1 m depth fluctuated most compared to the other two depths. *SM* was higher at the 1.0 m depth and lowest at the 0.1 m depth below the soil surface.

Validation of the SEBS and HYLARSMET Estimates

The SEBS daily *ET* estimates derived using the MODIS image (3rd of April 2012) were 3.9 and 4.0 mm for the maize and soybean sites respectively. These values are averages for the sites and contain two Modis pixels. The daily eddy covariance *ET* estimates were 2.0 mm for both the maize and soybean sites. The SEBS daily *ET* estimates were higher than the eddy covariance daily *ET* estimates. For the same day the average relative soil moisture estimates derived by SEBS were 0.7 and 0.5 at the maize and soybean sites respectively. These values were slightly lower than the measured relative soil moisture values of 0.8 (maize) and 0.6 (soybean).

The SEBS daily *ET* estimates derived using Landsat 7 EM+ images were higher for December 22, 2012 and January 23, 2013 compared to the rest of the images for both the maize and soybean sites respectively due to the higher incident solar radiation and air temperatures that occurred during these summer months. The SEBS daily *ET* estimates were higher than the eddy covariance daily *ET* estimates. This shows that the SEBS model overestimated the daily *ET* estimates for these days by approximately 15%.

The HYLARSMET daily *ET* estimates were lower than the EC and SEBS estimates by 4% and 16% respectively. The HYLARSMET estimates closely tracked the variation of the daily *ET* estimates for the different seasons. The HYLARSMET estimates of soil saturation index (SSI) estimates followed the drying and wetting patterns of the SEBS relative soil moisture. SEBS relative soil moisture estimates and HYLARSMET's SSI estimates compared well, although they differ in the way they are computed and have slightly different definitions (as defined in section 3 of this report).

6. CONCLUSIONS AND RECOMMENDATIONS FOR FUTURE RESEARCH

Spatial knowledge of land surface *ET* and *SM* is crucial for water resources management, crop modelling, optimizing irrigation water use, and flood forecasting. Seven months of eddy covariance *ET* estimates and profile soil water content measurements at two sites within Baynesfield were used for the validation of the SEBS and HYLARSMET models. SEBS model was used to derive *ET* and the relative soil moisture maps using MODIS TERRA and Landsat 7 ETM+ images. Landsat images provided better *ET* estimates when compared to MODIS images, possibly because of their higher spatial resolution (30 m compared to 1km).

The HYLARSMET daily *ET* estimates were lower than the EC and SEBS estimates. However, the HYLARSMET estimates followed the variation of the daily *ET* estimates for the different seasons. The HYLARSMET SSI estimates followed the drying and wetting patterns of the measured and SEBS relative soil moisture estimates. In general, the HYLARSMET estimates compared well with the measured and SEBS estimates. To gain confidence in these observations, more time series of spatially averaged HYLARSMET's estimates need to be compared with the field measurements and SEBS estimates.

Landsat 7 malfunctioned in 2003 and no longer provides complete image information for its entire coverage region due to the failure of the Scan Line Corrector. The result was that there was 22% data loss in each scene. Two Landsat 8 images were used in SEBS to derive *ET* maps in this study. The Landsat 8 images provided *ET* maps without stripes and without any data loss. Landsat 8 carries a Thermal infrared (TIR) instrument with two thermal bands that can provide a more accurate estimate of the land surface temperature than Landsat 7 and 5. The use of TIR remote sensing and Landsat 8 images can provide valuable information for future *ET* and *SM* estimation using surface energy balance models.

A new technology (Cosmic ray probes) for measuring soil moisture at spatial scales of up to 660 m in diameter (34 Ha) has been investigated during the course of this project. The proposed method involves measuring low-energy cosmic-ray neutrons above the ground, whose intensity is inversely correlated with soil water content and with water in any form above ground level (Note: the contributions from subsurface and surface waters are distinguishable). The instrument, called a "cosmic-ray moisture probe," is brand new, but it is built on existing technologies that are put together in an innovative way. The use of such tried and tested technologies means that the instrument and the technique are less likely to fail when deployed in the field and will be invaluable for future *SM* modelling and studies.

7. EXTENT TO WHICH THE CONTRACT OBJECTIVES HAVE BEEN MET

The purpose of this project was to provide a spatially explicit validation procedure for the 1 km grid of *SM* and *ET* produced by the SAHG UKZN and other hydrological models. The project was designed to build on the recent work in two WRC projects (Pegram *et al*, 2010; Sinclair and Pegram, 2013). A stakeholder workshop of the key role players from SAWS, UKZN, ARC, and Pegram & Associates was held at UKZN during the onset of the project. The aims of the workshop were to: (1) disseminate knowledge on the process of soil moisture modelling using the distributed PyTOPKAPI model, to spread capacity developed recently by Pegram & Associates; (2) establish the best method for verification of modelled results (3) identify suitable scales and replication of field measurements required and (4) select the most suitable catchment where data networks and suitable land uses are in place.

The objectives of the project were satisfactorily achieved by providing field measured *ET* and *SM* data during the two validation experiments using the eddy covariance method and profile soil water content measurements. The SEBAL model was proposed initially for the estimation of *ET* and *SM*. However, SEBAL could not be easily applied by the project team due to issues related to intellectual property rights. Instead, the SEBS model was used for *ET* and *SM* estimates for inter-comparison with the HYLARSMET model. In addition to spatial estimates of *ET*, the project was intended to use spatially distributed field based measurements of *SM* to verify *SM* sensors which were planned to be rolled out by SAWS at weather stations. The project team has made numerous attempts to encourage SAWS to provide their soil moisture probes for testing. All of these attempts have failed and the project team has therefore abandoned these efforts.

8. CAPACITY BUILDING AND TECHNOLOGY TRANSFER

Nicholas Moyo is currently studying towards a PhD in the field measurements of *ET* and spatial variability of *SM* over soybean and maize crops. The project provided funding and support for all his data and technical capacity building.

UKZN has also over the past invested in building capacity on the use of surface energy balance models together with remote sensing for improving the spatial estimates of *ET*, biomass and water use of different vegetation types. Through this project these skills were further developed in members of the project team Michael Mengistu (Post doc), Alistair Clulow (PhD student) and Caren Jarmain. Siphiwe Mfeka (field assistant) also received technical training on the project.

Expertise in flood hydrology and flood forecasting is scarce in South Africa. Prof Geoff Pegram and his associates are seen as the only existing experienced research capacity in this discipline in the country. This project is a planned initiative to build closer research relationships with Prof Pegram and in doing so increase the capacity in this domain in the country.

9. DATA

All processed and raw data used in the report have been catalogued and stored at the Centre for Water Resources Research (CWRR), University of KwaZulu-Natal, P/Bag X01, Scottsville, Pietermaritzburg, 3209.

Contact person: Dr Michael Mengistu (mengistu@ukzn.ac.za).

ACKNOWLEDGEMENTS

The research in this report emanated from a non-solicited project funded by the Water Research Commission in KSA1 (Water Resources Management). We are sincerely grateful to the Water Research Commission for funding and managing the project. Our special thanks go to the Farm Manager, G. Stopforth and staff of the Baynesfield Estate for providing access to the research sites.

We also gratefully acknowledge the following members of the Reference Group for their time and invaluable expertise:

Mr Wandile Nomquphu	Water Research Commission (Chairman)
Dr S Sinclair	Pegram and Associates
Prof GGS Pegram	Pegram and Associates
Prof GPW Jewitt	University of KwaZulu-Natal
Prof JG Annandale	University of Pretoria
Mr T Newby	Agriculture Research Council
Prof LD van Rensburg	University of the Free State
Mr NJ Kroese	South African Weather Services

The following people provided valuable assistance during the field experiments: Siphiwe Mfeka, Alistair Clulow, and ES Nile.

CONTENTS

LIST OF FIGURES

LIST OF SYMBOLS

ARC	Agricultural Research Council
ASL	Atmospheric Surface Layer
ATI	Applied Technologies, Inc
AWS	Automatic Weather Station
CWRR	Centre for Water Resources Research
DOY	Day of Year
EC	Eddy Covariance
ET	Evapotranspiration
FFGS	Flash Flood Guidance system
GC	Global Circulation
HYLARSMET	Hydrologically Consistent Land Surface Model for Soil Moisture and Evapotranspiration
ILWIS	Integrated Land and Water Information System
IRGA	Infrared Gas Analyzer
LAI	Leaf Area Index
METRIC	Mapping Evapotranspiration with Internalized Calibration
MODIS	Moderate Resolution Imaging Spectroradiometer
MOST	Monin-Obukhov Similarity Theory
NDVI	Normalized Difference Vegetation Index
NIR	Near-infrared
OPEC	Open Path Eddy Covariance
PBL	Planetary Boundary Layer
SAFFG	South African Flash Flood Guidance model
SAHG	Satellite Applications and Hydrology Group
SAWS	South African Weather Service
SEB	Surface energy balance
SEBAL	Surface Energy Balance Algorithm for Land
SEBI	Surface Energy Balance Index
SEBS	Surface Energy Balance System
SM	Soil Moisture
SR	Surface Renewal
S-SEBI	Simplified Surface Energy Balance Index
SSI	Soil Saturation Index
TDR	Time Domain Reflectometer
TIR	Thermal Infrared
TOPKAPI	Topographic Kinematic Approximation and Integration
UKZN	University of KwaZulu-Natal
WRC	Water Research Commission

Roman symbols:

e	Actual measured vapour pressure
s	Concentration of a scalar
f_c	Fractional canopy coverage
e_s	Saturation vapour pressure
H_{wet}	Sensible heat flux at the wet limit
w	Vertical wind speed
d	Zero plane displacement height
H_{dry}	Sensible heat flux at the dry limit
z_o	Surface roughness length
c_p	Specific heat capacity of air at constant pressure
dT	Surface to air temperature difference
EF	Evaporative Fraction
ETr	Alfalfa reference evapotranspiration
$ETrF$	Ratio of ET to ETr
G	Soil heat flux (Wm^{-2})
H	Sensible heat flux (Wm^{-2})
Kc	Crop coefficient
LE	Latent heat flux ($W\ m^{-2}$),
r_{ah}	Aerodynamic resistance to heat transport ($s\ m^{-1}$)
$R_{l\uparrow}$	Outgoing long wave radiation ($W\ m^{-2}$)
$R_{l\downarrow}$	Incoming long wave radiation ($W\ m^{-2}$)
R_n	Net radiation ($W\ m^{-2}$)
R_{n24}	Daily (24 hrs) net radiation ($W\ m^{-2}$)
R_s	Incident solar radiation ($W\ m^{-2}$)
T_{air}	Air temperature (K)
T_H	Reflectance dependent extreme temperature for the dry limit
T_{LE}	Reflectance dependent extreme temperature for the wet limit
T_s	Land surface temperature (K)

Greek symbols:

ρ_{red}	Atmospherically corrected ground reflectance in the red band
ρ_a	Density of air
r_{ew}	External resistance at the wet limit
γ	Psychrometric constant
Γ	Soil heat flux to net radiation ratio
Γ_c	Soil heat flux to net radiation ratio for full vegetation canopy
Γ_s	Soil heat flux to net radiation ratio for bare soil
α	Surface albedo
ρ_{nir}	Atmospherically corrected ground reflectance in the near infrared band
Δ	The rate of change of saturation vapour pressure with temperature
ε	Surface emissivity
ε'	Apparent atmospheric emissivity (air emissivity)
λ	Latent heat of vaporization (J kg^{-1})
ρ_w	Density of fresh water (kg m^{-3}).
σ	Stefan-Boltzmann constant ($5.67*10^{-8}$ W $m^{-2}K^{-4}$)
$\overline{\Lambda}$	Daily average evaporative fraction
Λ	Evaporative fraction
θ	Volumetric soil moisture content
ϑ_{sat}	Saturated soil moisture content

1. INTRODUCTION

The vulnerability of Southern African countries such as South Africa to climate and environmental change is likely to increase as demands on resources continue to rise in conjunction with rapidly growing populations. The implementation of effective and sustainable water resources management strategies is then imperative, to meet these increasingly growing demands for water. Disaster management agencies will have to adapt to the increasing number of natural disasters, including droughts and floods.

Spatial knowledge of land surface total evaporation (*ET*) and soil moisture (*SM*) is crucial for water resources management, crop modelling, optimizing irrigation water use, and flood forecasting. However, there is a lack of basic understanding of the spatial and temporal variability of hydrological parameters which is the main concern and challenge for water resource managers. This will only be feasible through remote sensing technologies and it is therefore essential to further the development and integration of space-based technologies within already existing national disaster management plans.

ET and *SM* have only been available at isolated sites until recently, when work carried out during two WRC research projects (Pegram *et al*., 2010; Sinclair and Pegram 2013) developed a detailed spatial product of real time estimates of *SM* and *ET*. These variables are routinely calculated in real time and made available as up-to-date images on the SAHG UKZN web-site. The model has shown great promise, but still requires further development by the UKZN team, as errors in the input data streams are hampering the quality of the product (Pegram and Sinclair, pers comm.). During the Reference Group meeting of K5/1683 (Pegram *et al*., 2010) held in May 2009, the need to provide an independent validation of the model was recognised. The purpose of this project is to provide a spatially explicit validation procedure for the 1 km grid of *SM* and *ET* produced by the SAHG UKZN and other hydrological models. Automatically tracking the current soil moisture state is a core function that allows the Flash Flood Guidance system (FFGS) to provide alerts, based on current and predicted rainfall. In addition, the current South African Flash Flood Guidance model (SAFFG) run by SAWS, by Eugene Poolman and his team under WRC project K5/2068, uses a relatively crude *ET* model. Therefore, validating *ET* estimates with better temporal and spatial resolution are likely to make improvements to the SAFFG.

This project was designed to build on the recent work in WRC project K5/1683: Soil moisture from Satellites and the aims of this project were:

- Provide data for the continued support of Soil moisture modelling of South Africa using a hydrologically consistent Land Surface Model in "HYLARSMET: A Hydrologically Consistent Land Surface Model for Soil Moisture and Evapotranspiration Modelling over Southern Africa using Remote Sensing and Meteorological Data" under WRC project K5/2024, (the follow-on project to K5/1683).
- Provide accurate field and satellite estimates of *ET* and *SM* for the calibration of Hydrometeorological models.
- Evaluate the spatial variability of *SM* at catchment scale.

2. SURFACE ENERGY BALANCE METHODS

2.1 Introduction

The estimation of total evaporation (*ET*), which includes evaporation from land and water surfaces and transpiration by vegetation, is one of the most important processes in the determination of the exchanges of energy and mass between the hydrosphere, atmosphere and biosphere (Sellers *et al*., 1996). In agriculture, *ET* is a major consumptive extractor of irrigation water and precipitation on agricultural land (Gowda *et al*., 2007). *ET* varies regionally and seasonally according to meteorological conditions (Hanson, 1991). Conventional micrometeorological methods such as eddy covariance (Meyers and Baldocchi, 2005), Bowen ratio (Fristchen and Simpson, 1989), scintillometry (Hill, 1992; Thiermann and Grassl, 1992; De Bruin *et al*., 1995), surface renewal (Paw U *et al*., 1995; Snyder *et al*., 1996), and lysimeters may be used to estimate *ET*. However, these methods estimate *ET* based on point or line averaged measurements of components of the energy balance, which are only representative of local scales and cannot easily be extended to large areas because of land surface heterogeneity (French *et al*., 2005). Remote sensing based *ET* models can provide representative measurements of several physical parameters at scales from field (local), catchments, to regional, and are better suited for estimating the water use of different vegetation surfaces (Allen *et al*., 2007).

Research on the use of remotely sensed land surface temperature data to estimate *ET* started towards the end of 1970's (Jackson *et al*., 1977) and early 1980's (Carlson *et al*., 1981; Price *et al*., 1982; Seguin and Itier, 1983; Gurney and Camillo, 1984). Over the years numerous remote sensing based models that vary in complexity have been developed for estimating regional *ET*. The complexity of these different methods depends on the balance between the empirical and physically based formulations used (Courault *et al*., 2005). Residual methods of the surface energy balance combine some empirical relationships and physical modules. Most current operational models (such as SEBAL, METRIC, SEBS, and S-SEBI (Moran *et al*.,1996; Bastiaanssen *et al*., 1998a; Su *et al*., 1999; Allen *et al*., 2007) use remote sensing directly to estimate input parameters and *ET*.

2.2 Radiation and Energy Balance

A brief review of the energy budget at a soil surface is needed for a better understanding of *ET* and *SM* estimation using remote sensing to derive the relevant surface properties such as albedo, vegetation cover, and surface temperature. The shortened energy balance equation is expressed as:

$$R_n = LE + H + G \tag{1}$$

where R_n is the net radiation (Wm^{-2}), LE is the latent heat flux (Wm^{-2}), H is the sensible heat flux (Wm^{-2}), and G is the soil heat flux (Wm^{-2}). The latent heat flux, representing the energy required for evaporation is computed as a residual of the energy balance as:

$$LE = R_n - H - G \tag{2}$$

The net radiation (R_n), can be computed using the expression described in Bastiaanssen *et al*., (1998), Timmermans *et al*. (2007) and Koloskov *et al*. (2007), as:

$$\begin{aligned} R_n &= (1-\alpha)R_{s\downarrow} + R_{l\downarrow} - R_{l\uparrow} - (1-\varepsilon)R_{l\downarrow} \\ &= (1-\alpha)R_{s\downarrow} + \varepsilon' \sigma T_{air}^{\ 4} - \varepsilon\sigma T_s^{\ 4} - (1-\varepsilon)\varepsilon' \sigma T_{air}^{\ 4} \end{aligned} \tag{3}$$

where R_s is the incident solar radiation (Wm^{-2}), $R_{l\downarrow}$ and $R_{l\uparrow}$ are the incoming and outgoing long wave radiations respectively (Wm^{-2}), ε' is the apparent atmospheric emissivity (air emissivity), α is surface albedo, ε is the surface emissivity, σ is the Stefan-Boltzmann constant (5.67*10^{-8} W m^{-2}K^{-4}), T_{air} is the air temperature (K) and T_s is the land surface temperature (K).

Net radiation (R_n) can be computed from satellite-measured narrow-band reflectances and surface temperature; G can be estimated from R_n, surface temperature, and a vegetation index; and H can be estimated from surface temperature, surface roughness, and wind speed using buoyancy corrections (Allen *et al*., 2005).

2.3 Eddy Covariance Method

In fully turbulent flow, the mean vertical fluxes of heat, water vapour, and momentum can be defined directly in terms of the turbulent (eddy) components of vertical velocities and of the properties being transferred (Rosenberg *et al*., 1983; Kaimal and Finnigan, 1994). Mean flux across any plane implies covariance between the wind component normal to that plane and the scalar entity of interest (Kaimal and Finnigan, 1994; Arya, 2001).

The eddy covariance (*EC*) method provides a direct measure of the vertical turbulent flux of a scalar entity of interest F_s across the mean horizontal stream lines (Swinbank, 1951) providing fast response sensors (≈ 10 Hz) for the wind vector and scalar entity of interest are available (Meyers and Baldocchi, 2005). For a sufficiently long averaging period of time over horizontally homogeneous surface, the flux is expressed as:

$$F_s = \rho_a \overline{w's'} \tag{4}$$

where ρ_a is the density of air, w is the vertical wind speed and s is the concentration of the scalar of interest. The primes in Equation (4) indicate fluctuation from a temporal average (i.e., $w' = w - \overline{w}$; $s' = s - \overline{s}$) and the over bar represents a time average. The vertical wind component is responsible for the flux across a plane above a horizontal surface. Based on Equation (4), the sensible heat flux H can be expressed as:

$$H = \rho_a c_p \overline{w'T_s'} \tag{5}$$

where c_p is the specific heat capacity of air, w' denotes the fluctuation from the mean of the vertical wind speed, and T_s' is the fluctuation of air temperature from the mean. The averaging period of the instantaneous fluctuations, of w' and s' should be long enough (30 to 60 minutes) to capture all of the eddy motions that contribute to the flux (Meyers and Baldocchi, 2005).

The *EC* technique, when properly applied, can be used routinely for direct measurements of surface layer fluxes of momentum, heat, water vapour, and carbon dioxide between a surface and turbulent atmosphere (Savage *et al*., 1997; Massman, 2000; Massman and Lee, 2002; Finnigan *et al*., 2003). Like other micrometeorological methods, an adequate fetch is required for the *EC* method; a fetch to height ratio greater than 100 is usually considered adequate (Wieringa, 1993). The *EC* measurements of w' should ideally be at a height that allows small-sized eddies between the anemometer transducer to be sensed (Savage *et al*., 1995). If the sensor height is too close to the canopy small-sized eddies may not be sensed, resulting in a possible underestimation of the flux. Savage *et al*. (1995) suggested that measurements, under unstable conditions above short turf grass surface, at a height of 1 m above the plant canopy should be sufficient without need of corrections for spectral attenuation of the eddy structures from spatial averaging.

The *EC* method requires sensitive, expensive instruments to measure high frequency wind velocities and scalar quantities. Besides, eddy covariance data need rigorous quality control and filtering, such as anemometer tilt correction (coordinate rotation, planar fit), spike detection, and trend removal (Meyers and Baldocchi, 2005). Sensors must measure vertical wind speed, sonic temperature and atmospheric humidity with sufficient frequency response to record the most rapid fluctuations important to the diffusion process (Drexler *et al*., 2004).

2.4 Remote Sensing Based Surface Energy Balance (SEB) Models

Surface energy balance (SEB) models combine some empirical relationships and physical modules, and are based on a shortened energy balance for each pixel where *ET* is estimated as a residual of the energy balance. The SEB models use Equations 1 to 3 to estimate the energy balance components. The following SEB models will be discussed: Surface Energy Balance Algorithm for Land (SEBAL); Mapping EvapoTranspiration with high Resolution and Internalised Calibration (METRIC); and Surface Energy Balance System (SEBS).

2.4.1 Surface Energy Balance Algorithm for Land (SEBAL) model

The SEBAL model was developed by Bastiaanssen and its formulation is discussed in detail by Bastiaanssen *et al*. (1998a) and Bastiaanssen (2000). SEBAL uses remotely sensed images, from satellites measuring Thermal Infrared (TIR) radiation in addition to visible and Near-infrared (NIR), to compute both the instantaneous and 24-hr integrated surface heat flux for each pixel of a satellite image. The latent heat flux (*ET*) is estimated as a residual of the energy balance Equation 2 and the net radiation is calculated using Equation 3 (Bastiaanssen *et al*. (1998a).

The SEBAL algorithm computes most of the necessary hydro-meteorological parameters (e.g. surface albedo, Normalized Difference Vegetation Index or *NDVI* and surface temperature) with limited ancillary meteorological data (air temperature, relative humidity and wind speed). The surface albedo, α is determined by integrating spectral reflectances in the six shortwave bands of the Landsat images, and the surface emissivity, ε is computed from vegetation indices derived from two of the shortwave bands (Tasumi, 2005).

The *NDVI* is computed from the reflectance in the red (band 3 of Landsat) and near infrared (band 4 of Landsat) channels as:

$$NDVI = \frac{\rho_{nir} - \rho_{red}}{\rho_{nir} + \rho_{red}} \tag{6}$$

where ρ_{nir} and ρ_{red} are atmospherically corrected ground reflectance in the near infrared and red bands respectively.

The soil heat flux *G* is empirically estimated using a function by Bastiaanssen (2000) based on albedo, surface temperature, and NDVI as:

$$G = \left[\frac{T_s - 273.16}{\alpha}(0.0038\alpha + 0.0074\alpha^2)(1 - 0.98NDVI^4)\right]R_n \tag{7}$$

The sensible heat flux *H* is estimated from wind speed and surface temperature using an internal calibration process as described by Bastiaanssen *et al*. (1998a):

$$H = \frac{\rho_a c_p (a + b * T_s)}{r_{ah}} \tag{8}$$

where ρ_a is air density (kg m^{-3}); which is a function of atmospheric pressure, c_p is the specific heat capacity of air (≈ 1004 J kg^{-1} K^{-1}) at constant pressure, r_{ah} is aerodynamic resistance to heat transport (s m^{-1}) between two near surface heights (generally 0.1 and 2 m) computed as a function of estimated aerodynamic roughness of the particular pixel and using wind speed extrapolated to some blending height above the ground surface (typically 100 to 200 m), with an iterative stability correction scheme based on the Monin-Obhukov functions (Allen *et al.*, 1996, Koloskov *et al.*, 2007) and *"a"* and *"b"* are empirical coefficients calibrated for each image. The term $a + b*T_s$ represents the near surface to air temperature T_a difference (*dT*). The use of *dT* eliminates problems caused by differences between radiometric to aerodynamic surface temperatures.

The definition of the coefficients *"a"* and *"b"* requires the selection of two extreme pixels within the scene (image). These extreme pixels are termed "cold" and "hot" pixels, where the *dT* values can be back-calculated using known *H* at the two pixels. According to Bastiaanssen *et al*. (1998a,b), the "cold" pixel is assigned T_s from the surface temperature of a local water body (or a well vegetated field) pixel while the "hot" pixel is typically assigned to a dry surface pixel. The sensible heat is assumed zero for the "cold" pixel, and to be equal to $R_n - G$ for the "hot" pixel. The coefficients *"a"* and *"b"* are calibrated for each image using linear interpolation based on surface temperature *(T_s)* between these two extreme pixels. However, there is no absolute method for the user to select wet/dry pixels in a satellite image and hence experience in the SEBAL computational approach is useful in this regard. Once latent heat flux *(LE)* at the image acquired time is estimated, an Evaporative Fraction *(EF)* for each pixel can be calculated (Bastiaanssen, 2000) as:

$$EF = \Lambda = \frac{LE}{R_n - G} \tag{9}$$

The evaporative fraction *EF* is fairly constant during the day time (Mohammed *et al*., 2004) thus allowing estimation of daytime evaporation from only one or two estimates of *EF* (Courault *et al*, 2005).

The daily total evaporation can then be estimated using the following expression:

$$ET = \frac{\Lambda(R_{n24} - G)}{\lambda \rho_w} 86400 * 10^3 \tag{10}$$

where *ET* is actual evaporation (mm d^{-1}), R_{n24} is the daily (24 hrs) net radiation (W m^{-2}), λ is the latent heat of vaporization (J kg^{-1}) and ρ_w is the density of fresh water (kg m^{-3}).

SEBAL has been validated at a number of locations around the world including locations in Spain, Italy, Turkey, Pakistan, India, Sri Lanka, Egypt, Niger, China, Western USA (Bastiaanssen *et al*., 1998b, 2005; Bastiaanssen & Bos, 1999; Morse *et al*., 2000, 2001; Allen *et al*., 2002; Hemakumara *et al*., 2003).

2.4.2 Mapping EvapoTranspiration with high Resolution and Internalised Calibration (METRIC) model

METRIC is a variation of the SEBAL model (Allen *et al*., 2007). The algorithms used in METRIC are similar to those described for SEBAL (Bastiaanssen, 1998a), and its modelling of *ET* is refined by incorporating reference *ET* computed from ground based weather data. METRIC differs from SEBAL mainly in the way that the sensible heat flux *H* is calibrated for each specific satellite image (Allen *et al*., 2005).

In METRIC, the same approach and assumptions are made for the hot pixel as in SEBAL, but for the lower calibration point of *dT* (Equation 8), a well vegetated (alfalfa reference ET) pixel is selected as the "cold pixel" and is therefore partly calibrated with ground-based alfalfa reference ET.

METRIC also differs from SEBAL in the way the daily *ET* is estimated from instantaneous *ET* calculated at the time of the satellite overpass. The evaporative fraction (*EF*) is assumed to be the same at both the observation time and for the 24 hr period for SEBAL. In METRIC, the extrapolation from observation time to the 24 hr period is done using the fraction of reference *ET* (*ETrF*) rather than *EF*. *ETrF* is defined as the ratio of *ET* to *ETr* (alfalfa reference), and is the same as the crop coefficient, *K*c (Allen *et al*., 2005).

The instantaneous *ET* is estimated as the residual of the energy balance equation for each pixel.

$$ET_{inst} = 3600 \frac{LE}{\lambda \rho_w} \quad \text{(mm hr}^{-1}\text{)} \tag{11}$$

where 3600 for conversion from seconds to hours, ρ_w is the density of fresh water (kg m^{-3}), and λ latent heat of vaporization. In METRIC, extensions have also been made to SEBAL to refine its accuracy by incorporating a relatively complex geometric equations to integrate solar radiation incident to sloping terrain over 24 hr period (Allen *et al*., 2002).

In METRIC daily *ET* estimates are up-scaled from the instantaneous *ET* using,

$$ET_{24} = C_{rad}\left(ET_rF\right)\left(ET_{r\_24}\right) \tag{12}$$

where C_{rad} is a correction term used in sloping terrain to correct for variation in 24 hr versus instantaneous energy availability which is a function of clear-sky solar radiation, ET_r is the reference *ET* from a standard 0.5 m alfalfa, and ET_{r_24} is the reference *ET* for the 24 hr period.

The daily evaporation is further up-scaled to a seasonal *ET* estimates by interpolating the reference ET_rF between processed images and multiplying it with daily ET_r values. METRIC assumes that a change in evaporation for an entire image (area) is proportional to the reference alfalfa evaporation ET_r. Generally one satellite image per month is sufficient to construct a good ET_rF curve to estimate seasonal *ET*. However, in areas with a rapid vegetation change, more than one image is required.

2.4.3 Simplified Surface Energy Balance Index (S-SEBI) model

The surface energy balance index (SEBI) algorithm (Menenti and Choudhury, 1993) is a modification of the "Crop water stress index" developed by Jackson *et al*. (1981, 1988), which was later updated by Moran *et al*. (1996). SEBI is based on the principle that surface temperature varies with evaporation (Van den Hurk, 2001). A simplified version of SEBI, called S-SEBI (Roerink *et al*., 2000) was developed using the minimum and maximum surface temperatures from Landsat-TM image.

S-SEBI determines a reflectance dependent maximum temperature for dry conditions and a reflectance dependent minimum temperature for wet conditions; subsequently the sensible and latent heat fluxes are partitioned according to the actual surface temperature. S-SEBI requires scanned spectral radiances under cloud-free conditions in the visible, near-infrared and thermal infrared range to determine surface properties (surface reflectance, surface temperature, and NDVI) used to calculate the energy budget at the surface (Roerink *et al*., 2000).

The net radiation (R_n) is calculated in S-SEBI as the difference of all incoming and outgoing shortwave and longwave radiation (Equation 3). The soil heat flux (G) is derived with an empirical relationship of the vegetation and surface characteristics as:

$$G = \Gamma R_n \tag{13}$$

where Γ is the soil heat flux to net radiation ratio, which is an empirical relationship of the surface reflectance, surface temperature and *NDVI*.

Evaporative fraction (*EF*) is calculated by determining surface reflectance to temperature relationships for wet (LE_{max}) and dry (H_{max}) limits, where temperature is related to soil moisture and the convective fluxes. For each pixel in a scene, the surface reflectance (α), and surface temperature (T_s), and reflectance dependent extreme temperatures for wet and dry limits (T_{LE} and T_H) are determined (Roerink *et al*., 2000).
The evaporative fraction is estimated then as:

$$EF = \Lambda = \frac{T_H - T_s}{T_H - T_{LE}} \tag{14}$$

where T_H is surface reflection dependent temperature for the dry limit, and T_{LE} is surface reflection dependent temperature for the wet limit.

The S (of Simplified) in the S-SEBI model stands for the case where the extreme temperatures T_{LE} and T_H can be determined from the image itself (Roerink *et al*., 2000). This is possible when the atmospheric conditions are constant over the image and sufficient wet and dry pixels are present throughout the reflectance spectrum. Wind speed can affect the values of the extreme temperatures, but as long as the wet and dry pixels are present the S-SEBI method will work (Roerink *et al*., 2000).

2.4.4 Surface Energy Balance System (SEBS) model

The Surface Energy Balance System (SEBS) uses the SEBI algorithm as its foundation to estimate the atmospheric turbulent fluxes using remote sensing data. SEBS consists of a set of tools for the determination of the land surface physical parameters, such as albedo, emissivity, temperature, vegetation cover from spectral reflectance and radiance (Su *et al*., 1999), an extended model for the determination of the roughness length for heat transfer (Su *et al*., 2001) and a new method for the determination of the evaporative fraction on the basis of energy balance at limiting cases (Su, 2002).

The SEBS model requires three sets of information or data. The first set of data consists of land surface albedo, emissivity, temperature, fractional vegetation coverage, leaf area index and the height of the vegetation. If vegetation information is not available, *NDVI* is used as a surrogate. These input data can be derived from remote sensing data in conjunction with other information about the surface of interest. The second set includes meteorological data, such as air pressure, temperature, humidity, and wind speed at a reference height. The reference height is the measurement height for point application and the height of the planetary boundary layer (PBL) for regional application. This data set can be variables estimated by large scale meteorological models. The third data set includes downward solar radiation, and downward long wave radiation which can either be measured or estimated as model output or parameterization.
The SEBS model also applies the surface energy balance equation (Equation 1) to partition the available energy into sensible and latent heat flux density and Equation (3) to calculate the net radiation (R_n). The equation to estimate soil heat flux *G* is parameterized as

$$G = R_n\left[\Gamma_c + (1 - f_c)(\Gamma_s - \Gamma_c\right] \quad (15)$$

in which it is assumed that the ratio of soil heat flux to net radiation Γ_c is 0.05 for full vegetation canopy by Monteith cited in Su (2002) and Γ_s is 0.315 for bare soil (Kustas and Daughtry, 1989), and f_c is the fractional canopy coverage that is used to separate non-vegetated, partially vegetated and densely vegetated land surfaces using *NDVI*.

SEBS uses the Monin-Obukhov similarity theory (MOST) to estimate the sensible heat and latent heat fluxes. MOST relates surface fluxes to surface variables and variables in the atmospheric surface layer (ASL) (Su *et al*., 2001). The aerodynamic (d and z_{om}) and thermal dynamic roughness parameters (z_{oh}) need to be known to estimate sensible heat flux. The aerodynamic parameters, d and z_{om} can be estimated from near surface wind speed and vegetation parameters (height and leaf area index). When wind speed and vegetation parameters are not available, the aerodynamic parameters can be related to vegetation indices derived from satellite data (Su, 2002).

The actual sensible heat flux (*H*) is constrained by the sensible heat flux at the wet limit, H_{wet} and the sensible heat flux at the dry limit H_{dry} in SEBS. Under the dry-limit, the latent heat (evaporation) becomes zero due to the limitation of soil moisture and the sensible heat flux is at its maximum value. The dry limit is given as:

$$H_{dry} = R_n - G \quad (16)$$

$$LE_{dry} = R_n - G - H_{dry} \quad (17)$$

Under the wet-limit, where evaporation takes place at potential rate, LE_{wet} (evaporation is limited only by the energy available under the given surface and atmospheric conditions), the sensible heat flux takes its minimum value, H_{wet}, i.e.

$$H_{wet} = ((R_n - G) - \frac{\rho Cp(e_s - e)}{r_{ew}\gamma}) / (1 + \frac{\Delta}{\gamma}) \quad (18)$$

$$LE_{wet} = R_n - G - H_{wet} \quad (19)$$

where e is the actual measured vapour pressure, e_s is the saturation vapour pressure, γ is the psychrometric constant, Δ is the rate of change of saturation vapour pressure with temperature, and r_{ew} is the external resistance at the wet limit.

The relative evaporation (Λ_r) then can be given as:

$$\Lambda_r = \frac{LE}{LE_{wet}} = 1 - \frac{LE_{wet} - LE}{LE_{wet}} \tag{20}$$

$$\Lambda_r = 1 - \frac{H - H_{wet}}{H_{dry} - H_{wet}} \tag{21}$$

The evaporative fraction is then estimated as:

$$\Lambda = \frac{LE}{H + LE} = \frac{LE}{R_n - G} = \frac{\Lambda LE_{wet}}{R_n - G} \tag{22}$$

The actual sensible heat and latent heat fluxes can be finally obtained by inverting Equation (22) as:

$$\begin{aligned} H &= (1 - \Lambda)(R_n - G) \\ LE &= (R_n - G) \end{aligned} \tag{23}$$

When the evaporative fraction is known, the daily evaporation (mm day^{-1}) can be determined as:

$$E_{daily} = 8.64x10^7 \, x\overline{\Lambda}(\frac{\overline{R_n} - \overline{G}}{\lambda \rho_w}) \tag{24}$$

where $\overline{\Lambda}$ is the daily average evaporative fraction, and ρ_w is the density of water. Since the daily soil heat flux *G* is close to zero because the downward daytime and upward flux at night balance each other approximately, the daily evaporation is determined by assuming the daily evaporative fraction is approximately equal to the instantaneous value as:

$$E_{daily} = 8.64x10^7 \, x \frac{\Lambda \overline{R_n}}{\lambda \rho_w} \tag{25}$$

By summing up the corresponding daily evaporation for a certain period the actual evaporation for a week, month, season, and year can be determined. However errors will occur due to cloud effects, and such effects can be removed by using the time series processing or by data assimilation procedures (Su *et al*., 2003).

2.5 Estimation of Soil Moisture using SEB Models

Soil moisture is an important hydrologic parameter linked to water availability, land surface evapotranspiration, runoff generation, ground water recharge, and irrigation scheduling (Scott *et al*., 2003). Spatial knowledge of land surface evapotranspiration and root zone soil moisture is of prime interest for environmental applications, such as optimizing irrigation water use, irrigation system performance, crop water deficit, drought mitigation strategies (Hafeez *et al*., 2007) and indicates where water is physically present in water sheds and river basins (Scott *et al*., 2003). The deviation between actual and desirable values of soil moisture is critical for the water resources management decision making process (Scott *et al*., 2003). Flood prediction, including information on the spatial extent of inundation, discharge, and timing of the flood peak, and duration of recession, is critically dependent on soil moisture data (Scott *et al*., 2003).

In situ soil moisture measurements are difficult to obtain due to the significant spatial variability of the variable. Therefore, it is necessary to investigate other soil moisture measurement methods at a larger scale. Remote sensing techniques can be used to assess spatial and temporal variation of soil moisture (Moran *et al*., 2002). Remote sensing techniques based on different parts of the electromagnetic spectrum such as passive microwave, active microwave, visible, and thermal infrared can be used to estimate soil moisture. Microwave remote sensing of soil moisture has good physical basis and operates under all weather conditions. The limitation of microwave methods is that they cannot be used to estimate soil moisture in the root zone under lush green vegetation, such as in agriculture or in wetlands and other environmentally sensitive zones (Scott *et al*., 2003). Thermal infrared technique provides an integrated soil moisture value for the root zone. The advantages of thermal infrared method include good physical basis, is applicable at a range of spatial and temporal scale, and is a cost effective technique (Scott *et al*., 2003).

The effect of soil wetness is clearly evident in the magnitude of surface energy balance variables such as sensible heat *H* and latent heat fluxes *LE*. If a soil is dry, *H* will be large and *LE* will be small, and the contrary holds true for wet soil (the sum of *H* and *LE* does not change significantly with soil moisture). Measurements or estimates of *H* and *LE*, can therefore be used to quantitatively express soil moisture content. An empirical relationship between evaporative fraction (Λ) and volumetric soil moisture content (ϑ) was developed by Bastiaanssen *et al*. (1997) using evaporative fraction data from SEBAL and *in situ* measured soil moisture data. Scott *et al*. (2003) modified this relationship by normalizing soil moisture ϑ with saturated soil moisture content ϑ_{sat}:

$$\theta/\theta_{sat} = \exp\{(\Lambda - 1.0)/0.421\} \qquad (26)$$

The value of relative soil moisture content $\vartheta/\vartheta_{sat}$ varies between 0 (oven dry) to 1 (full saturation) and is a standard relationship that can be applied to a wide range of soils. Scott *et al*. (2003) have further validated the accuracy of the relationship using data collected from irrigated plains in Pakistan and Mexico.

The value of Λ under non-advective conditions ranges between 0 and 1, which represents zero to maximum evapotranspiration. Since the evaporative fraction Λ can also be calculated over large areas using satellite imagery (e.g. Bastiaanssen *et al*., 1998a), the evaporative fraction is a suitable indicator for the description of soil moisture conditions at the regional scale.

3. TOPKAPI AND HYLARSMET MODELS

As part of a Water Research Commission funded research project (Pegram *et al.*, 2010), the TOPKAPI model was adapted and coded using algorithms from the literature. One of the objectives of the project was to use the distributed TOPKAPI catchment model to estimate the soil moisture from hydrological data and then to compare this estimate with remote-sensing estimates using satellite data. The model was adapted to South African conditions and applied to model the hydrology of the Liebenbergsvlei catchment.

TOPKAPI is an acronym which stands for **TOP**ographic **K**inematic **AP**proximation and **I**ntegration and is a physically-based distributed rainfall-runoff model. TOPKAPI is a fully distributed model with the spatial range of the grid cell discretisation within which the model is valid up to 1 km (Martina, 2004). It is physically-based, meaning that it explicitly represents the hydrological processes on the basis of the fluid mechanics and soil physics, while the input parameters can be directly obtained from existing spatial datasets. In the original version proposed by Liu and Todini (2002), TOPKAPI consists of 5 main modules comprising soil, overland, channel, evapotranspiration and snow modules. The first 3 modules take the form of non-linear reservoirs controlling the horizontal flows. The evapotranspiration module has been slightly modified in this application (Vischel *et al.*, 2008), compared to the original module presented in Liu and Todini (2002). The improvement of the TOPKAPI module, by the addition of an infiltration filter in the guise of the Green-Ampt model (Green and Ampt, 1911) is shown in Figure 1. The detailed theory and development of the TOPKAPI model is described in Pegram *et al*. (2007).

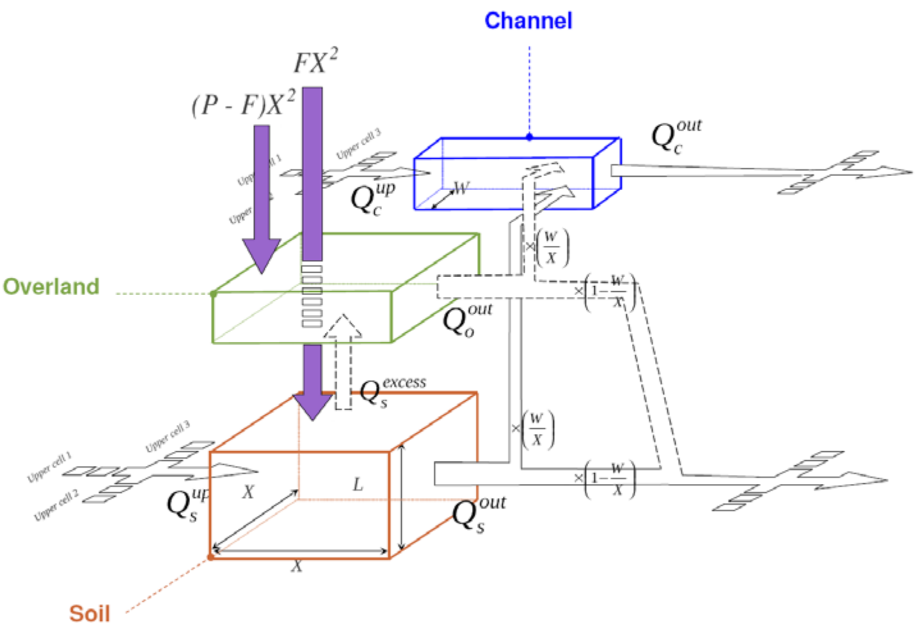

Figure 1. Schematic showing the water transfers for a single cell in the revised PyTOPKAPI model formulation (Sinclair and Pegram, 2012).

The TOPKAPI model was extended by adding a Green-Ampt infiltration module (Sinclair and Pegram, 2013a; Sinclair and Pegram 2013b) and the model and source code was made freely available on the internet as PyTOPKAPI. The purpose of the WRC project K5/2024 (Sinclair and Pegram, 2013a) was to make substantial improvements to the existing methodology and software implementation for modelling Soil Moisture information/maps over South Africa (generated in WRC project K5/1683) in order to provide Soil Moisture and Evapotranspiration data at appropriate scales to institutions responsible for Flood forecasting, Drought monitoring, Crop modelling and Catchment Management (Sinclair and Pegram, 2013a). Through this project an automated modelling system that produces country-wide estimates of Soil Moisture state (and actual evapotranspiration as a by-product) at a 3 h time-step on a 12 km spatial grid over South Africa has been established as a practical and useful product, which could be adopted for operational use by the South African Weather Service (SAWS) in their national Flash Flood Guidance (FFG) system. An updated version of the HYLARSMET model data flow is shown in Figure 2. The dynamic forcing includes the meteorological and remotely sensed data to obtain ET_o and rainfall inputs. The static data provide the slopes, soil parameters and surface roughness. NDVI is obtained at 10 day intervals as it changes relatively slowly. The calculations of Soil Saturation Index (SSI) are performed daily at 3-hour intervals and archived. SSI is defined as the percentage of soil void space taken up by water

$$SSI = (\theta - \theta_r)/(\theta_{sat} - \theta_r) \qquad (27)$$

where ϑ is the soil moisture content, ϑ_{sat} is the saturated moisture content and ϑ_r is the residual moisture content.

Figure 2/...

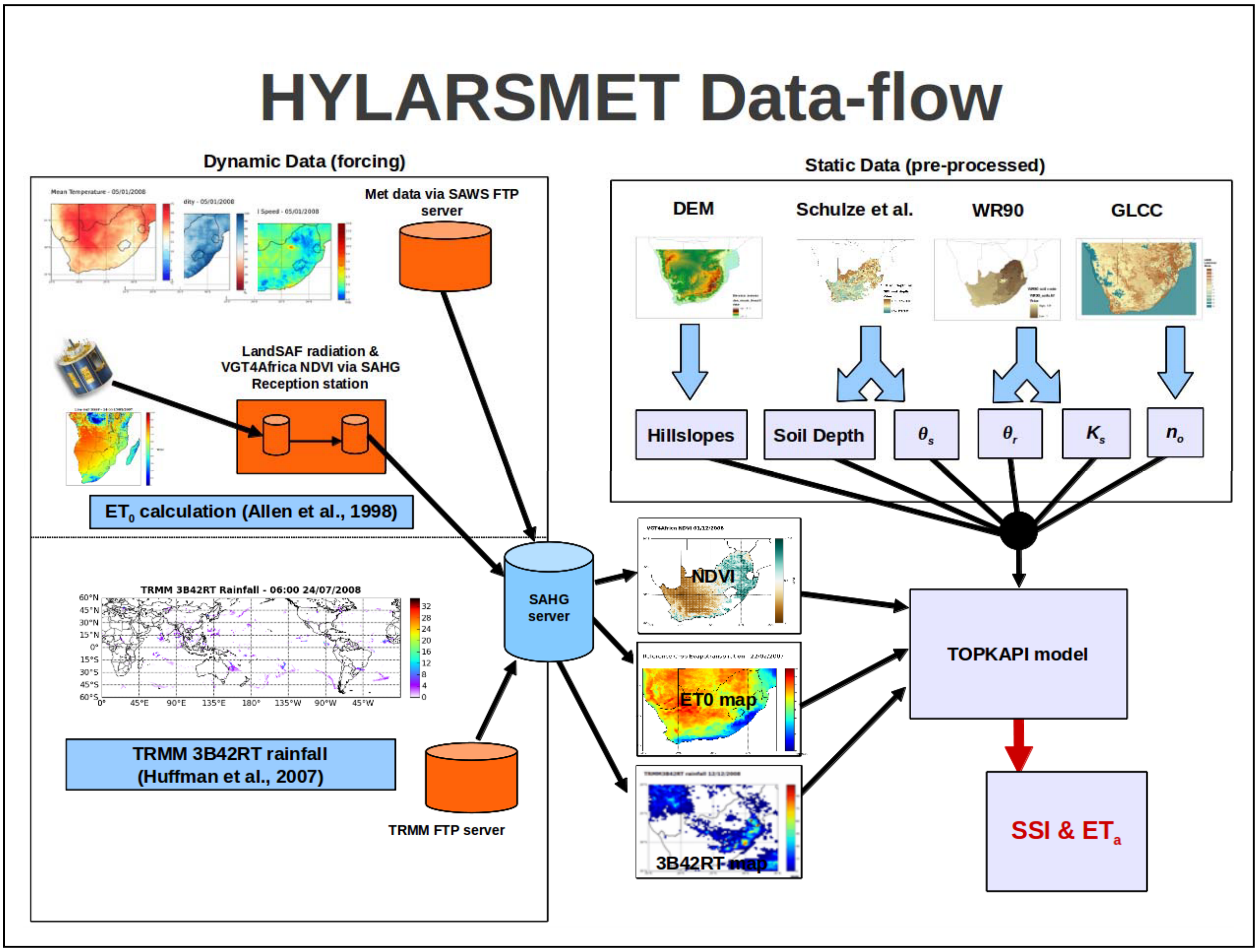

Figure 2. Data-flow diagram showing sources of the dynamic and static data to produce the main information streams: Soil Saturation Index and Actual Evapotranspiration in HYLARSMET model (Sinclair and Pegram, 2013a).

4. STUDY SITE

4.1 Site Selection

A stakeholder workshop of the key role players from SAWS, UKZN, ARC, and Pegram & Associates was held at UKZN, Pietermaritzburg in the 2nd of August 2011. The aims of the workshop were to: (1) disseminate knowledge on the process of soil moistures behind the real time Hydrometeorological modelling, to spread capacity developed recently by Pegram & Associates; (2) establish the best method for verification of modelled results (3) identify suitable scales and replication of field measurements required and (4) select the most suitable catchment where data networks and suitable land uses are in place.

The participants were invited for their extensive knowledge of hydrological modelling, remote sensing and evaporation measurement as well as knowledge of suitable research sites and potential interest/involvement in the project. The workshop comprised of three presentations by Prof Pegram, Dr Sinclair and Prof Everson on hydrological modelling, soil water prediction and evaporation measurement from satellites respectively. The presentations were followed by open discussions where the workshop members had an opportunity to suggest sites and provide inputs on the experimental design and raise concerns relating to the presentations. The suggestions and ideas were referred back to the project objectives to ensure that they were realistic and achievable. The information gained from this meeting assisted in the selection of a suitable field site and experimental design for validation of the measurements of evaporation and soil moisture from satellites.

At the workshop, it was suggested that both homogenous and heterogeneous sites should be selected with a good degree of sampling variability. It was decided that a site in the Baynesfield area would be suitable. The selected site should cover a 3x3 km area, preferably have a 1 km grid, and be representative of the vegetation in the area.

4.2 Site Description

The study site selected for the validation experiment was at Baynesfield Estate in KwaZulu-Natal, South Africa (Figure 3). Baynesfield climate is classified as sub-humid with dry and cool winters and warm and rainy summers. The mean monthly air temperature ranges from a maximum of 21.1^{o}C in January to a minimum of 13.3^{o}C in June with mean annual precipitation of 844 mm. The predominant wind direction is easterly.

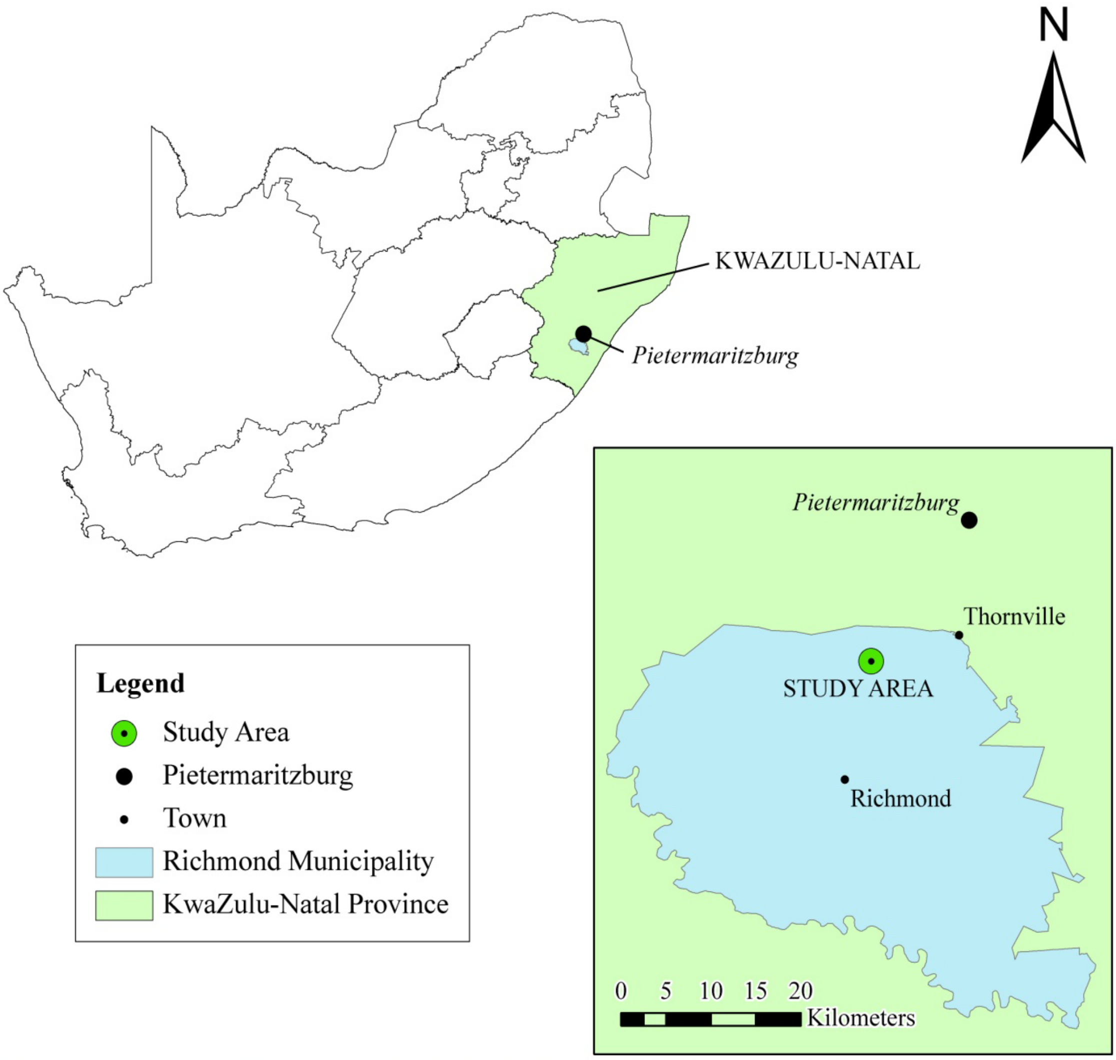

Figure 3. Location of the study area (Baynesfield) near Pietermaritzburg, South Africa.

The research area has a variety of crops grown on a large scale. The crops grown mainly at the study site are maize, soybean, sugarcane, and avocados. Two different sites were selected within Baynesfield which were suitable for this study (Figure 4).

Figure 4. Map showing the two sites selected (sites 1 and 2) within Baynesfield Estate**.**

5. MATERIALS AND METHODS

5.1 First Validation Experiment

5.1.1 Field measurements

5.1.1.1 Site 1 (Maize)

An EC150 open path gas analyser and a 3D sonic anemometer (Campbell Scientific Inc., Logan, Utah, USA) were used as an eddy covariance system to measure fluxes of water vapour and carbon dioxide (Figure 5). The EC150 is an integrated *in-situ* open path analyser and sonic anemometer specifically designed for eddy covariance flux measurements. The EC150 system consists of a CR3000 datalogger, a CSAT3 three-dimensional sonic anemometer, an EC150 open path gas analyser, a HMP45C temperature and humidity probe, and energy balance sensors consisting of NR-LITE net radiometer, two soil heat flux plates, one soil temperature averaging probe, and one CS616 soil moisture reflectometer. The system measures carbon dioxide flux, latent energy flux, barometric pressure, momentum flux, a computed sensible heat flux, net radiation, a computed soil heat flux density, temperature, humidity, horizontal wind speed, and wind direction.

The EC150 system was installed on a lattice mast at 5.0 m above the soil surface (Figure 6). The average height of the maize was 3.0 m. The average leaf area index (LAI) of the maize measured using LAI-2200 (LI-COR Inc, Lincoln, Nebraska, USA) was 2.50 m^2 m^{-2}.

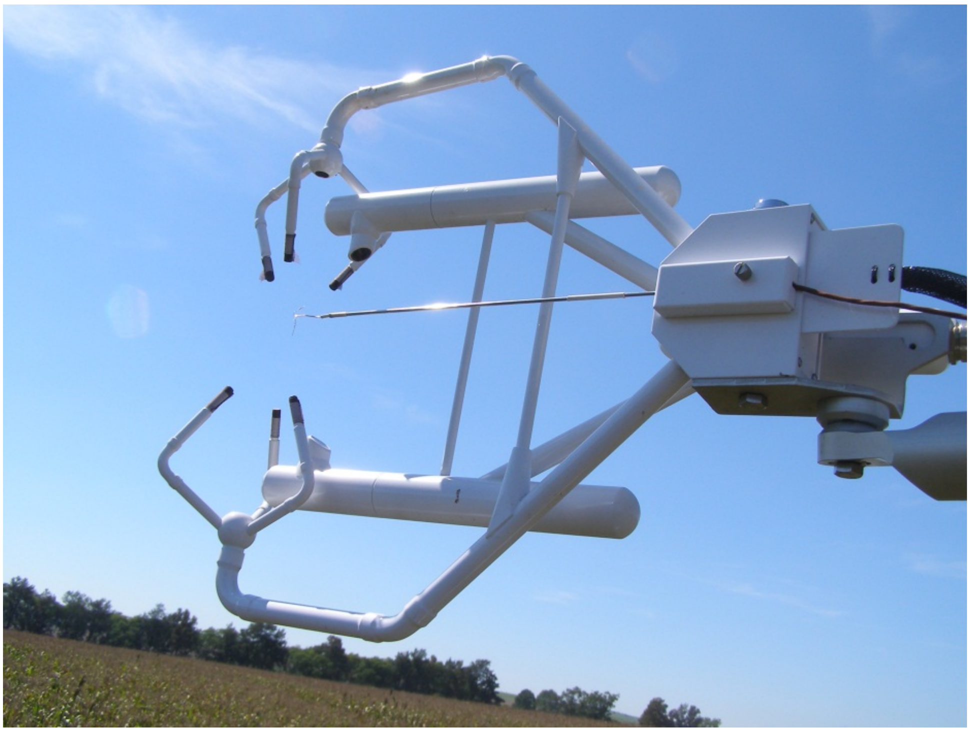

Figure 5. EC150 CO2 and H2O Open-Path Gas Analyzer and 3D Sonic Anemometer with fine wire thermocouple in the middle.

Four CS616 Campbell Scientific probes were used for volumetric soil moisture measurement. Three CS616 probes were installed by excavating a pit 1 m deep to measure volumetric soil water content at 0.1, 0.5 and 1.0 m depths as shown in Figure 7. The three CS616 probes were connected to a CR10X datalogger (Campbell Scientific Inc., Logan, Utah, USA). The fourth CS616 probe was installed as part of the EC150 system to measure volumetric soil water content of the top 60 mm of the soil surface. The measurements were sampled every hour with a Campbell CR10X and hourly and daily volumetric soil water content measurements were computed and stored for further analysis.

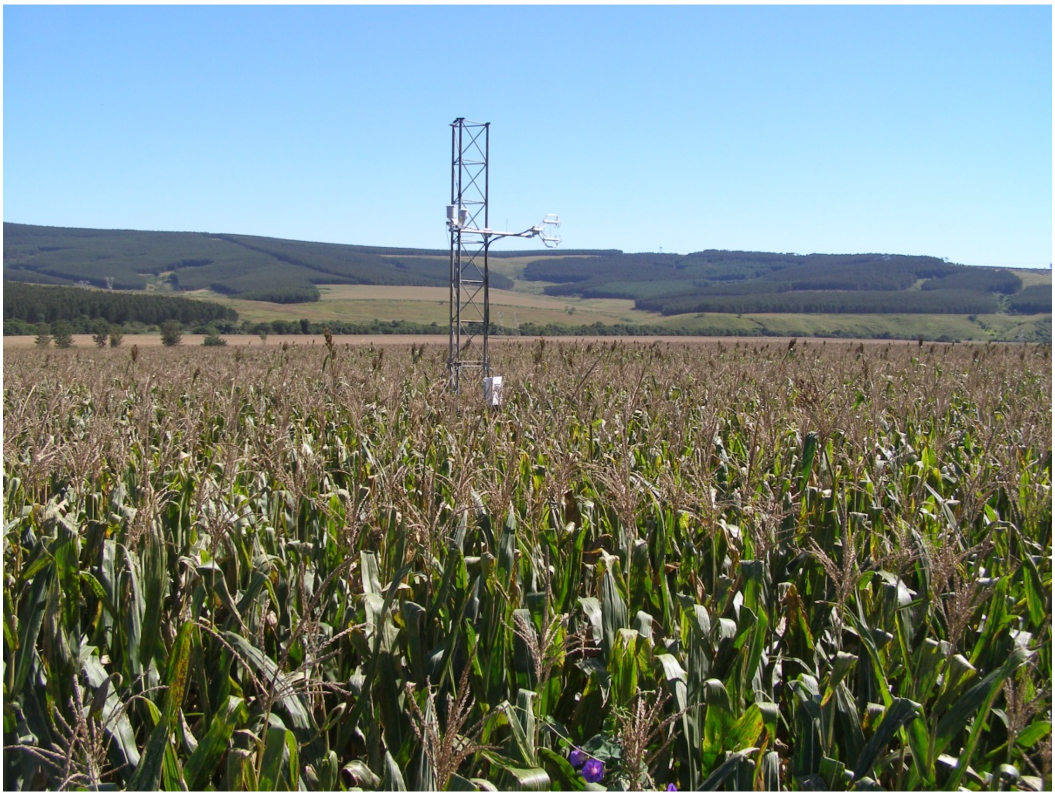

Figure 6. The EC150 system installed on a lattice mast at 5.0 m above the soil surface in the middle of the maize field.

Figure 7. Three CS616 probes installed at 0.1, 0.5, and 1.0 m depths below the soil surface.

5.1.1.2 Site 2 (Soybean)

An Applied Technologies, Inc. (ATI) Sonic Anemometer (“Sx” style probe) was used as an eddy covariance system (Figure 8) to measure three dimensional wind velocity components by transmitting and receiving sonic signals along fixed orthogonal directions and sensible heat flux density. The sonic anemometer was mounted on a lattice mast at 2.0 m above the soil surface. All eddy covariance data were sampled at a frequency of 10 Hz and data processed online in the datalogger. The high frequency data, the two-minute, and thirty-minute averages of the covariances between wind speed (u, v, and w), sonic temperature, T_s and wind direction were calculated and stored for further analysis. The surface renewal (SR) technique was also used to estimate sensible heat flux density. The SR technique is based on high frequency air temperature measurements. Air temperature was measured using two unshielded type-E fine-wire thermocouples (75 µm diameter) placed at heights of 1.0 and 2.0 m above the ground surface. Air temperature data were sampled at a frequency of 10 Hz and then lagged by 0.4 s and 0.8 s. The second, third and fifth air temperature structure function values required by the Van Atta (1977) approach were then formed after lagging the air temperature data by specified amounts - either by 0.4 and 0.8 s. The data were then averaged and stored every two minutes in the datalogger. All sensors were connected to a CR3000 datalogger (Campbell Scientific Inc., Logan, Utah, USA).

Additional sensors for measuring the remaining energy balance components were also connected to the CR3000 datalogger. Net irradiance was measured using a Q*7 net radiometer (REBS, Seattle, Washington, USA) placed at 2.0 m above the ground surface. The soil heat flux was measured using two Hukse flux plates (HFP01-15, Delft, The Netherlands) which were placed at a depth of 80 mm below the soil surface. A system of parallel thermocouples at depths of 20 and 60 mm were used for measuring the soil heat stored above the soil heat flux plates. Volumetric soil water content in the first 60 mm was also measured using a CS615 time domain reflectometer (TDR).

The average height of the soybean was 1.0 m. The average leaf area index (LAI) of the soybean measured using LAI-2200 (LI-COR Inc, Lincoln, Nebraska, USA) was 3.0 m^2 m^{-2}.

Figure 8. An Applied Technologies, Inc. (ATI) sonic anemometer, two surface renewal arms with fine wire thermocouples, and a net radiometer mounted on a lattice above the soybean canopy.

Three Hydra Probe II soil moisture sensors (Stevens Water Monitoring Systems, Inc., Portland, Oregon, USA) were used to measure soil moisture in the soybean field. The Stevens Hydra Probe II soil moisture sensor is an *in-situ* soil probe which instantly calculates soil moisture, electrical conductivity, salinity, and temperature as well as supplying raw voltages and complex permittivity for research applications. The Hydra Probe II soil moisture sensors were installed by excavating a pit 1 m deep to measure volumetric soil water content at 0.1, 0.5. and 1.0 m depths as shown in Figure 9. All sensors were connected to a CR200 datalogger (Campbell Scientific Inc., Logan, Utah, USA). The volumetric water content of the soil was measured at the three depths every 30 minutes and daily.

Figure 9. Three Hydra Probe II soil moisture sensors installed at 0.1, 0.5, and 1.0 m depths below the soil surface.

5.1.2 Satellite estimates

The purpose of this project was to provide a spatially explicit validation procedure for the 1 km by 1 km grid of *ET* and *SM* produced by the SAHG UKZN and other hydrological models. In this study, Surface energy balance algorithm for land (SEBAL) was proposed for the estimation of *ET* and *SM*. However, SEBAL could not be easily applied by the project team due to intellectual property rights. WaterWatch, the original developer and intellectual owner of SEBAL was taken over by a company called eLEAF. Instead, the Surface Energy Balance System (SEBS) was used for *ET* and *SM* estimates. The SEBS model is available in the Integrated Land and Water Information System (ILWIS) which is a free open-source software package.

Moderate Resolution Imaging Spectroradiometer (MODIS) TERRA image was used for SEBS total *ET* estimation. MODIS is a 36 band spectrometer providing a global data set every 1-2 days with a 16-day repeat cycle. The spatial resolution of MODIS (pixel size at nadir) is 250 m for channel 1 and 2 (0.6^{o}C m - 0.9 µm), 500 m for channel 3 to 7 (0.4-2.1 µm) and 1000 m for channel 8 to 36 (0.4-14.4 µm), respectively. The MODIS instrument consists of a cross-track scan mirror, collecting optics and individual detector elements. MODIS L1B (calibrated, but not atmospherically corrected) products for the 3rd of April 2012 was used in SEBS for *ET* estimation.

HDFView tool was used for browsing and viewing the contents of MODIS HDF files. The MODIS Swath Tool was used to re-project swath MODIS level-1 images. Pre-processing of the MODIS image for SEBS such as: Raw to radiance/reflectance; Brightness temperature computation; Water vapour content estimation; SMAC for atmospheric correction; Land surface albedo computation; Land surface emissivity, NDVI, vegetation proportion and emissivity difference computation; and Land surface temperature computation were done ILWIS. SEBS core packaged in ILWIS was used for bio-geophysical parameter extraction. It uses satellite earth observation data, in combination with meteorological information as inputs, to produce the evaporative fraction, net radiation, soil heat flux, daily total evaporation and other parameters.

5.2 Second Validation Experiment

5.2.1 Field measurements

Crop rotation is the normal practice at Baynesfield. The soybean and maize crops are grown in succession to preserve the productive capacity of the soil. For the second growing season (October 2012 to April 2013) the soybean and maize crops were rotated at the two sites.

5.2.1.1 Site 1 (Soybean)

An EC150 open path gas analyser and a 3D sonic anemometer (Campbell Scientific Inc., Logan, Utah, USA) were used as an eddy covariance system to measure fluxes of water vapour and carbon dioxide (Figure 10).

Figure 10/...

Figure 10. The EC150 eddy covariance system installed on a lattice mast in the middle of the soybean field.

Four CS616 Campbell Scientific probes were used for volumetric soil moisture measurement. Three CS616 probes were installed by excavating a pit 1 m deep to measure volumetric soil water content at 0.1, 0.5 and 1.0 m depths as shown in Figure 7. The three CS616 probes were connected to a CR10X datalogger (Campbell Scientific Inc., Logan, Utah, USA). The fourth CS616 probe was installed as part of the EC150 system to measure volumetric soil water content of the top 60 mm of the soil surface. The experimental setup was the similar to the maize site for the first validation experiment.

5.2.1.2 Site 2 (Maize)

An extended Open Path Eddy Covariance (OPEC) system (Campbell Scientific Inc., Logan, Utah, USA) was used as an eddy covariance system to measure fluxes of water vapour and carbon dioxide (Figure 11). The OPEC system consists of a CR5000 datalogger, a CSAT3 three-dimensional sonic anemometer, a LI-7500 open path infrared gas analyzer (IRGA), a HMP45C temperature and humidity probe, and energy balance sensors consisting of NR-LITE net radiometer, two soil heat flux plates, one soil temperature averaging probe, and one CS616 soil moisture reflectometer. The system measures carbon dioxide flux, latent energy flux, momentum flux, a computed sensible heat flux, net radiation, a computed soil heat flux density, temperature, humidity, horizontal wind speed, and wind direction.

Three Hydra Probe II soil moisture sensors (Stevens Water Monitoring Systems, Inc., Portland, Oregon, USA) were used to measure soil moisture in the maize field. The Hydra Probe II soil moisture sensors were installed by excavating a pit 1 m deep to measure volumetric soil water content at 0.1, 0.5 and 1.0 m depths as shown in Figure 9 for the first validation experiment. All sensors were connected to a CR200 datalogger (Campbell Scientific Inc., Logan, Utah, USA). The volumetric water content of the soil was measured at the three depths every 30 minutes and daily.

Figure 11. An extended Open Path (CSAT 3) eddy covariance system installed on a lattice mast above maize canopy.

5.2.2 Satellite estimates

Surface energy balance algorithm for land (SEBAL) could not be easily applied by the project team due to intellectual property rights as stated in section 5.1.2. Instead, the Surface Energy Balance System (SEBS) is used for *ET* estimates. The SEBS model is available in the Integrated Land and Water Information System ILWIS which is a free open-source software package.

High-resolution satellite images (Landsat 7 ETM+ and Landsat 8) were used to capture the heterogeneity of the land surface over the study site. The Landsat images can provide high-resolution information (30 m by 30 m) on the land surface temperature, land cover classification, albedo, and the *NDVI*. Seven scenes of Landsat 7 ETM+ datasets were collected on 09 March 2012, 10 April 2012, 26 April 2012, 22 December 2012, 23 January 2013, 28 March 2013, and 13 April 2013. In addition, two Landsat 8 scenes were collected on 23 May 2013 and 24 June 2013. Most of the images are for cloudless days where the fraction of cloud cover is not more than 5% on these days. Meteorological data (solar radiation, air temperature, wind speed, relative humidity, and atmospheric pressure) from an automatic weather station (AWS) at the site were used to compute surface fluxes over the area of the satellite images.

Erdas Imaging software was used for the preprocessing of the Landsat images. Erdas has several built in standard options, as well as convenient options for data exchange with ArcGIS. One of the strong features of Erdas is the model generator. This allows the user to set up a model with graphical interactions. SEBS uses a powerful open source GIS and remote sensing software, ILWIS, to pre-process satellite images. The land surface physical properties such as albedo, emissivity, temperature, vegetation coverage (*NDVI*), etc. were determined from the spectral reflectances and radiances of the Landsat bands. The images were then converted to GeoTiff format in Erdas before exporting the images to SEBS4ILWIS for the surface flux computations.

6. RESULTS AND DISCUSSION

6.1 First Validation Experiment

6.1.1 Field measurements

Total evaporation (*ET*) was estimated using the eddy covariance and surface renewal methods at the maize and soybean sites. Root zone soil moisture contents were also monitored for the two sites and are presented in the following sections.

6.1.1.1 Site 1 (Maize)

Energy flux measurements were carried out from 9 March to 28 May 2012 (Day of year 68 to 148). The diurnal fluctuations of the net radiation (R_n), soil heat flux (*G*), sensible heat flux (*H*), and the latent energy flux (*LE*) are presented in Figure 12. The maximum daily R_n varied from 200 to 700 W m^{-2} during the measurement period. The daily maximum soil heat flux densities (*G*) were less than 100 W m^{-2}, whereas the maximum daily sensible heat flux ranged (*H*) between 200 and 350 W m^{-2} (Figure 12).

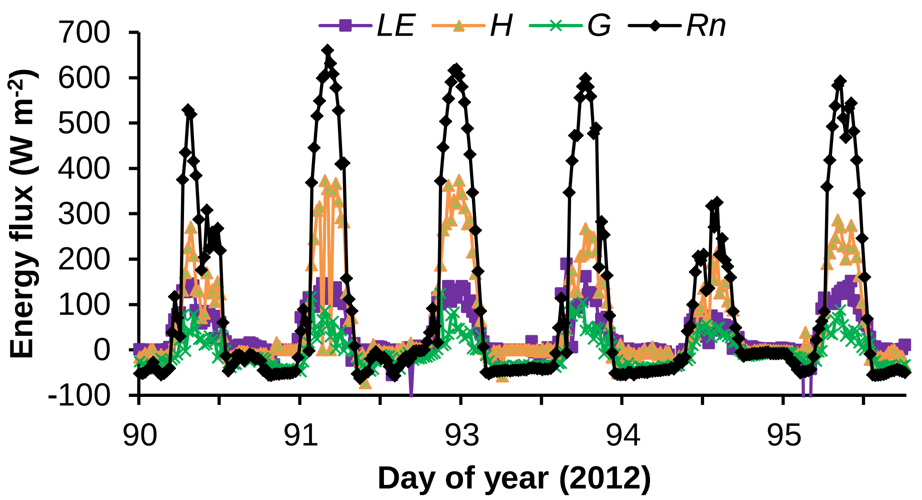

Figure 12. Diurnal variations of half-hourly net radiation (*Rn*), EC150 sonic anemometer sensible heat flux estimates (*H*), and the soil heat flux density (*G*) at the maize site for DOY 90 to 96 (2012).

The daily variations in *ET* estimates (mm) over the maize canopy are shown in Figure 13, along with rainfall (mm) for the measurement period. Daily *ET* from the maize crop ranged from 0.25 to 5.3 mm. Total evaporation was higher for March 2012 compared to April and May 2012 (Figure 13) due to the higher solar radiation and high air temperatures that existed during this month.

Daily fractional volumetric soil water content measurements using three CS616 probes installed at 0.1, 0.5 and 1.0 m depths are shown in Figure 14. Volumetric soil water content (*SM*) values varied between 0.35 and 0.44 during the measurement period. *SM* was the highest for the 0.5 m depth and lowest for the 1.0 m depth below the soil surface as shown in Figure 14.

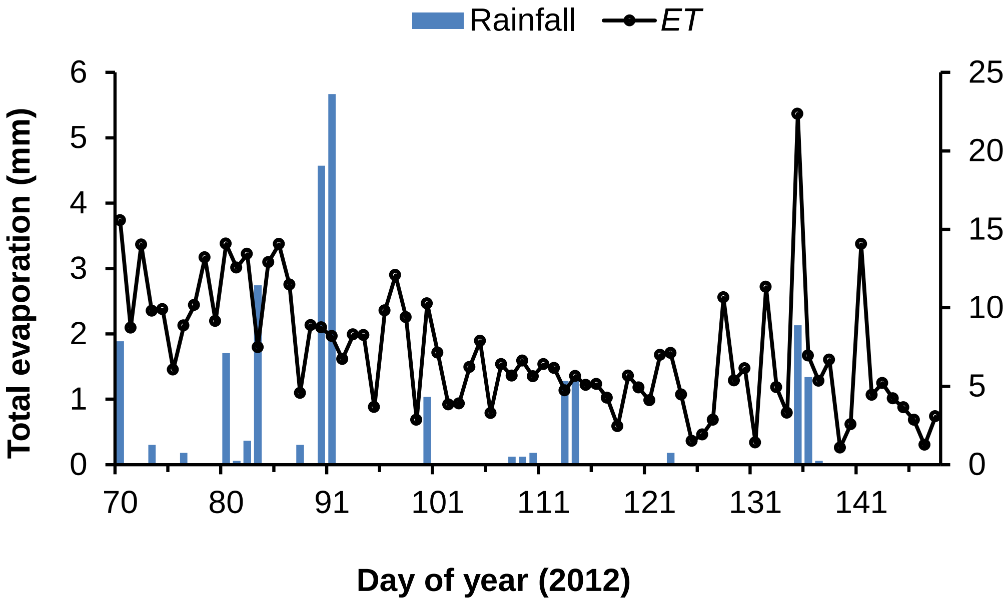

Figure 13. Total evaporation estimates (mm) from the maize canopy along with rainfall (mm) for DOY 70 to 148 (2012).

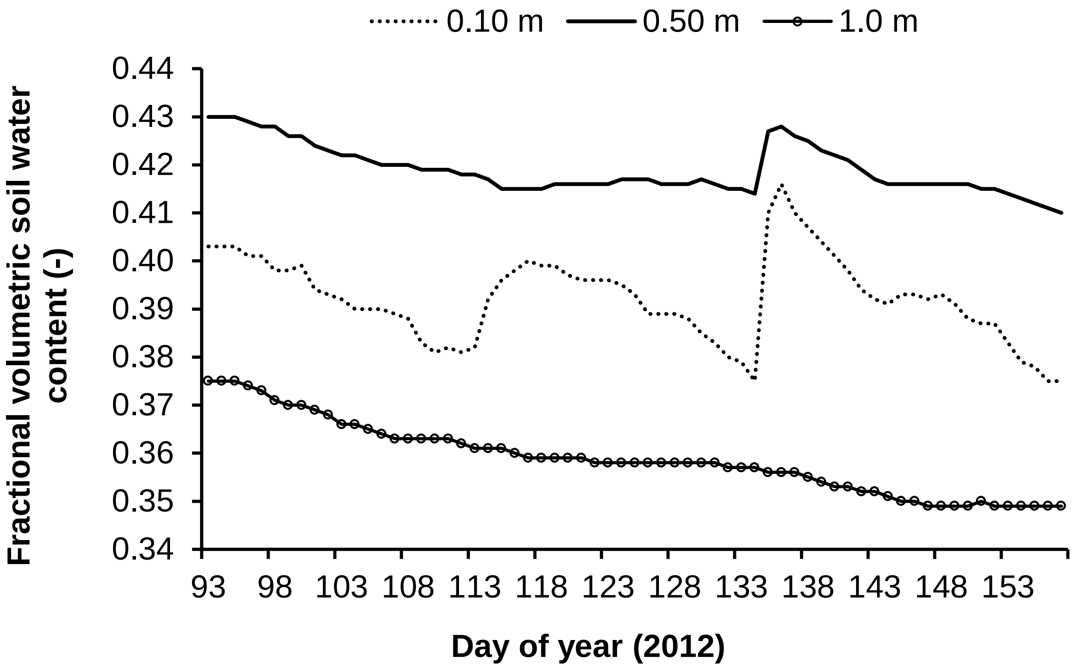

Figure 14. Fractional volumetric soil water content measurements using three CS616 probes in the maize field at 0.1, 0.5, and 1.0 m depths below the soil surface.

6.1.1.2 Site 2 (Soybean)

Energy flux measurements were carried out from 3 March to 17 April 2012 (Day of year 62 to 107). The diurnal fluctuations of the net radiation (R_n), soil heat flux (G), sensible heat flux (H), and the latent energy flux (LE) are presented in Figure 15. The maximum daily R_n varied from 200 to 600 W m^{-2}. The daily maximum G values were between 100 and 200 W m^{-2}. The maximum daily H values ranged between 100 and 300 W m^{-2} (Figure 15).

The daily variations in ET estimates (mm) over the soybean canopy are shown in Figure 16, along with rainfall (mm) on the secondary y-axis. Daily ET from the soybean crop varied between 0.50 and 5.0 mm. Total evaporation was higher for March 2012 compared to April 2012 (Figure 16).

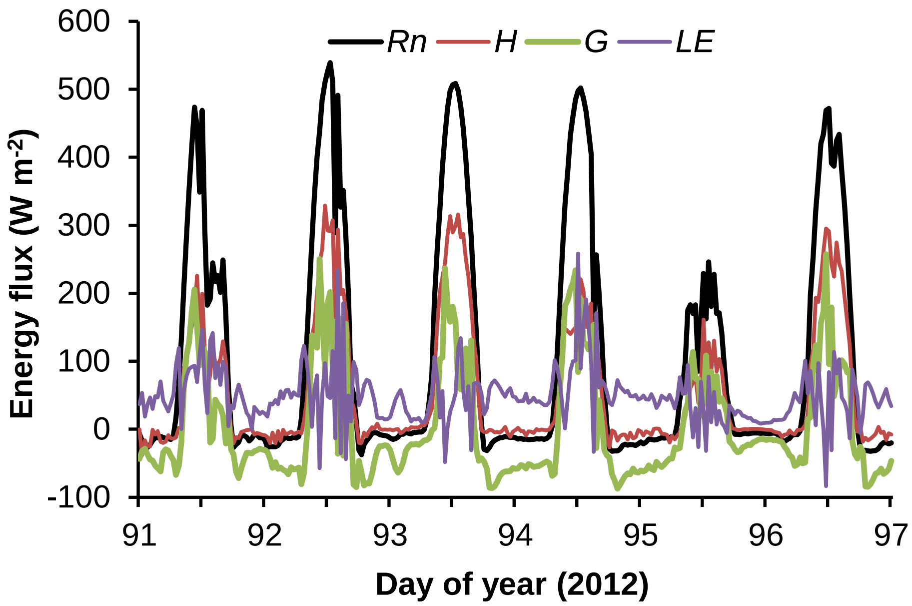

Figure 15. Diurnal variations of half-hourly net radiation (*Rn*), ATI sonic anemometer sensible heat flux estimates (*H*), and the soil heat flux density (*G*) at the soybean site for DOY 91 to 97 (2012).

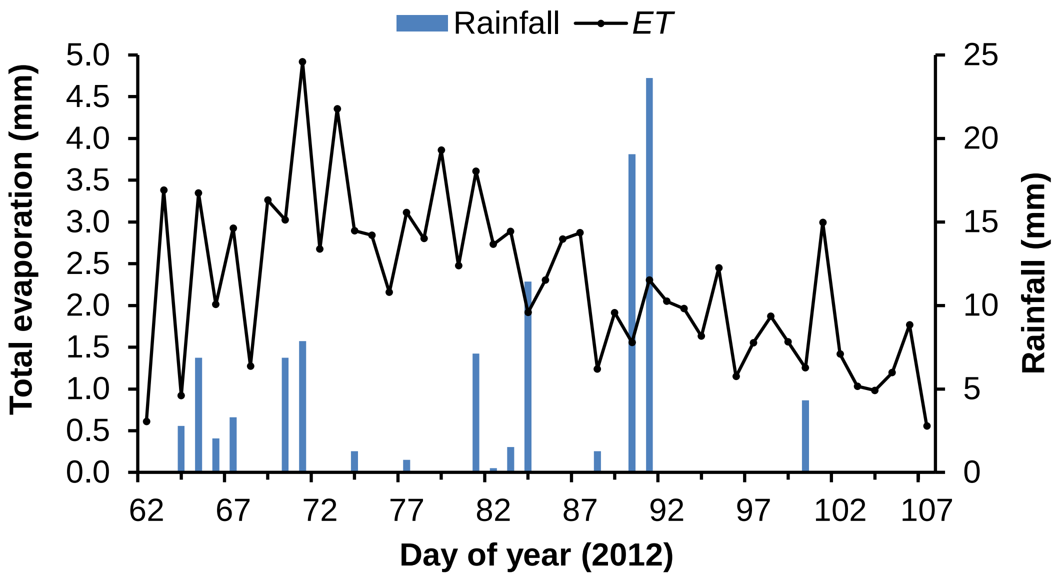

Figure 16. Total evaporation estimates (mm) from the soybean canopy along with rainfall (mm) for DOY 62 to 107 (2012).

Daily volumetric soil water content measurements using the three Hydra Probe II soil moisture sensors at 0.1, 0.5 and 1.0 m depths below the soil surface are shown in Figure 17. Volumetric soil water content (SM) values varied between 0.20 and 0.38 during the measurement period. Soil moisture at the 0.1 m depth fluctuated most compared to the other two depths as shown in Figure 17. SM was higher at the 0.5 m depth for most of the measurement days.

Figure 17/...

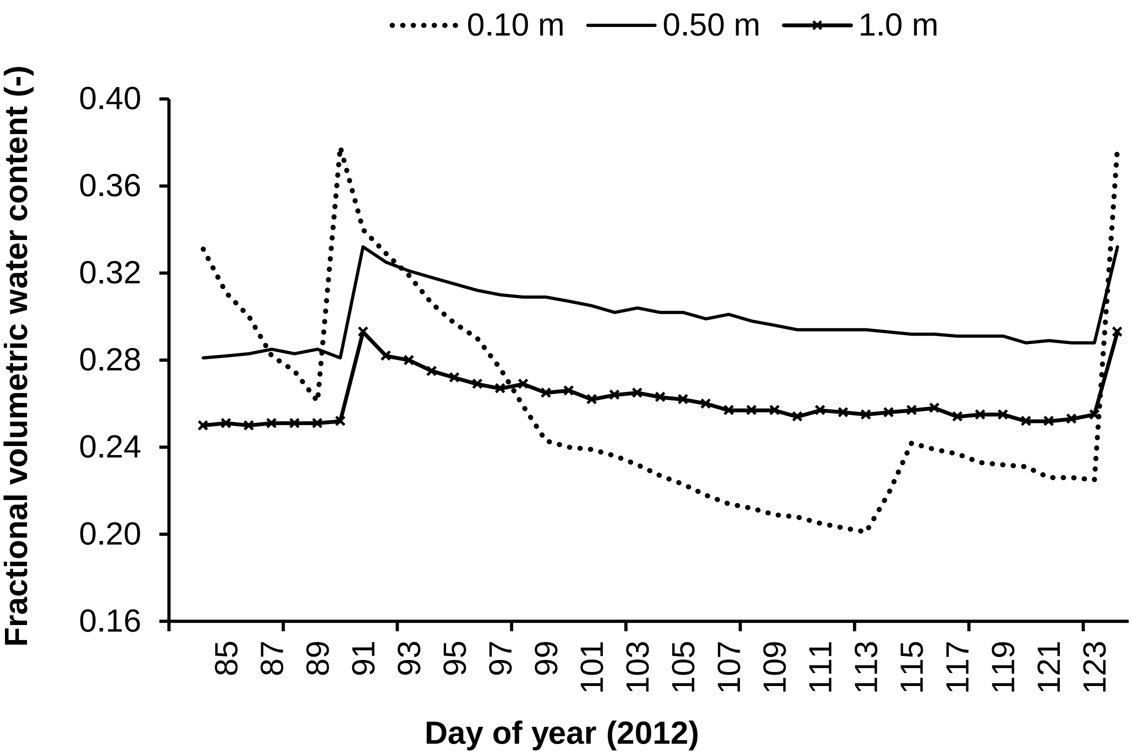

Figure 17. Fractional volumetric soil water content measurements in the soybean field at 0.1, 0.5, and 1.0 m depths below the soil surface**.**

6.1.2 Satellite estimates

Pre-processing and post processing of the MODIS image was done in ILWIS to create maps which are required for the SEBS model. The four maps required in SEBS for *ET* estimation are a land surface temperature map, an emissivity map, an albedo map, NDVI map, and vegetation cover map. Other maps required included a digital elevation map and sun zenith angle map. Land use map with associated surface parameters is also required in SEBS. If land use and vegetation cover maps are not available SEBS uses the NDVI map to estimate all surface parameters. Meteorological data from an AWS at Baynesfield next to the two sites was used in SEBS. Default values where used for all the remaining parameters.

Daily *ET* map for the Baynesfield area with *ET* value for the maize site for the 3rd of April 2012 is shown in Figure 18. Evaporative fraction and relative soil moisture maps are also presented in Figures 19 and 20 respectively. The SEBS daily *ET* estimates were 4.3 and 4.2 mm for the maize and soybean sites respectively. The daily eddy covariance *ET* estimates were 2.0 mm and 2.1 mm for the maize and soybean sites (Figures 13 and 16). The SEBS daily *ET* estimates were higher than the eddy covariance daily *ET* estimates.

The average relative soil moisture estimates using SEBS were 0.67 and 0.53 at the maize and soybean sites respectively (Figure 20). These values are lower than the measured relative soil moisture values of 0.80 (maize) and 0.61 (soybean). The shortened energy balance components: net radiation, soil heat flux, and sensible heat flux maps are presented in Figures 21, 22, and 23 respectively. *NDVI* map for the site is shown in Figure 24.

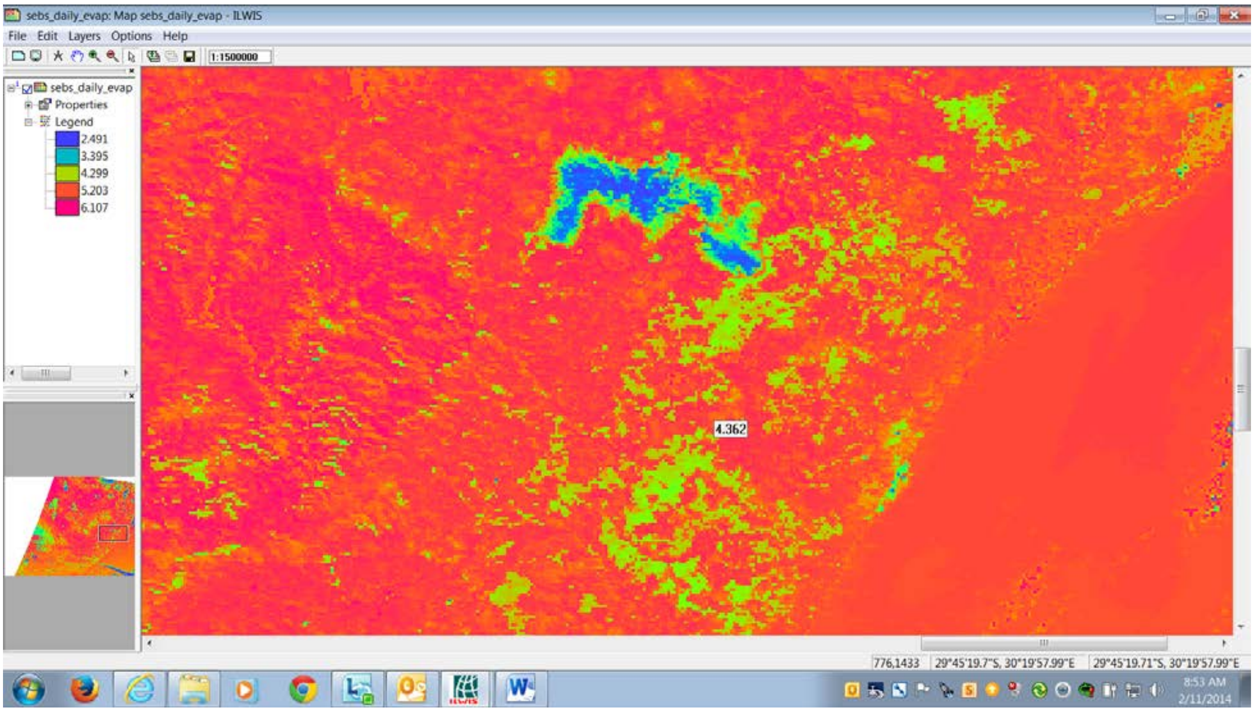

Figure 18. Daily *ET* map for the Baynesfield area with *ET* value for the maize site (April 3, 2012). Map scale (1:1500000).

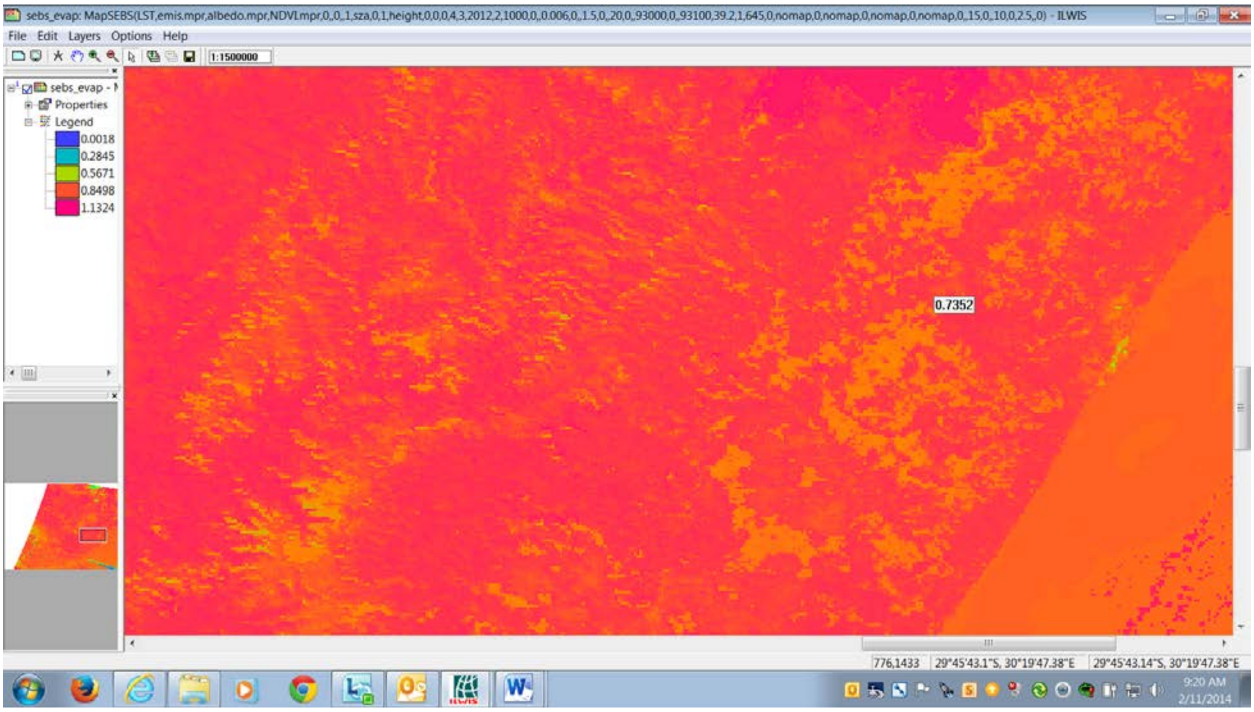

Figure 19. Evaporative fraction map for the Baynesfield area showing value for the maize site (April 3, 2012). Map scale (1:1500000).

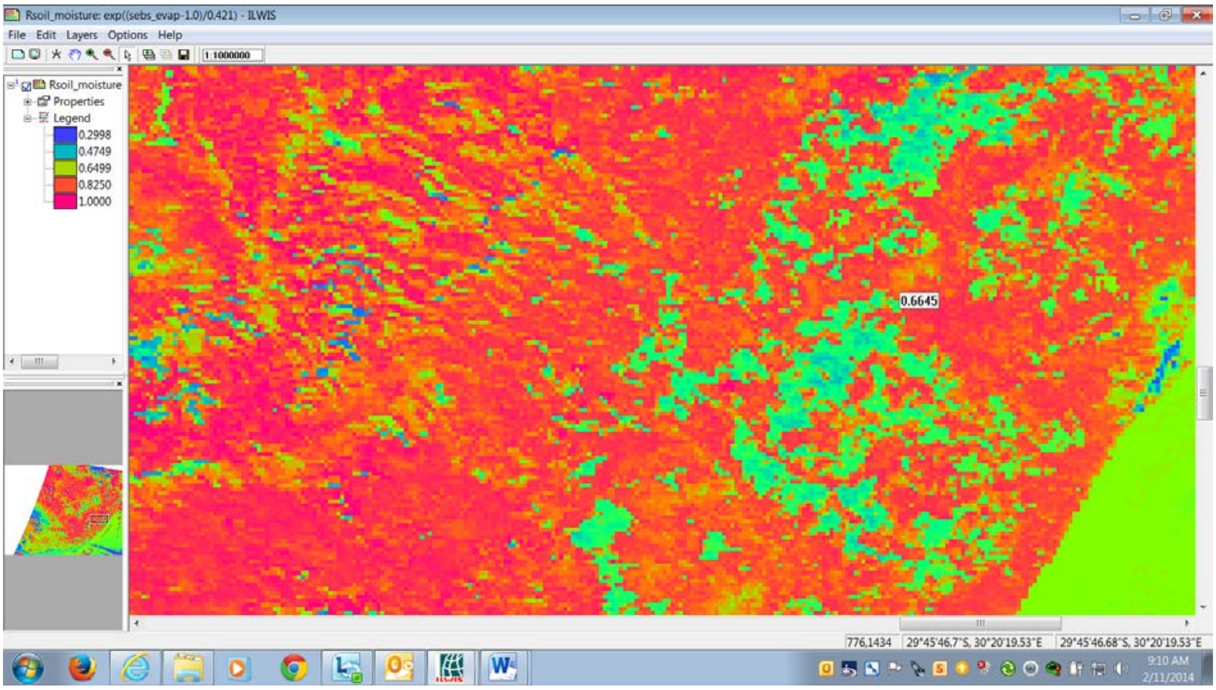

Figure 20. Relative soil moisture map for the Baynesfield area estimated using the Scott *et al*. (2003) equation. Map scale (1:1000000).

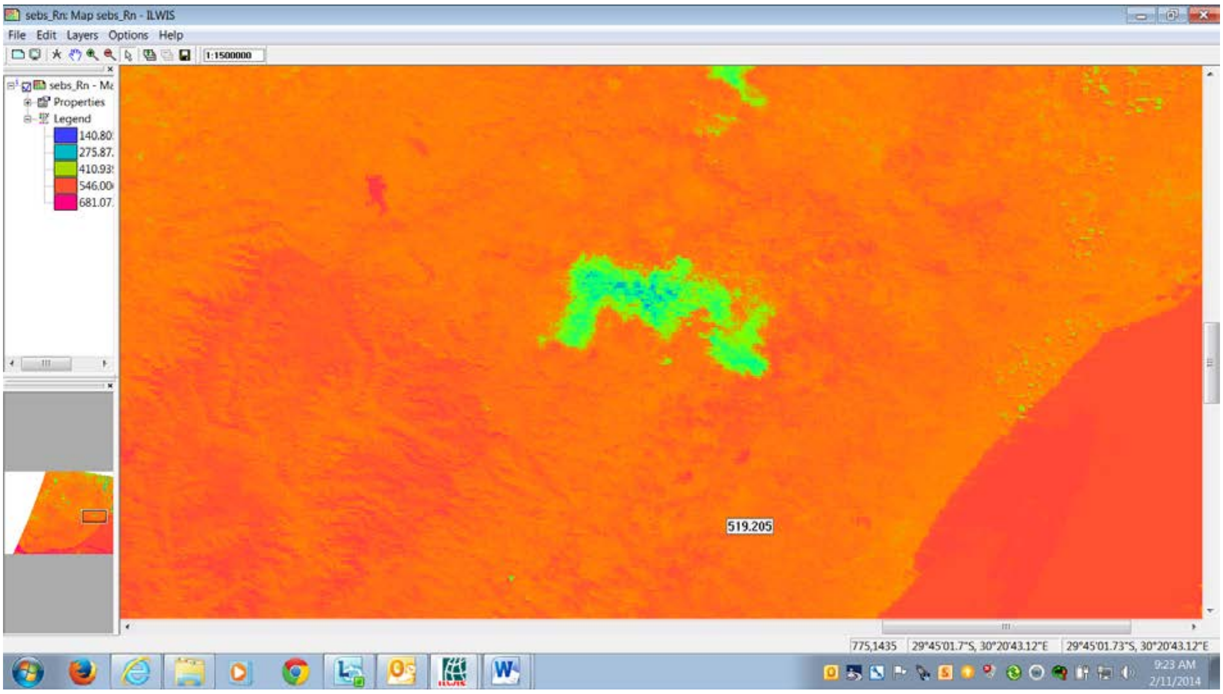

Figure 21. Net radiation (R_n) map during the satellite over pass time (10:00 A.M) for the Baynesfield area showing value for the maize site (April 3, 2012). Map scale (1:1500000).

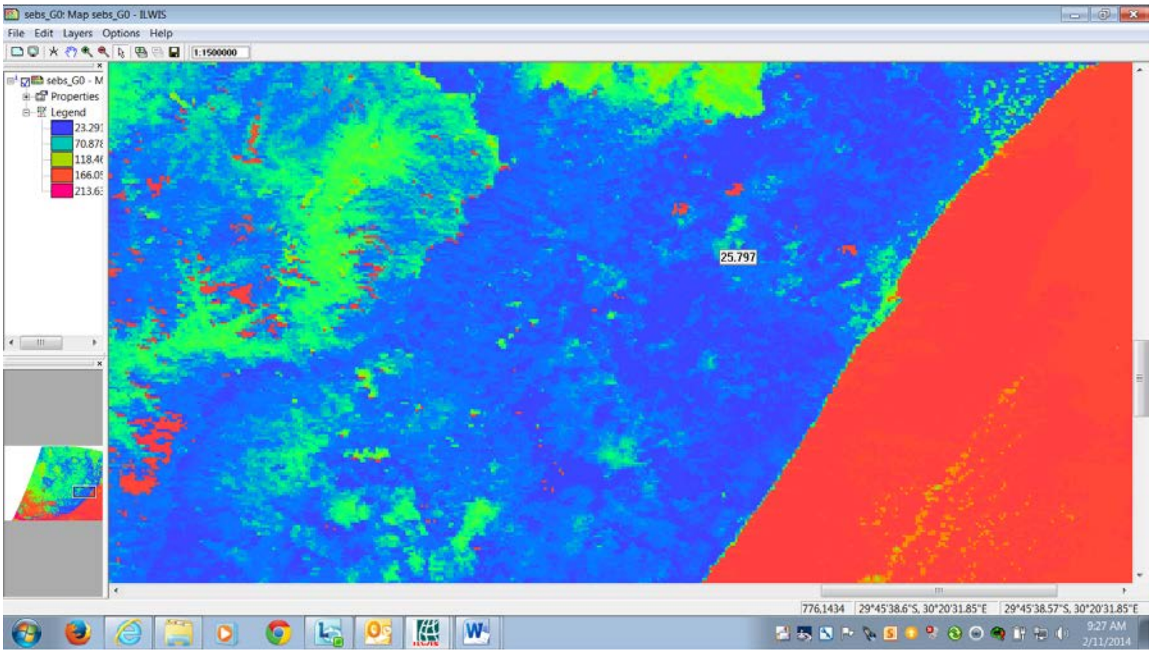

Figure 22. Soil heat flux (*G*) map during the satellite over pass time (10:00 A.M) for the Baynesfield area showing value for the maize site (April 3, 2012). Map scale (1:1500000).

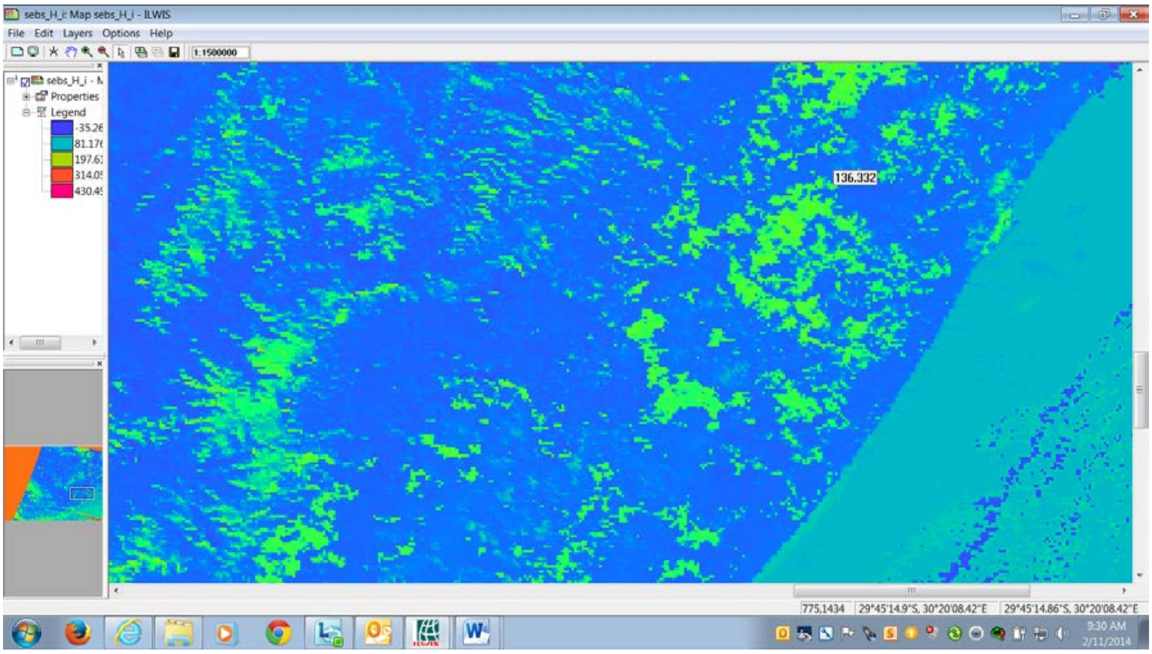

Figure 23. Sensible heat flux (*H*) map during the satellite over pass time (10:00 A.M) for the Baynesfield area showing value for the maize site (April 3, 2012). Map scale (1:1500000).

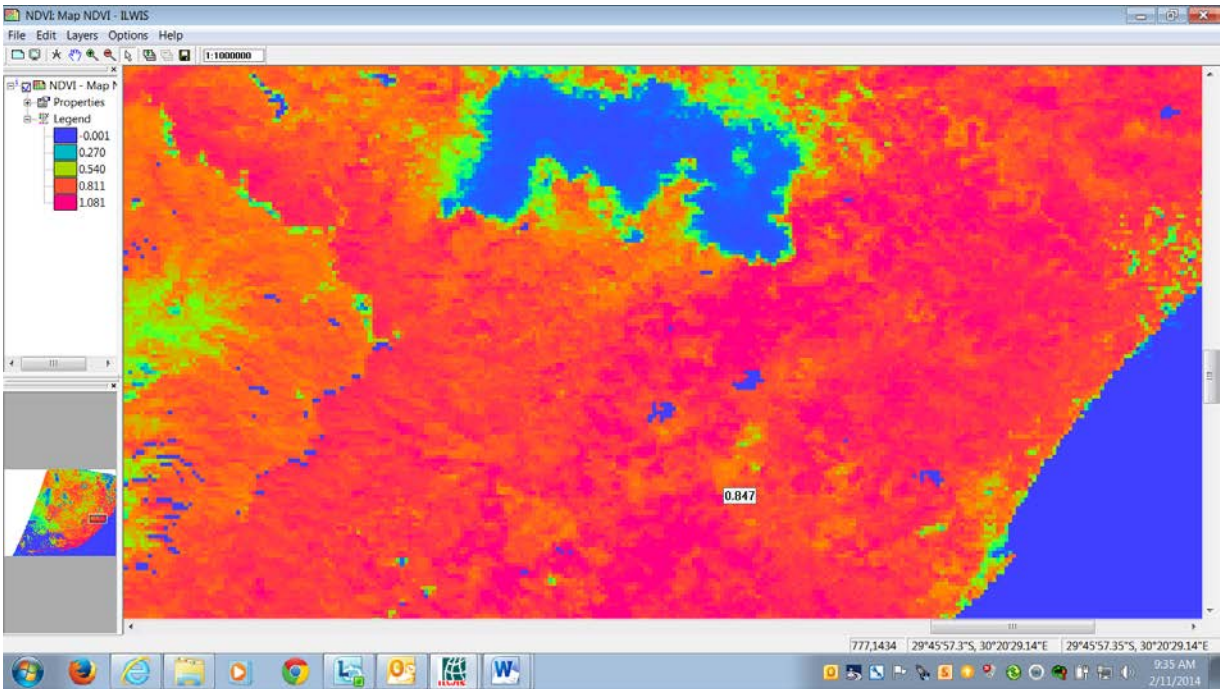

Figure 24. *NDVI* map for the Baynesfield area showing value for the maize site (April 3, 2012). Map scale (1:1000000).

Field measured energy flux estimates and SEBS estimates during satellite overpass time (10:00 A.M) for the maize site are presented in Figure 25. Net radiation and soil heat flux estimates compared well during the satellite over pass time. However, SEBS sensible heat flux (*H_sebs*) estimates are much lower compared to field estimates (Figure 25).

The daily *ET* estimates using SEBS model are presented in Figure 26 for four days in April 2012. The field measured daily eddy covariance *ET* estimates are presented in Figures 13 and 16 for the maize and soybean sites respectively. The SEBS daily *ET* estimates were higher than the eddy covariance daily *ET* estimates. This shows that the SEBS model overestimated the daily *ET* estimates for these days.

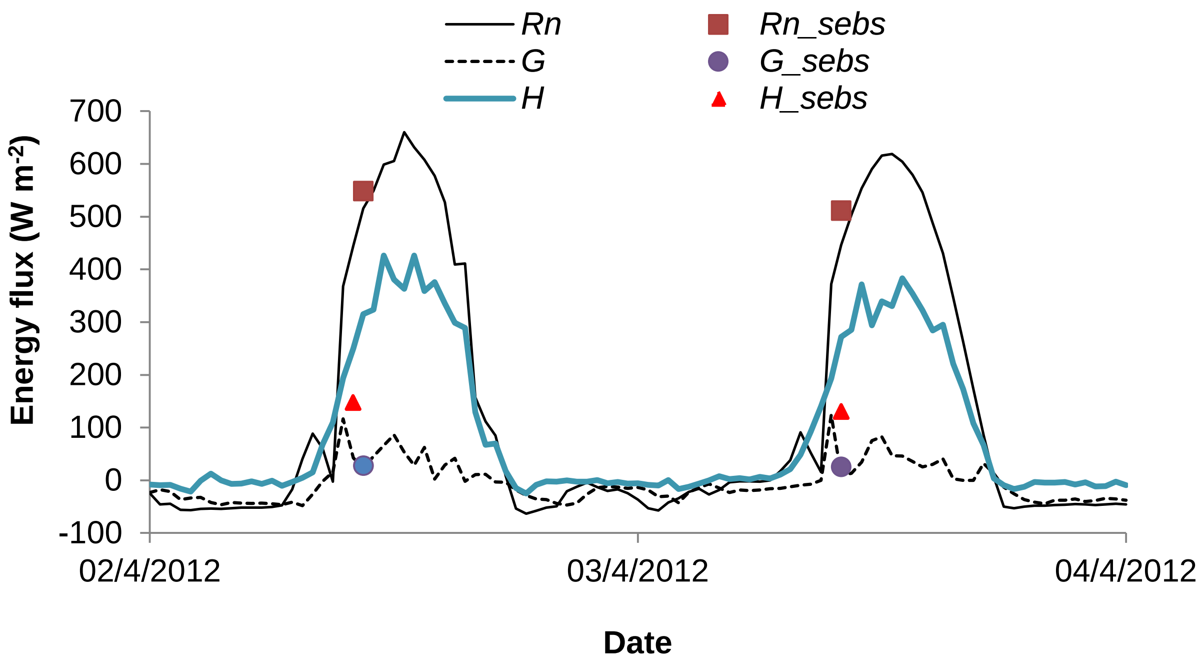

Figure 25. Field measured energy flux estimates and SEBS estimates during satellite overpass time (10:00 A.M) for the maize site.

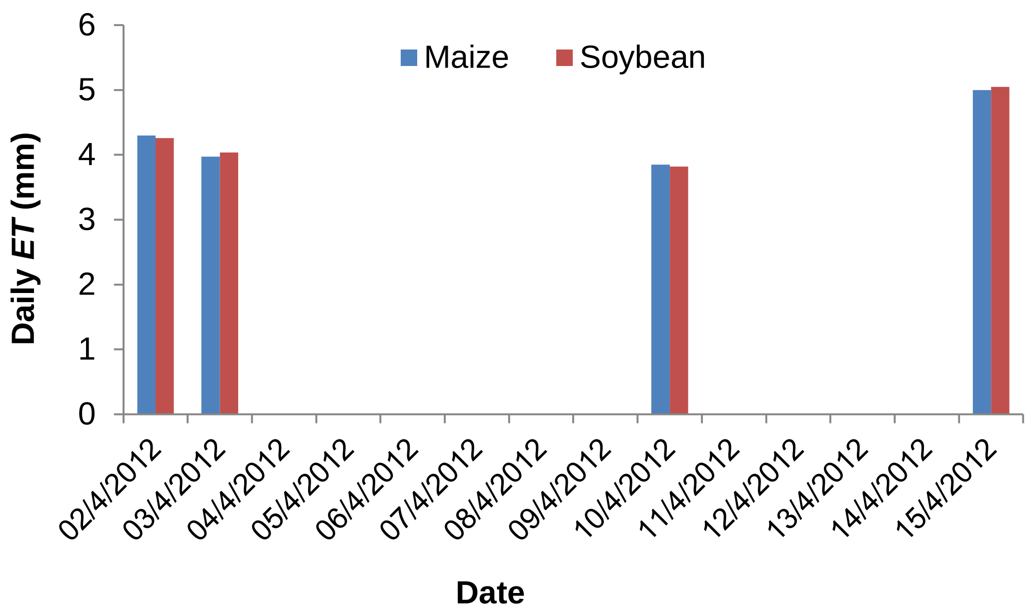

Figure 26. SEBS daily *ET* estimates for four days in April 2012 at the maize and soybean sites.

6.2 Second Validation Experiment

6.2.1 Field measurements

Total evaporation (*ET*) was estimated using the eddy covariance method at the maize and soybean sites. Root zone soil moisture contents were also monitored for the two sites and are presented in the following sections.

6.2.1.1 Site 1 (Soybean)

The daily variations in *ET* estimates (mm) over the soybean canopy are shown in Figure 27, along with rainfall (mm) for the measurement period. Daily *ET* of the soybean crop ranged from 0.5 to 6.7 mm. Total evaporation was higher for January and February 2013. Daily *ET* estimates from the soybean crop decreased to less than 3 mm for most of the days in March and April 2013.

Daily fractional volumetric soil water content measurements using three CS616 probes installed at 0.1, 0.5 and 1.0 m depths are shown in Figure 28. Volumetric soil water content (*SM*) values varied between 0.25 and 0.55 during the measurement period. Soil moisture increased with the increase in depth as shown in Figure 28. *SM* was the highest for the 1.0 m depth and lowest for the 0.1 m depth below the soil surface.

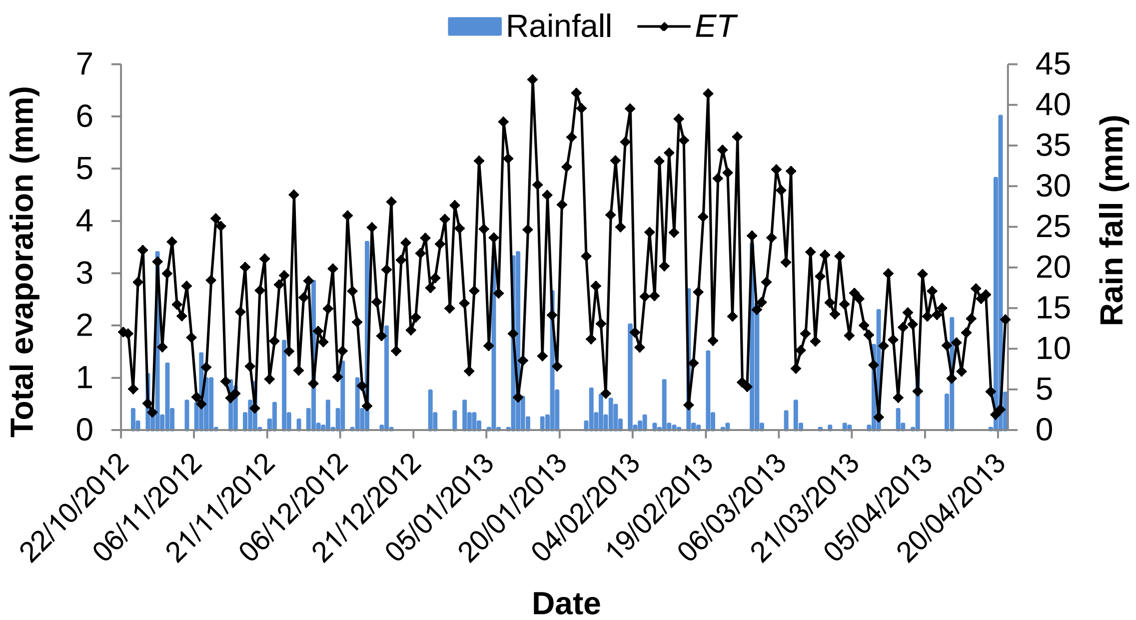

Figure 27. Total evaporation estimates (mm) from the soybean canopy along with rainfall (mm) for the 2012/2013 growing season.

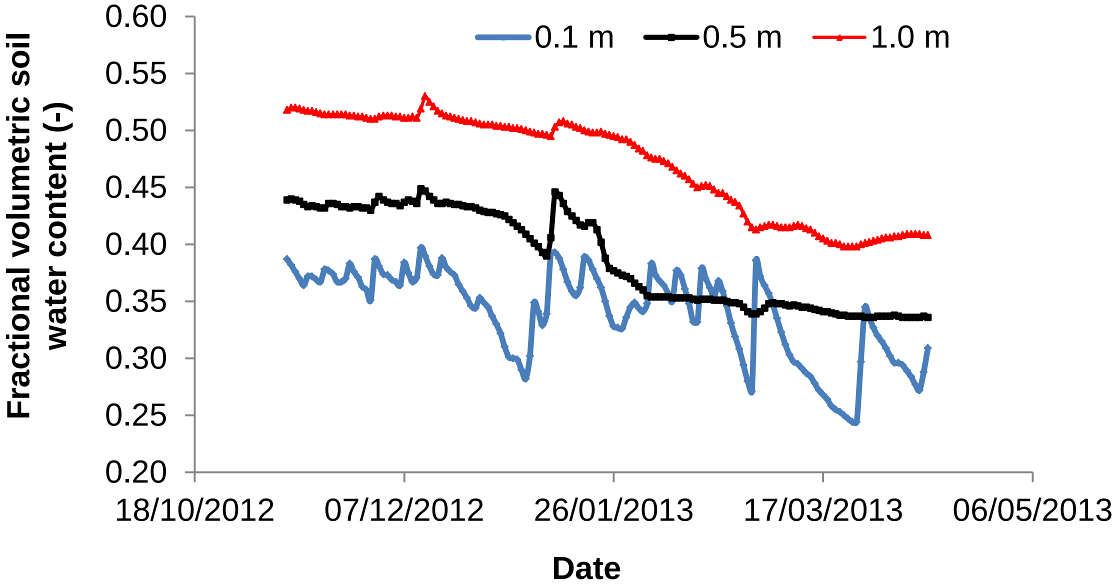

Figure 28. Fractional volumetric soil water content measurements using three CS616 probes in the soybean field at 0.1, 0.5, and 1.0 m depths below the soil surface.

6.2.1.2 Site 2 (Maize)

The daily variations in *ET* estimates (mm) over the maize canopy are shown in Figure 29, along with rainfall (mm) on the secondary y-axis. Daily *ET* from the maize crop varied between 0.5 and 5.0 mm. Total evaporation was higher for March 2012 compared to April 2012 (Figure 29). Total evaporation was higher for January and February 2013. Total evaporation from the maize crop decreased to less than 3 mm in March and April 2013.

Daily volumetric soil water content measurements using the three Hydra Probe II soil moisture sensors at 0.1, 0.5 and 1.0 m depths below the soil surface are shown in Figure 30. Volumetric soil water content (*SM*) values varied between 0.20 and 0.38 during the measurement period. Soil moisture at the 0.1 m depth fluctuated most compared to the other two depths as shown in Figure 30. *SM* was higher at the 1.0 m depth and lowest at the 0.1 m depth below the soil surface.

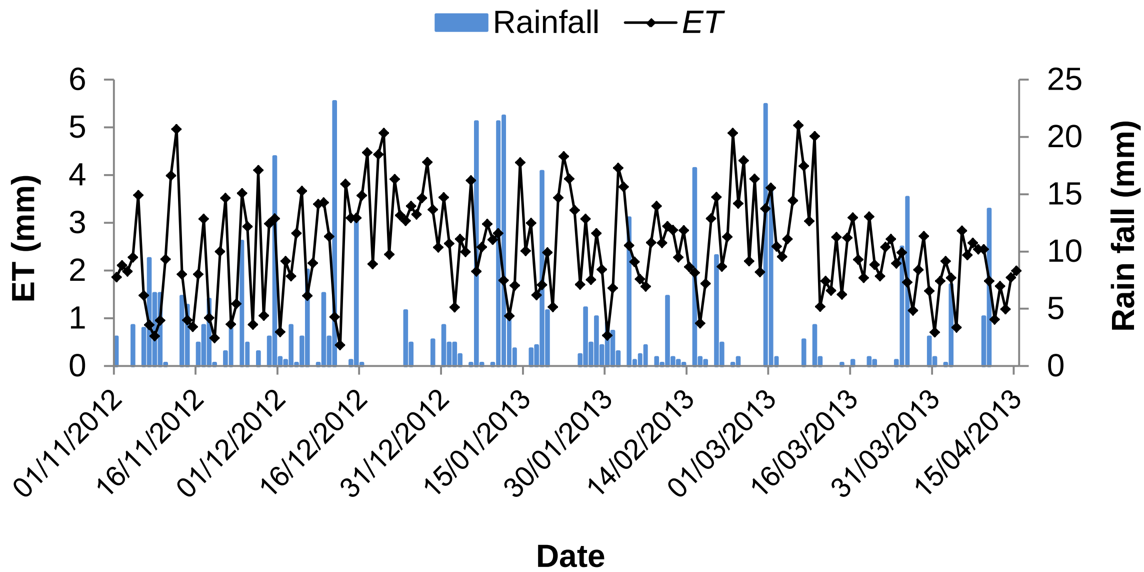

Figure 29. Total evaporation estimates (mm) from the maize canopy along with rainfall (mm) for the 2012/2013 growing season.

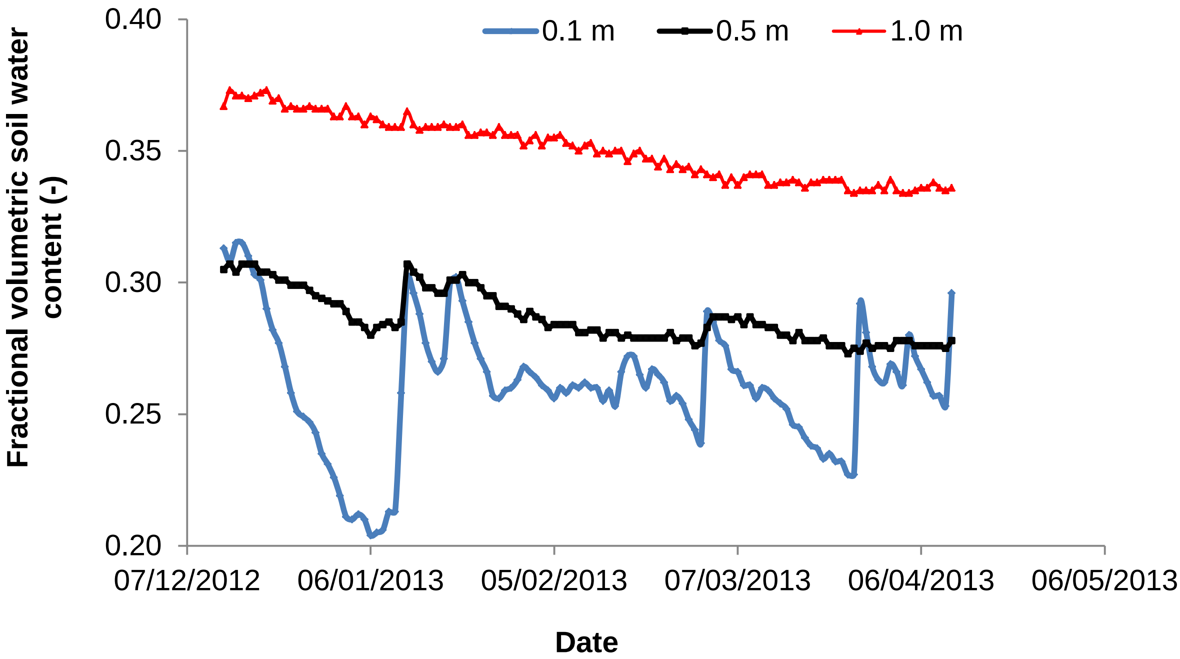

Figure 30. Fractional volumetric soil water content measurements in the maize field at 0.1, 0.5, and 1.0 m depths below the soil surface.

6.2.2 Satellite estimates

Pre-processing of the Landsat 7 and 8 images was done in Erdas Imaging and post processing of the images was done in ILWIS to create maps of the different surface fluxes using the SEBS model. The four maps required in SEBS for *ET* estimation are a land surface temperature map, an emissivity map, an albedo map, *NDVI* map, and vegetation cover map. Other maps required included a digital elevation map and sun zenith angle map. Land use map with associated surface parameters is also required in SEBS. If land use and vegetation cover maps are not available SEBS uses the *NDVI* map to estimate all surface parameters. Meteorological data from an AWS at Baynesfield next to the two sites was used in SEBS.

Daily *ET* map for the Baynesfield area using Landsat 7 scenes (WRS path 168, WRS row 81) for 09 March 2012, 10 April 2012, 26 April 2012, 22 December 2012, 23 January 2013, 28 March 2013, and 13 April 2013 are shown in Figures 31 to 36. Two Landsat 8 scenes (WRS path 168, WRS row 81) on 23 May 2013 and 24 June 2013 are also used in SEBS for daily ET estimates as shown in Figures 37 and 38. The SEBS daily *ET* estimates were higher for December 22, 2012 and January 23, 2013 compared to the rest of the images for both the maize and soybean sites respectively.

The average relative soil moisture estimates using SEBS for 09 March 2012, 22 December 2012, 23 January 2013, 28 March 2013 are presented in Figures 39 to 42. The relative soil moisture was calculated using an empirical relationship (Equation 17) between evaporative fraction (Λ) and volumetric soil moisture content (ϑ) following the Scott et al. (2003) method. The value of relative soil moisture content ($\vartheta/\vartheta_{sat}$) varied between 0.09 (dry) and 1 (full saturation).

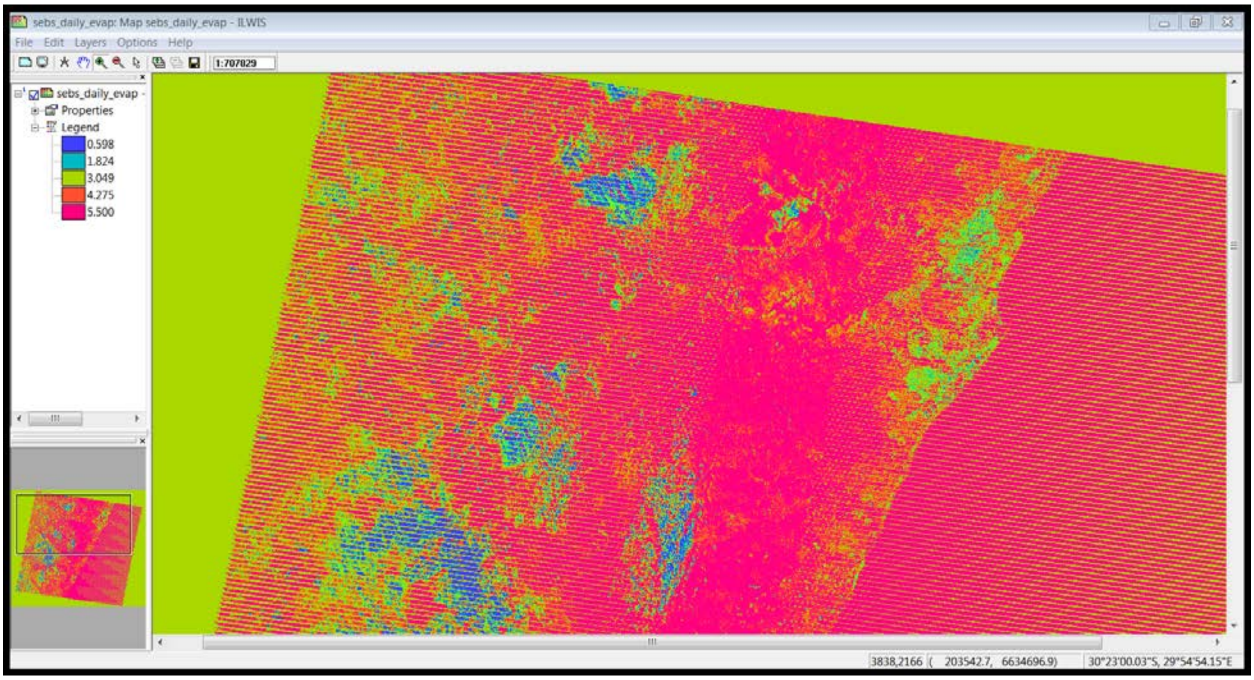

Figure 31. Daily *ET* map for the Baynesfield area using Landsat 7 scene (WRS path 168, WRS row 81) for March 9, 2012.

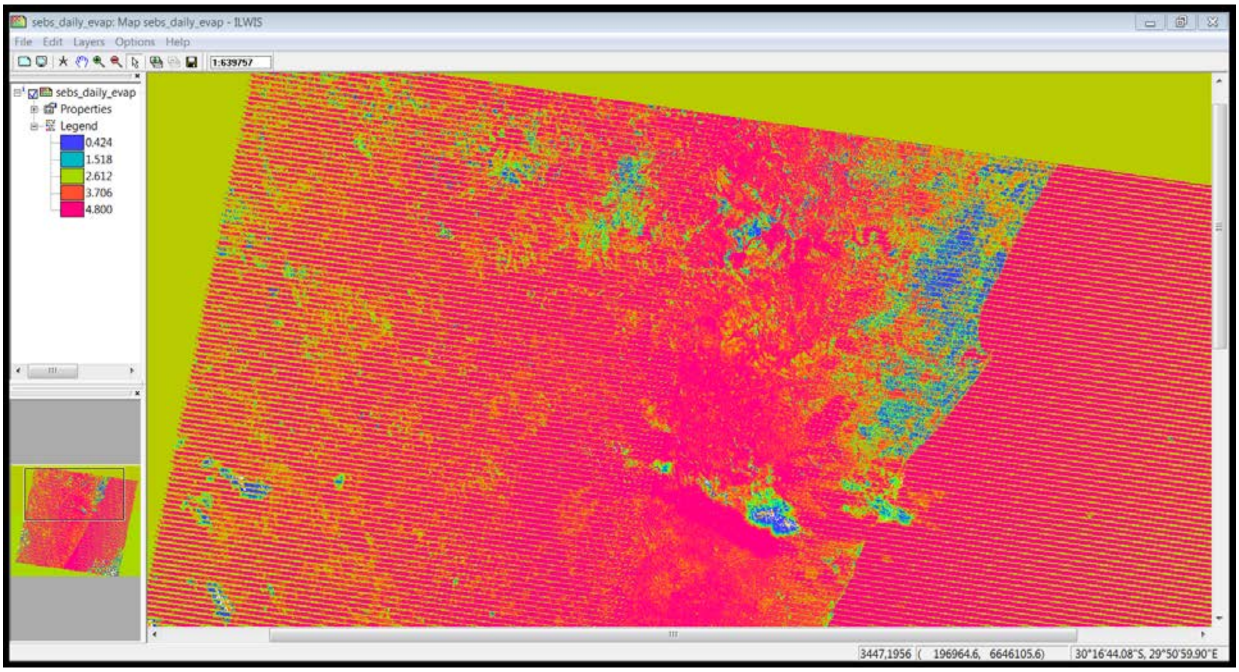

Figure 32. Daily *ET* map for the Baynesfield area using Landsat 7 scene (WRS path 168, WRS row 81) for April 10, 2012.

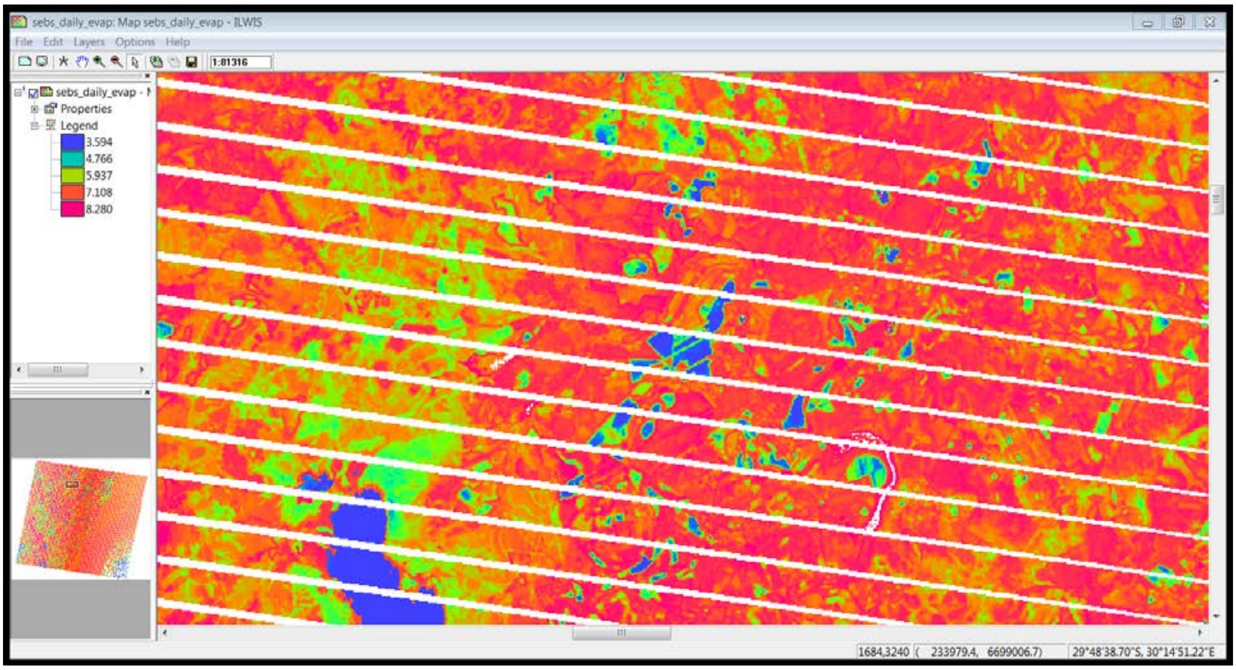

Figure 33. Daily *ET* map for the Baynesfield area using Landsat 7 scene (WRS path 168, WRS row 81) for December 22, 2012.

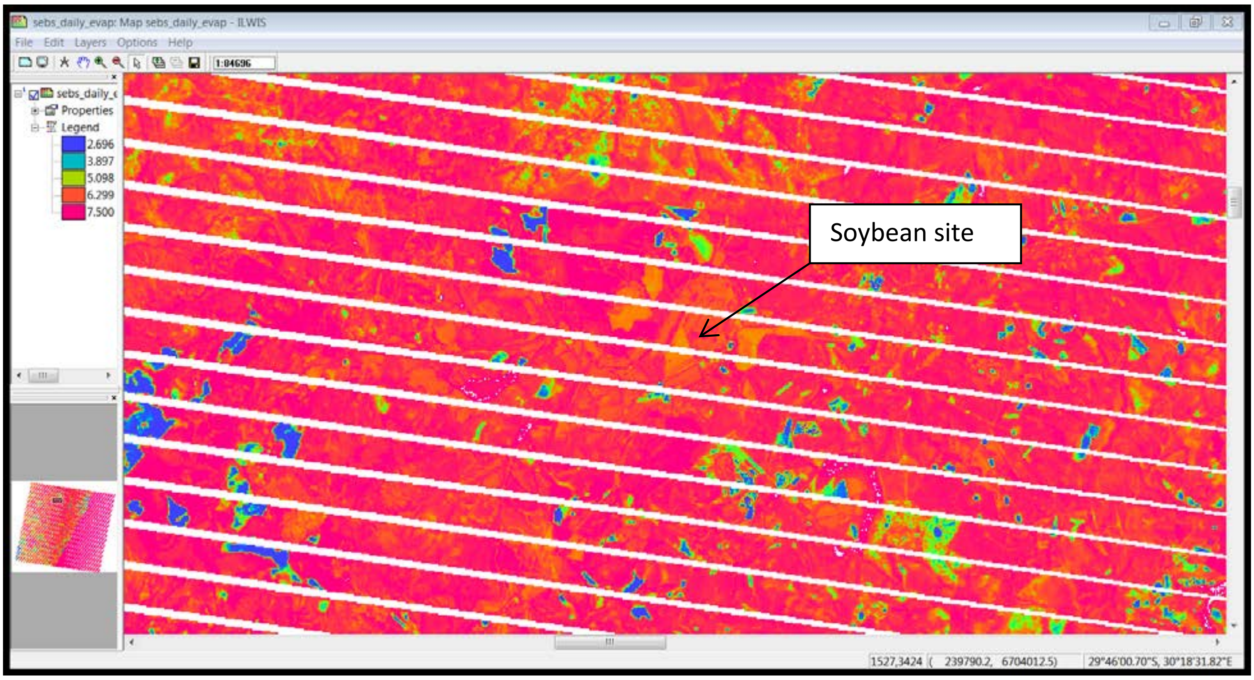

Figure 34. Daily *ET* map for the Baynesfield area using Landsat 7 scene (WRS path 168, WRS row 81) for January 23, 2013.

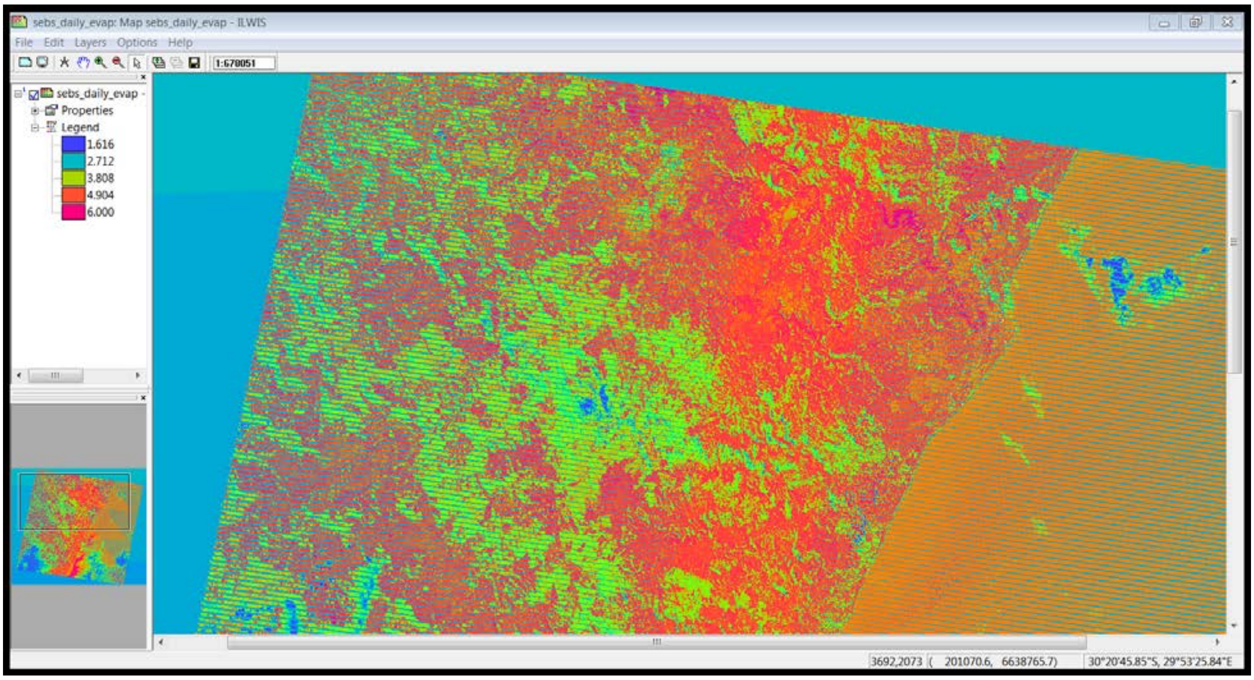

Figure 35. Daily *ET* map for the Baynesfield area using Landsat 7 scene (WRS path 168, WRS row 81) for March 28, 2013.

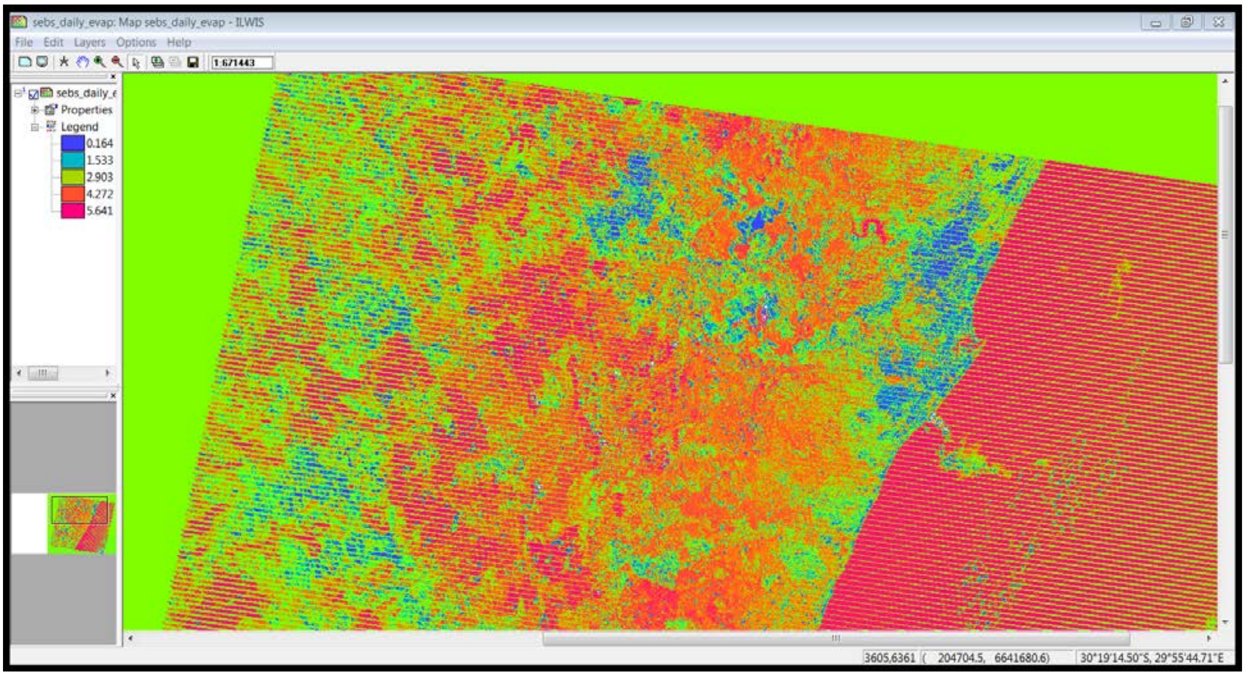

Figure 36. Daily *ET* map for the Baynesfield area using Landsat 7 scene (WRS path 168, WRS row 81) for April 13, 2013.

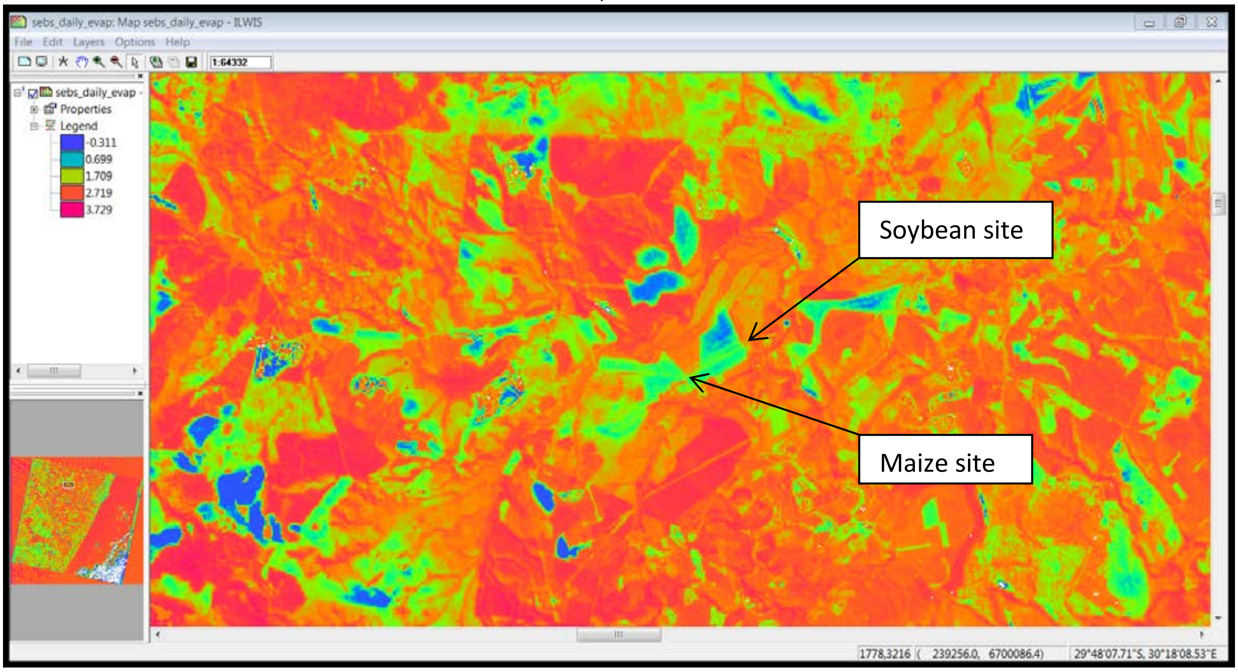

Figure 37. Daily *ET* map for the Baynesfield area using Landsat 8 scene (WRS path 168, WRS row 81) for May 23, 2013.

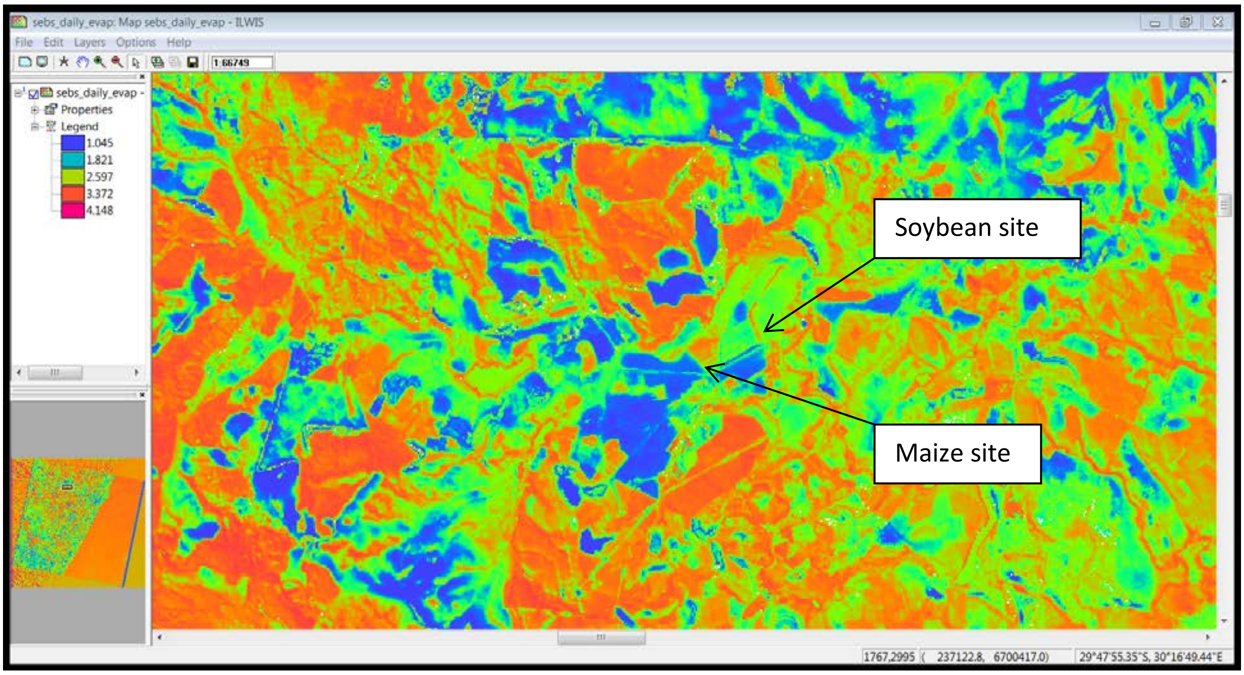

Figure 38. Daily *ET* map for the Baynesfield area using Landsat 8 scene (WRS path 168, WRS row 81) for June 24, 2013.

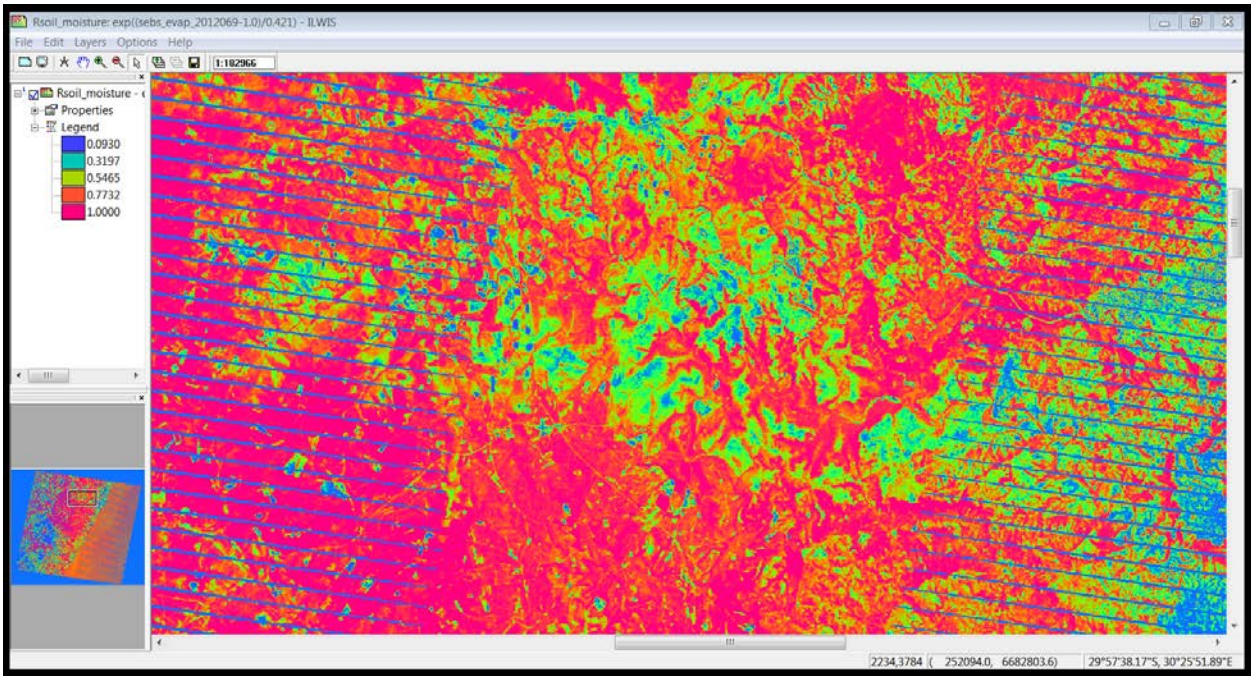

Figure 39. Relative soil moisture map (9 March, 2012) for the Baynesfield area estimated using the Scott *et al*. (2003) equation.

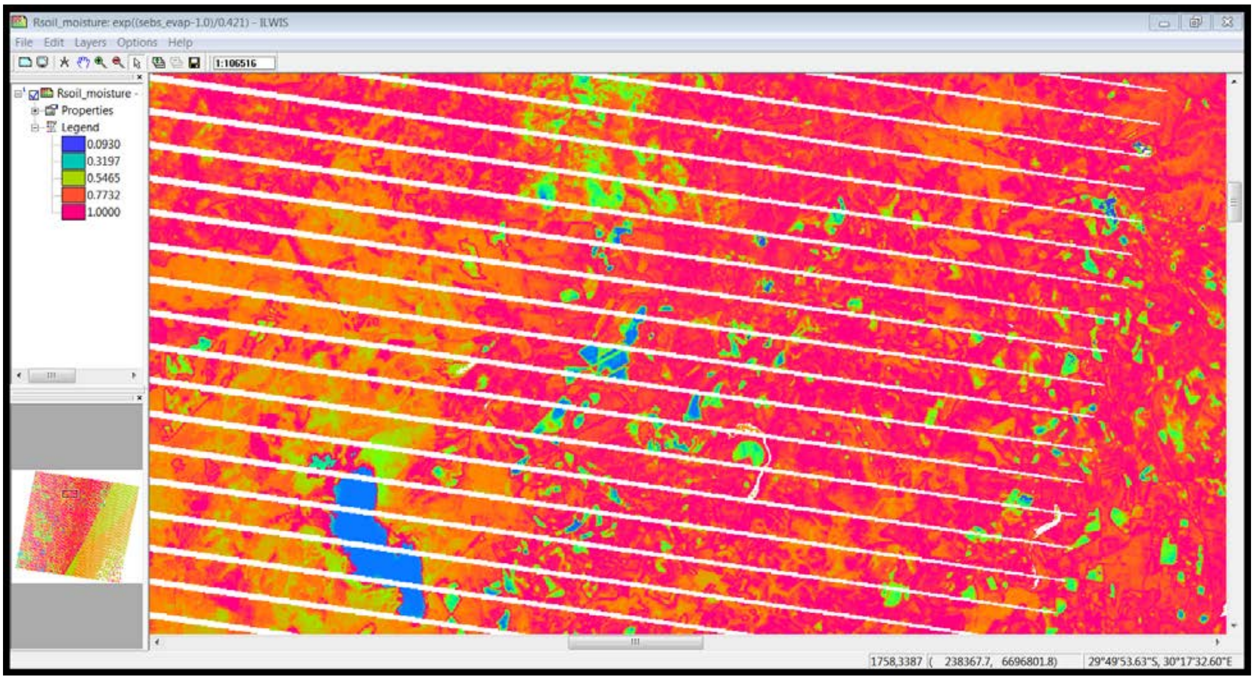

Figure 40. Relative soil moisture map (22 December, 2012) for the Baynesfield area estimated using the Scott *et al*. (2003) equation**.**

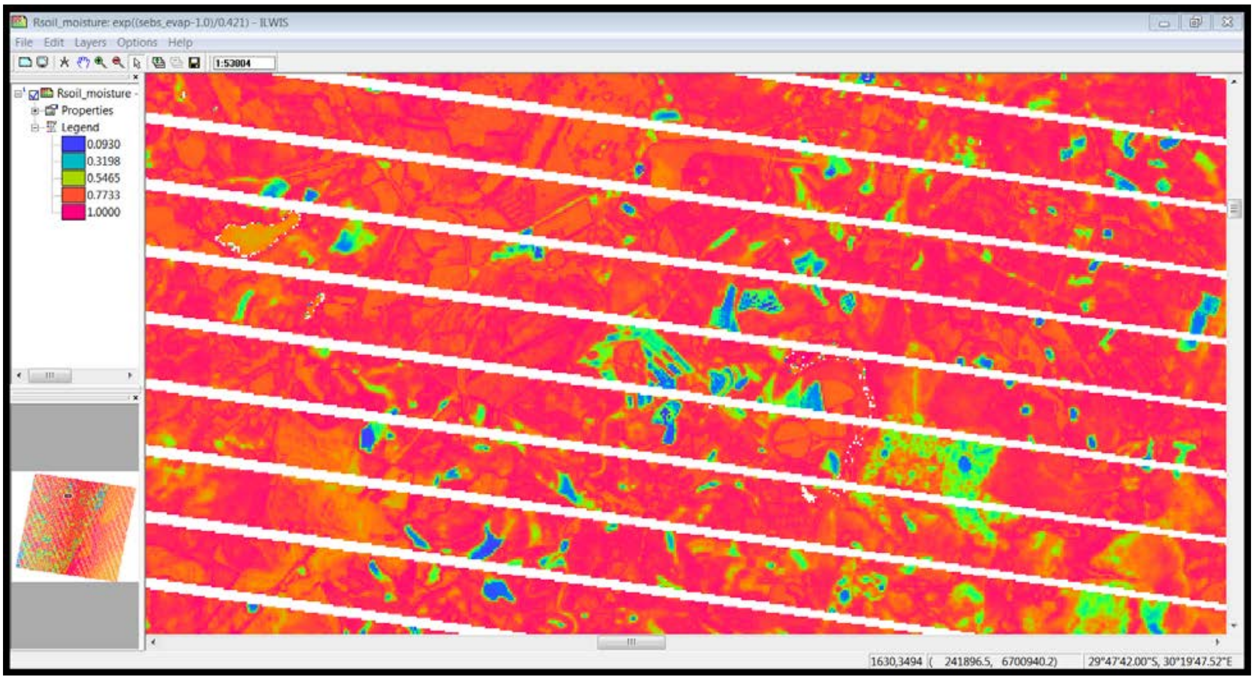

Figure 41. Relative soil moisture map (23 January, 2013) for the Baynesfield area estimated using the Scott *et al*. (2003) equation**.**

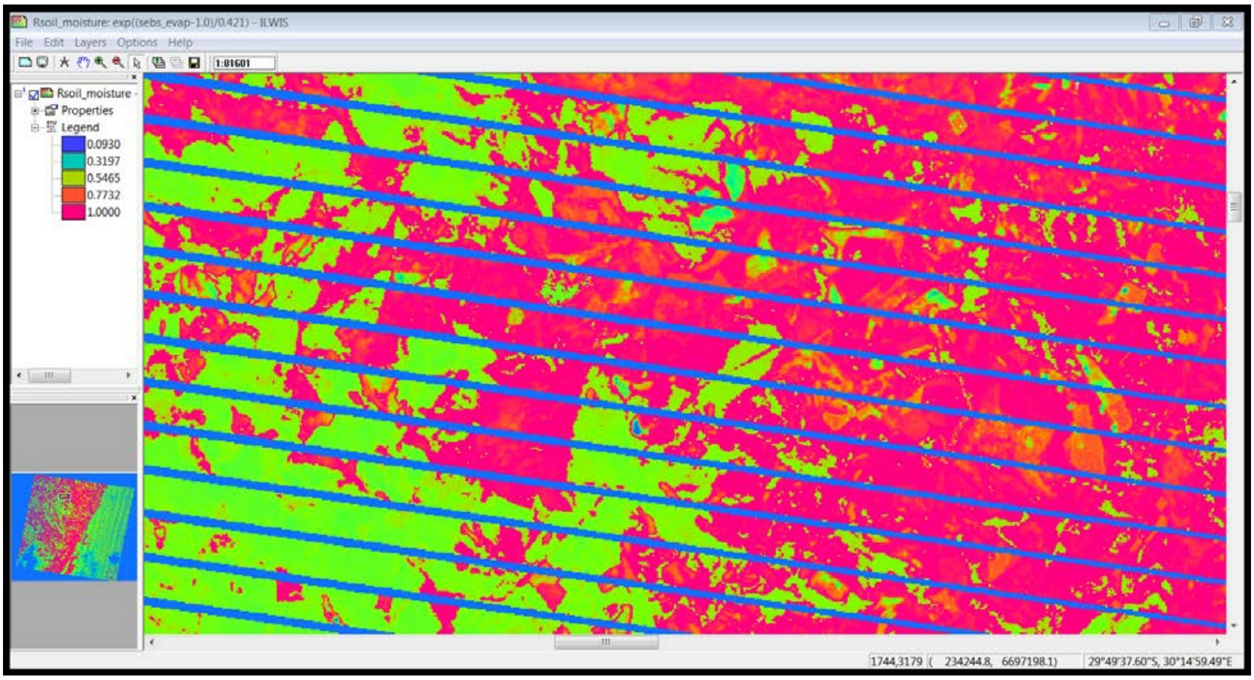

Figure 42. Relative soil moisture map (28 March, 2013) for the Baynesfield area estimated using the Scott *et al*. (2003) equation. Banding caused by missing scan lines in Landsat 7 data.

6.3 TOPKAPI/ HYLARSMET Model Estimates

PyTOPKAPI, an open source implementation of the TOPKAPI distributed hydrological model, was used to investigate soil moisture dynamics at national and catchment scales. The model is forced by 3-hourly spatially distributed rainfall (TRMM 3B42RT) and evapotranspiration (computed from reference crop *ET* modulated by vegetation health and available soil water). The advantage of this modelling approach is its ability to produce estimates at regular time steps over a range of locations, which can be selected depending on the requirements of a particular application (Sinclair and Pegram, 2012).

HYLARSMET model *ET* simulations (Pegram and Associates) for the same days of the Landsat scenes shown in the previous section are presented in Figures 43 to 49. Soil Saturation Index (SSI) maps are also presented in Figures 50 to 56.

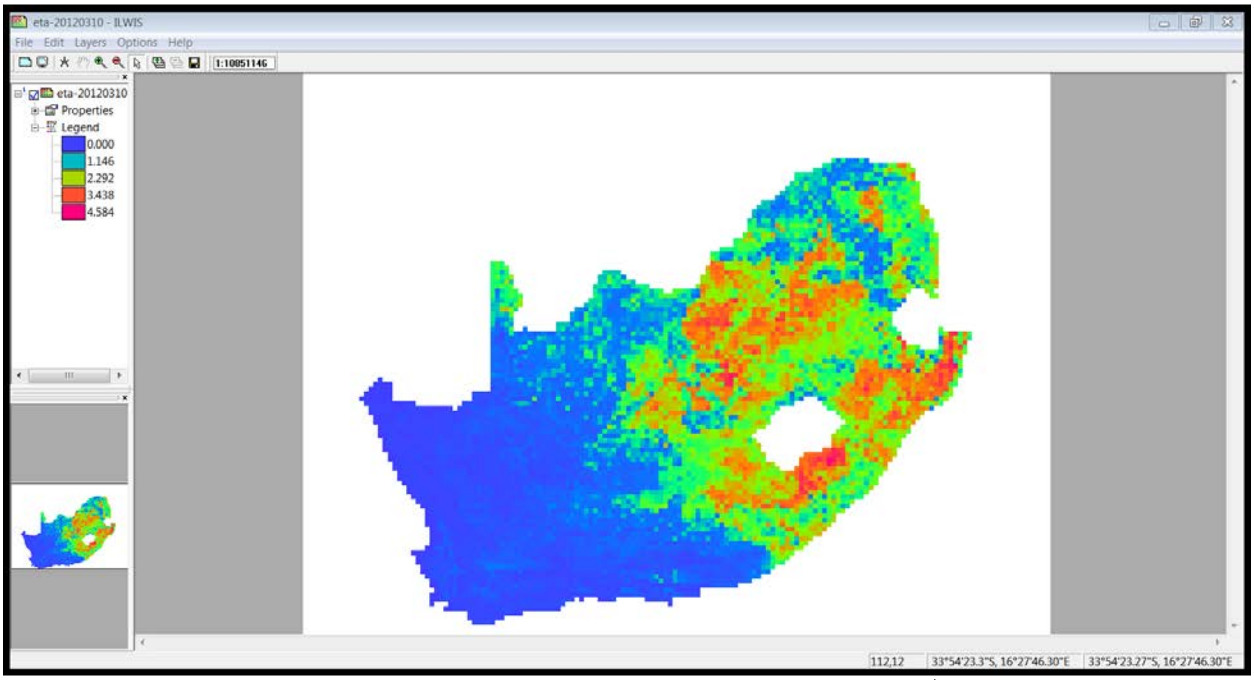

Figure 43. Daily *ET* estimates (mm) using the HYLARSMET model for the 9th of March 2012.

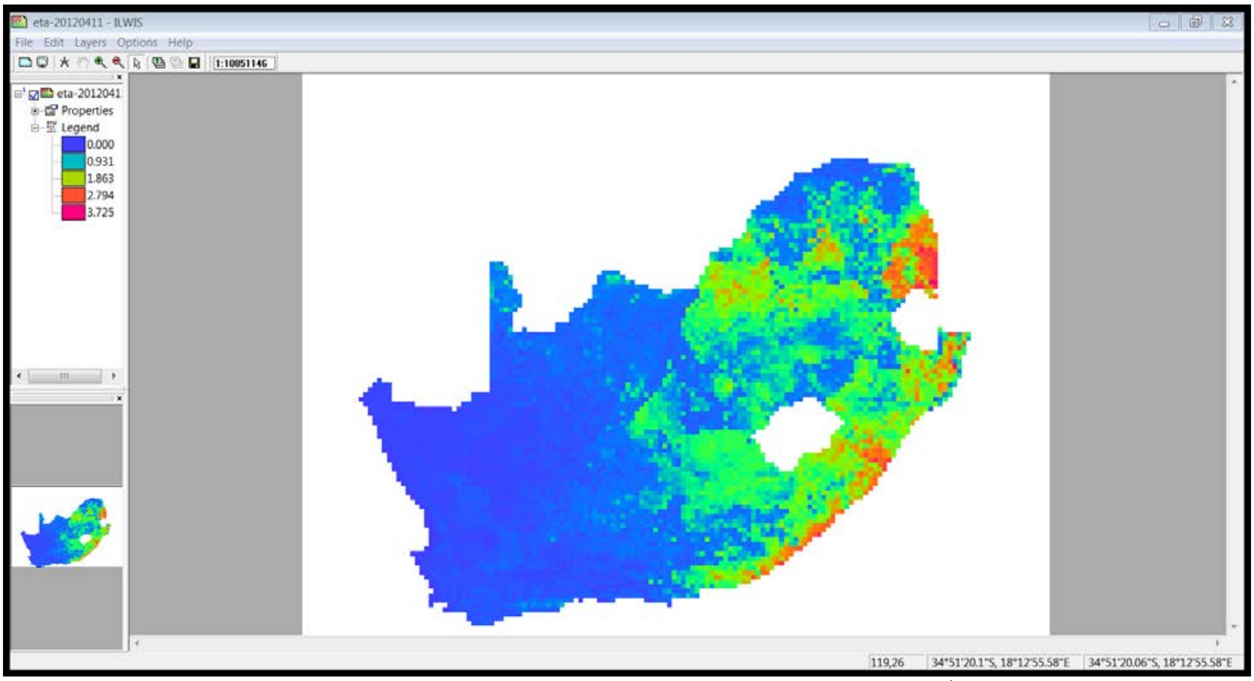

Figure 44. Daily *ET* estimates (mm) using the HYLARSMET model for the 10th of April 2012.

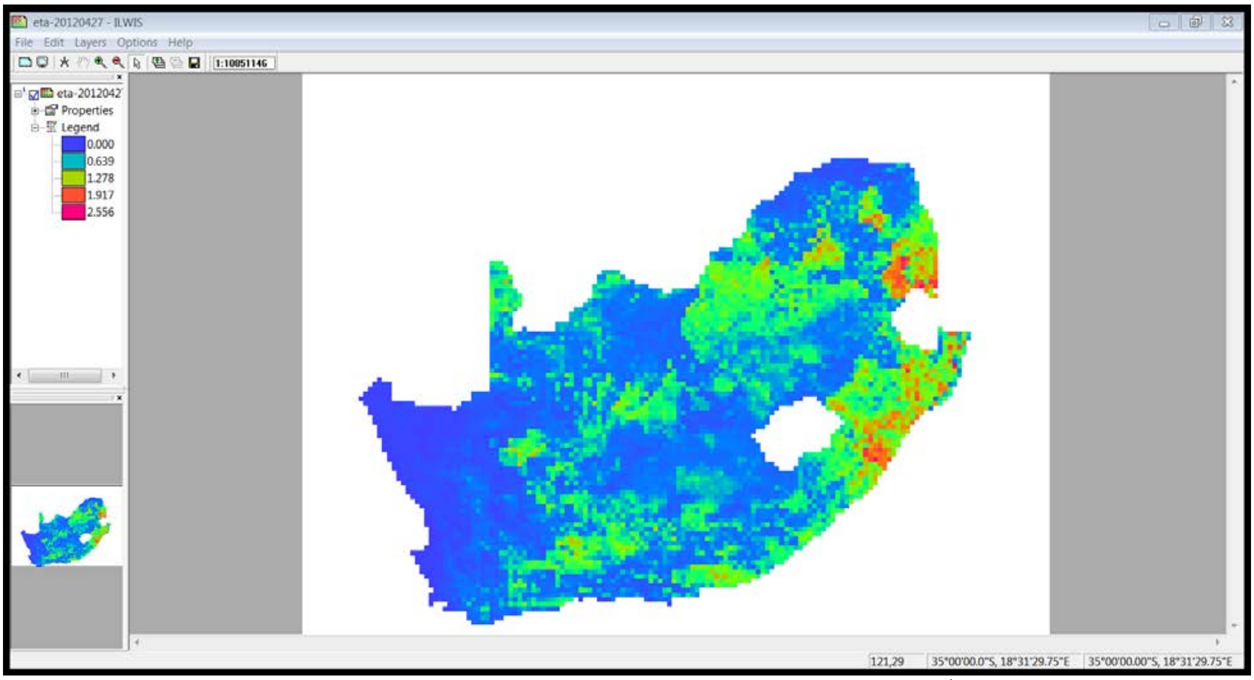

Figure 45. Daily *ET* estimates (mm) using the HYLARSMET model for the 26th of April 2012.

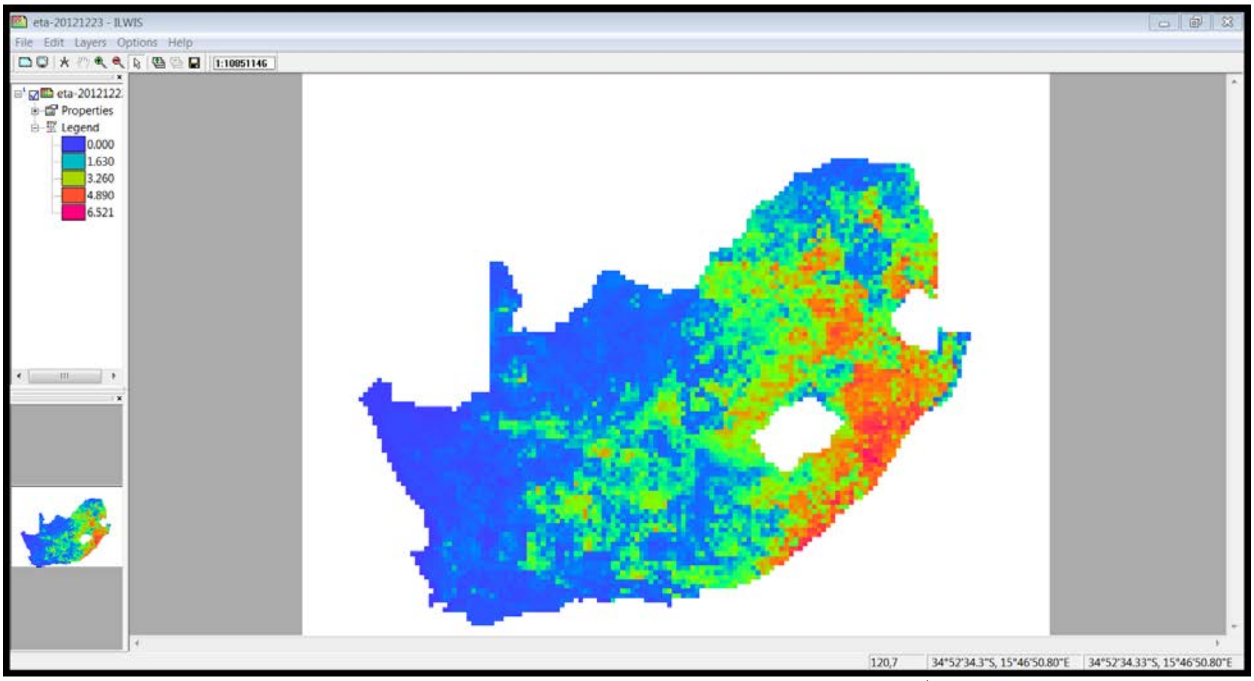

Figure 46. Daily *ET* estimates (mm) using the HYLARSMET model for the 22nd of December 2012.

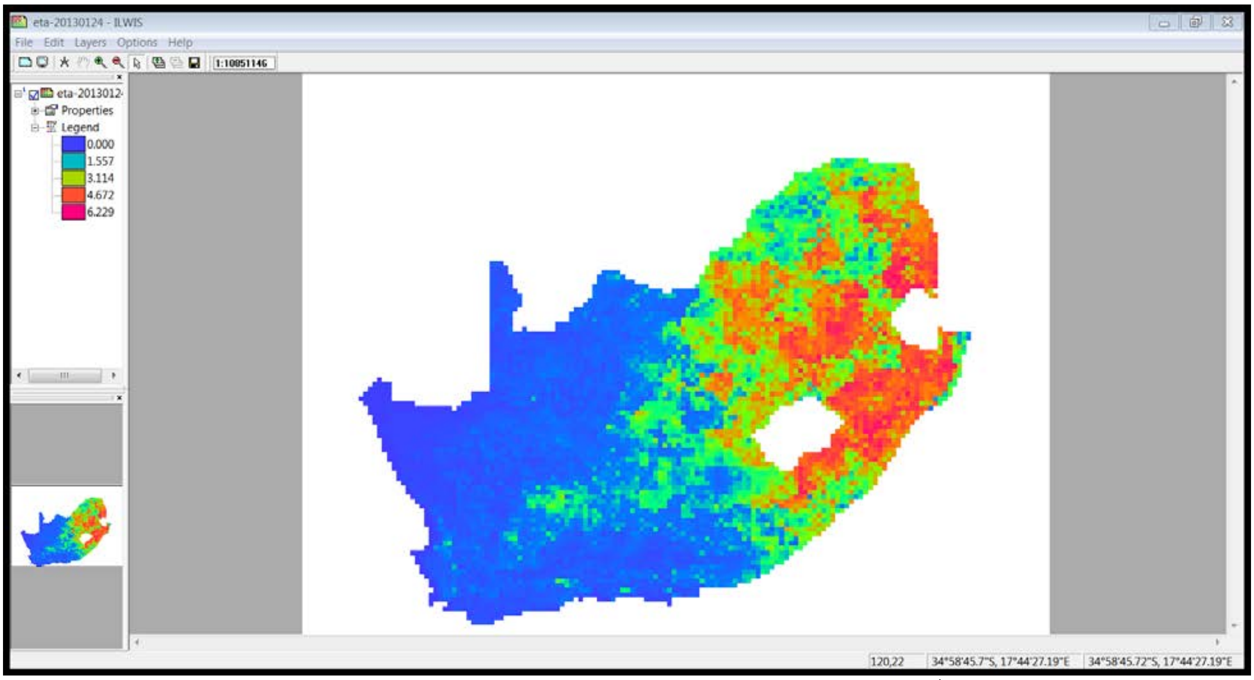

Figure 47. Daily *ET* estimates (mm) using the HYLARSMET model for the 23rd of January 2013.

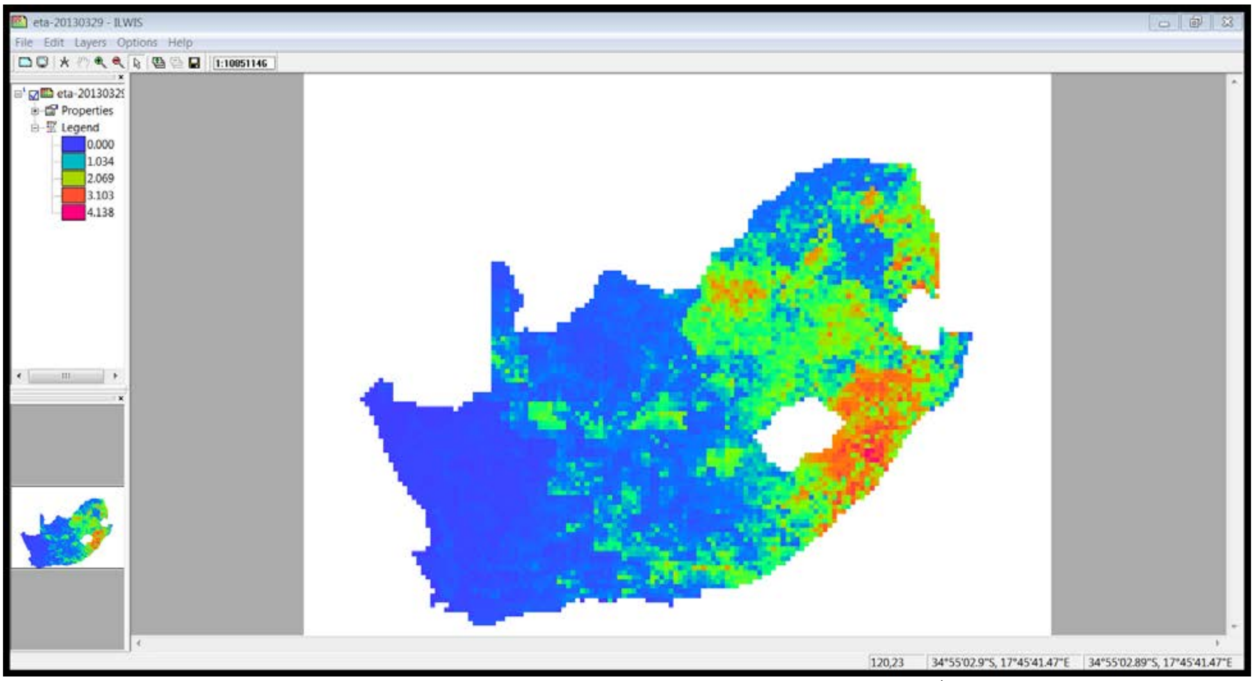

Figure 48. Daily *ET* estimates (mm) using the HYLARSMET model for the 28th of March 2013.

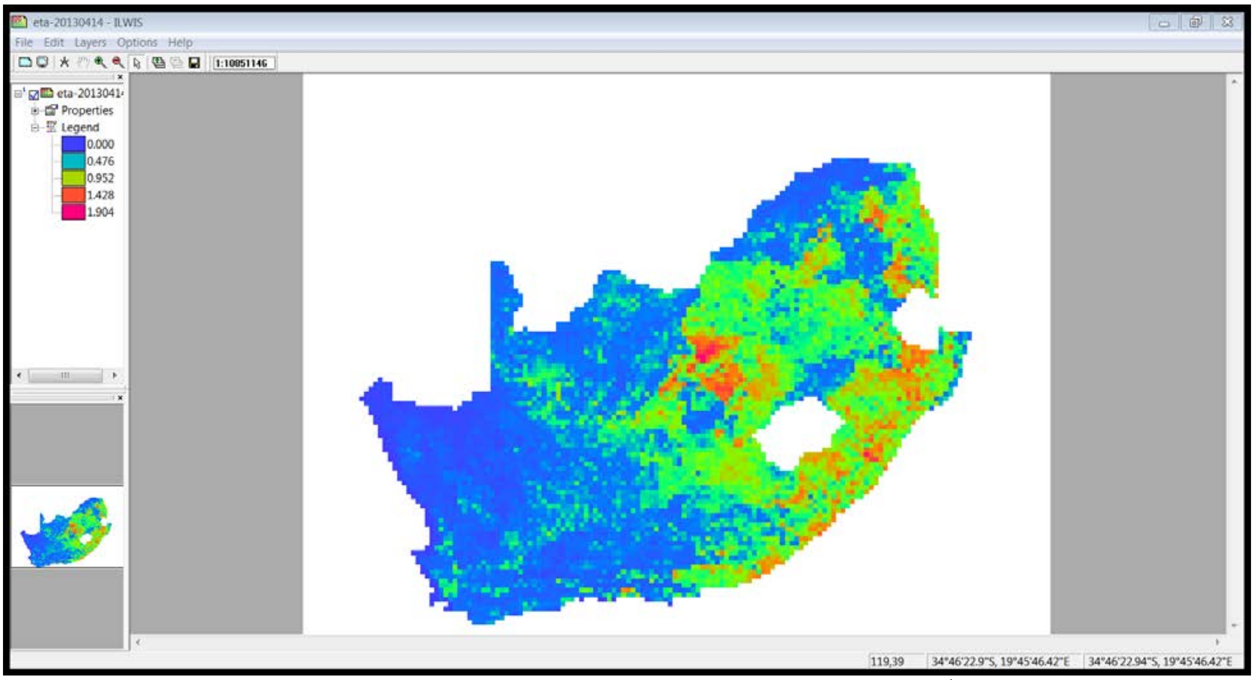

Figure 49. Daily *ET* estimates (mm) using the HYLARSMET model for the 13th of April 2013.

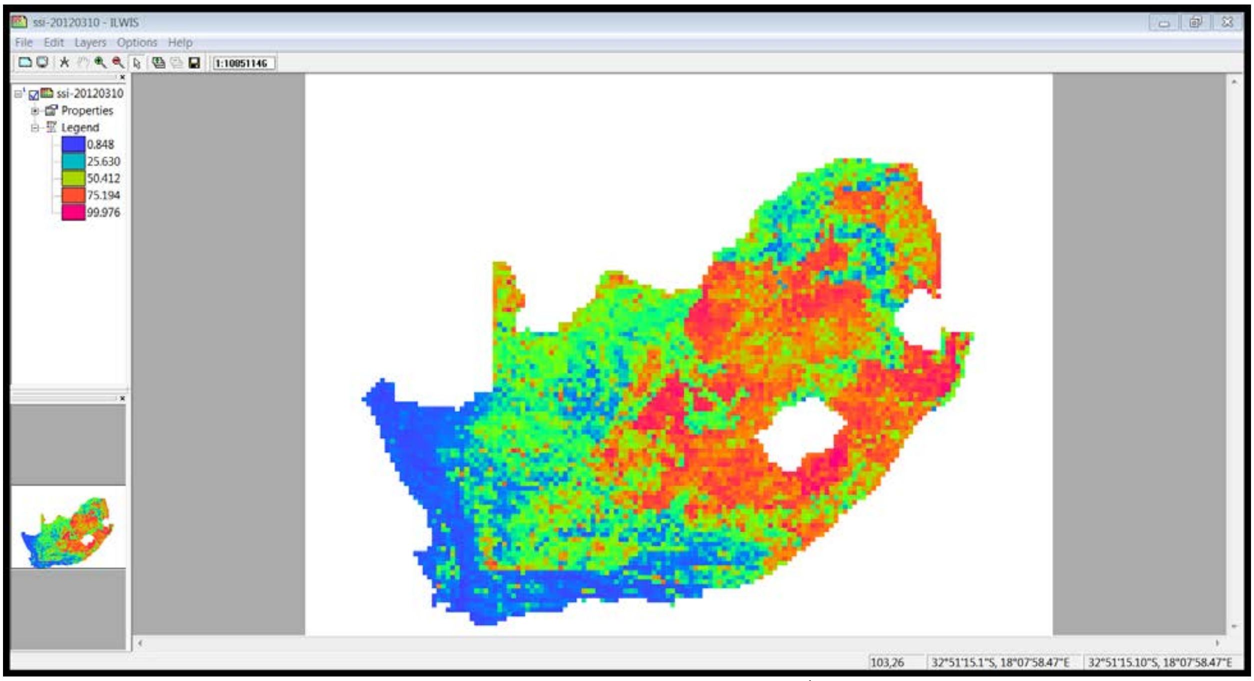

Figure 50. Soil Saturation Index (SSI) map for the 9th of March 2012.

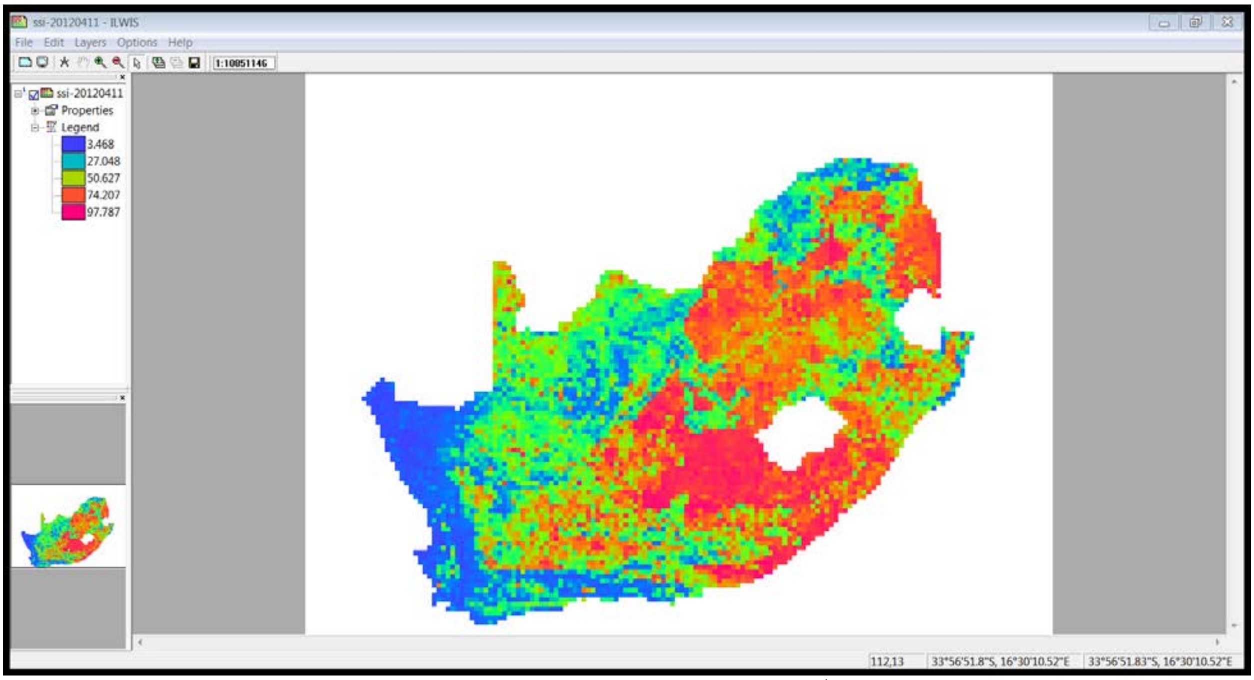

Figure 51. Soil Saturation Index (SSI) map for the 10th of April 2012.

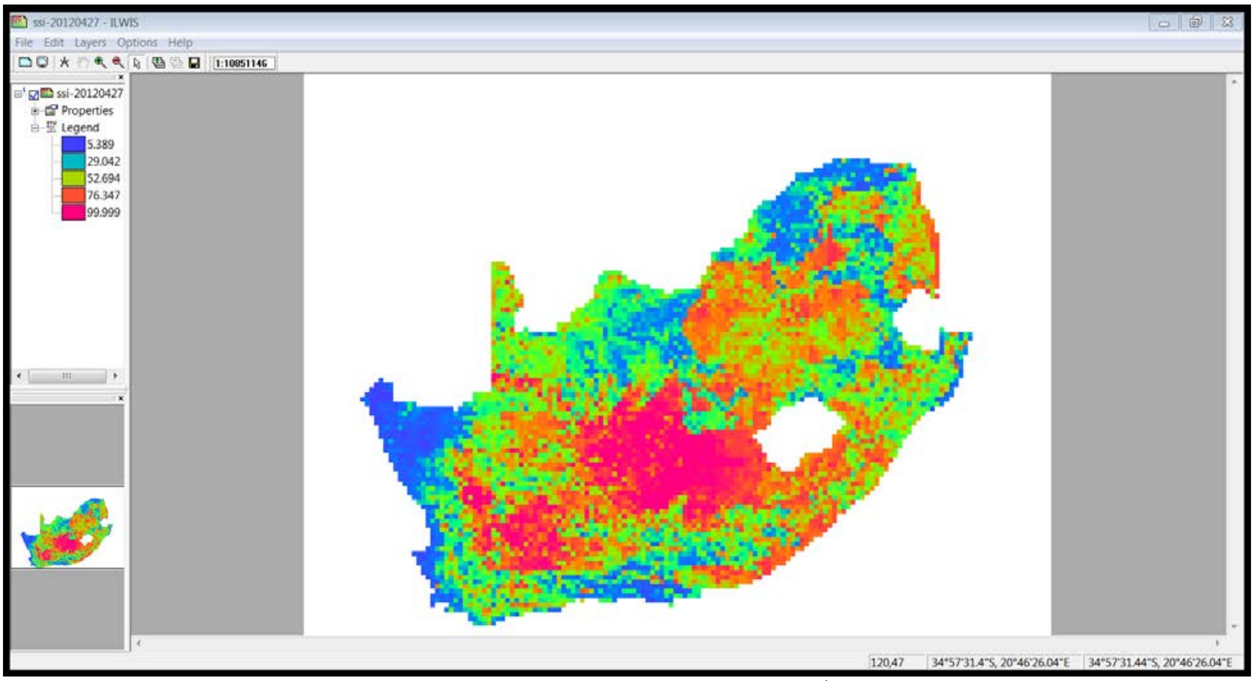

Figure 52. Soil Saturation Index (SSI) map for the 26th of April 2012.

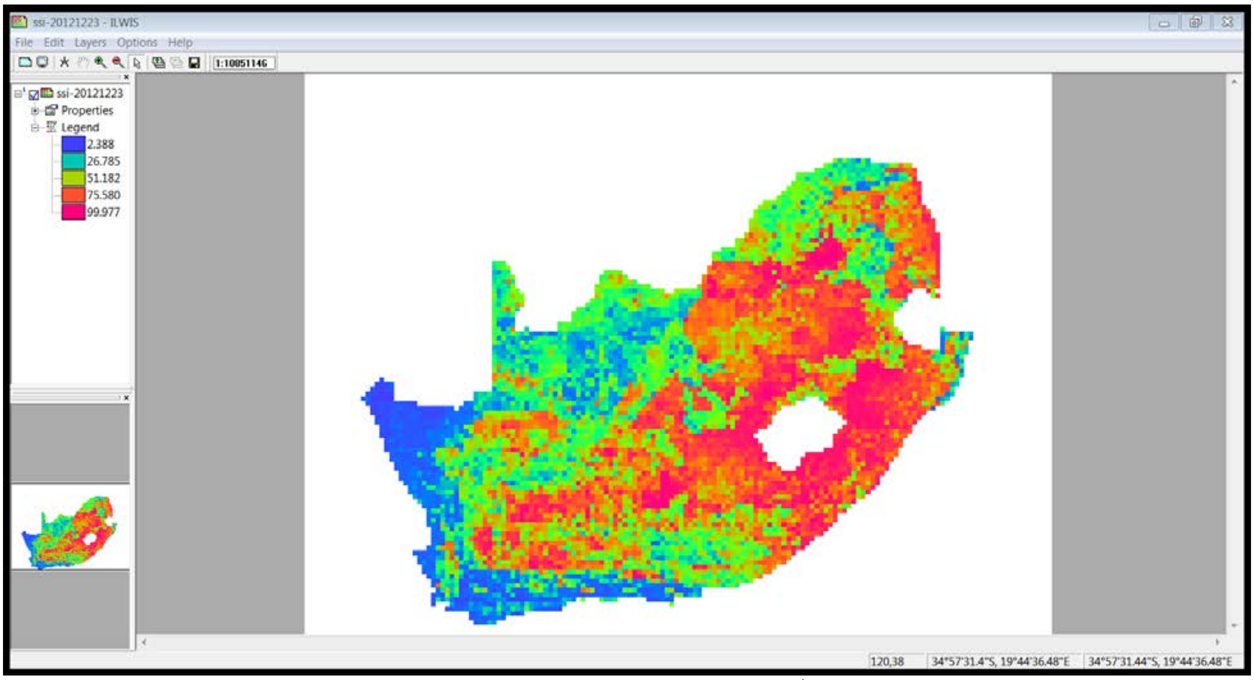

Figure 53. Soil Saturation Index (SSI) map for the 22nd of December 2012.

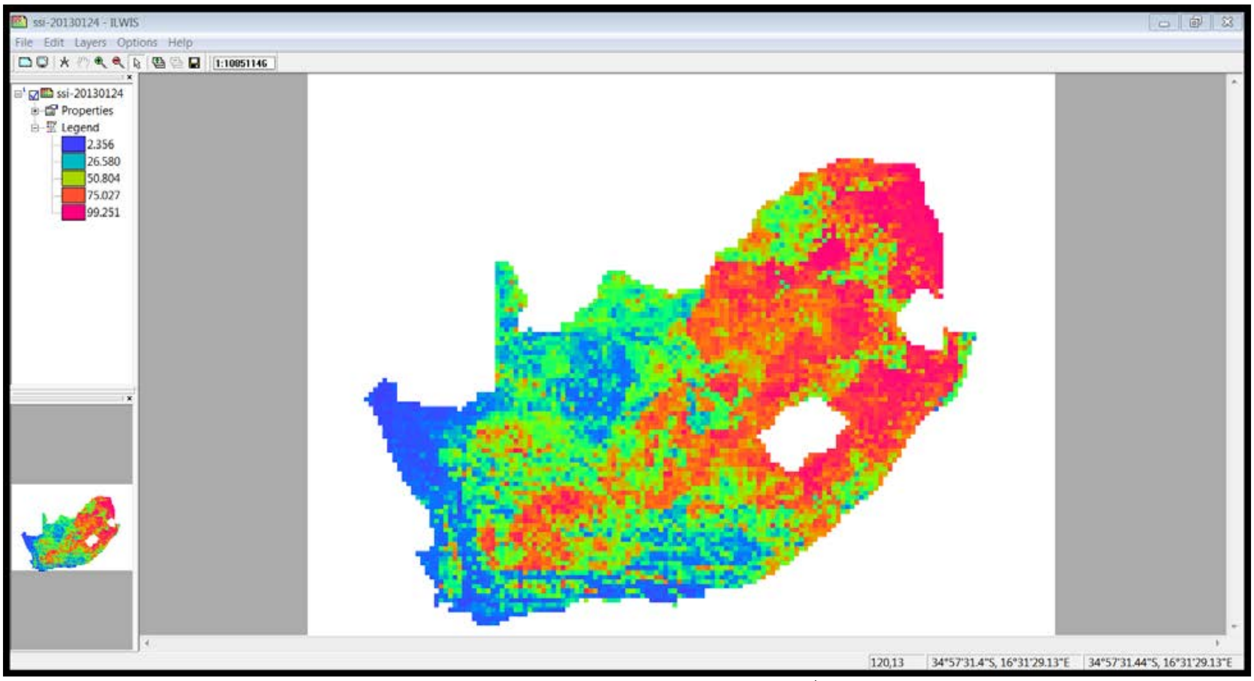

Figure 54. Soil Saturation Index (SSI) map for the 23rd of January 2013.

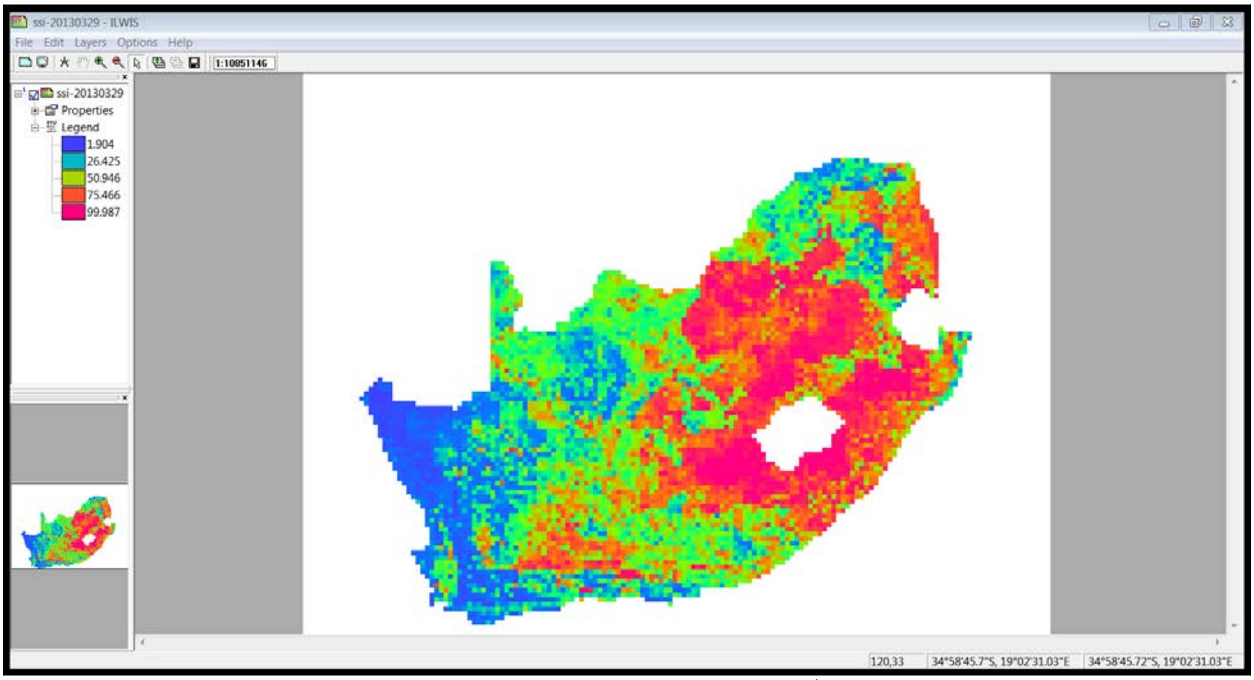

Figure 55. Soil Saturation Index (SSI) map for the 28th of March 2013.

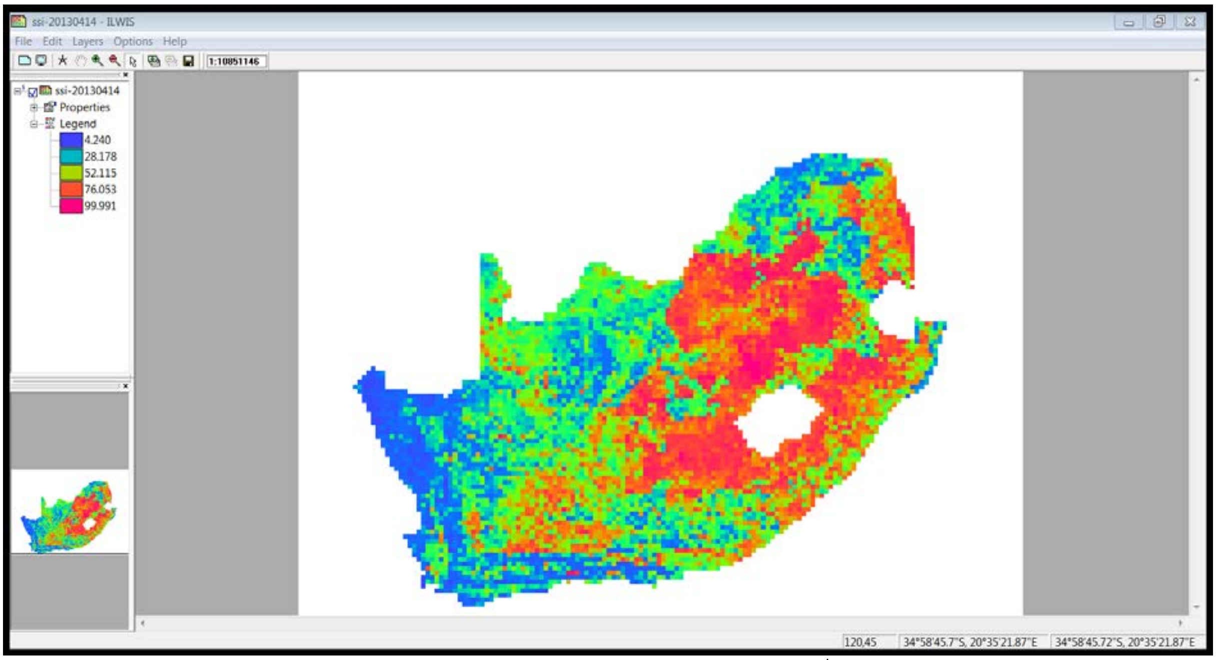

Figure 56. Soil Saturation Index (SSI) map for the 13th of April 2013.

6.4 Validation of the SEBS and HYLARSMET Estimates

Field measured energy fluxes and SEBS estimates during the satellite overpass time (10:00 A.M) for the soybean site are presented in Figures 57 and 58. Net radiation (R_n) and soil heat flux (G) estimates compared well during the satellite over pass time. SEBS sensible heat flux (*H_SEBS*) estimates were lower compared to the field estimates of *H*.

The daily *ET* estimates using SEBS and HYLARSMET models along with the eddy covariance estimates are presented in Figures 59 to 62 for four days of the second validation experiment. The field measured daily eddy covariance *ET* estimates are presented in Figures 27 and 29 for the soybean and maize sites respectively. The SEBS daily *ET* estimates were higher than the eddy covariance daily *ET* estimates. This shows that the SEBS model overestimated the daily *ET* estimates for these days. The HYLARSMET daily *ET* estimates were lower than the EC and SEBS estimates. The HYLARSMET estimates followed the variation of the daily *ET* estimates for the different seasons.

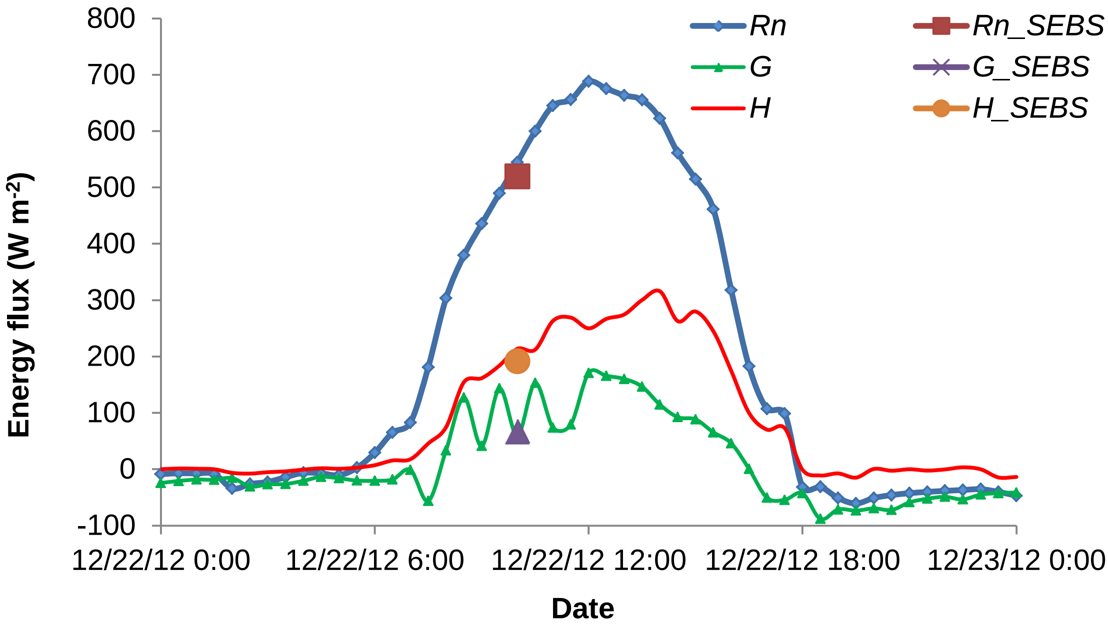

Figure 57. Field measured energy flux estimates and SEBS estimates during the satellite overpass time (10:00 A.M) for the soybean site (22 December, 2012).

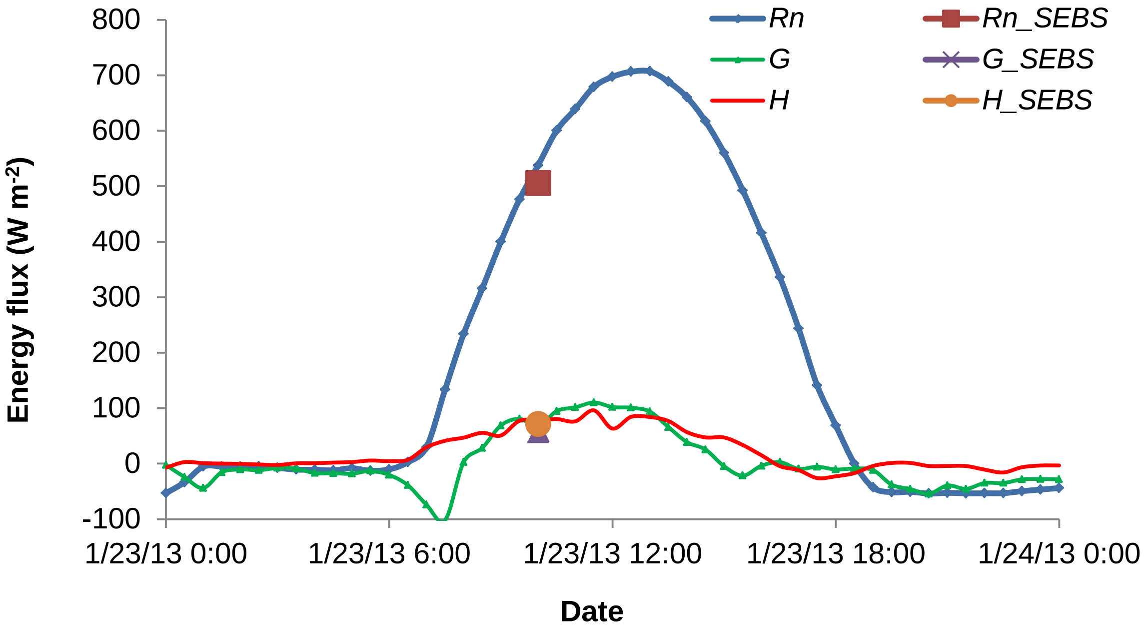

Figure 58. Field measured energy flux estimates and SEBS estimates during the satellite overpass time (10:00 A.M) for the soybean site (23 January, 2013).

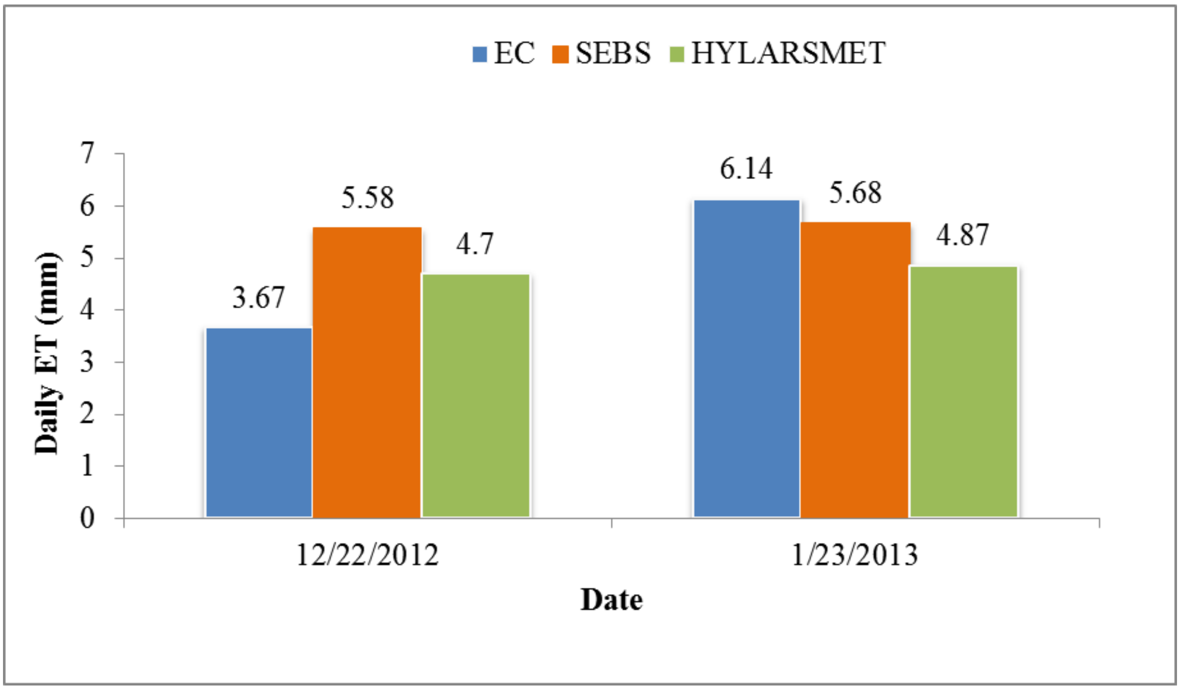

Figure 59. Comparison of the daily *ET* estimates for December 22, 2012 and 23 January 2013 at the soybean site.

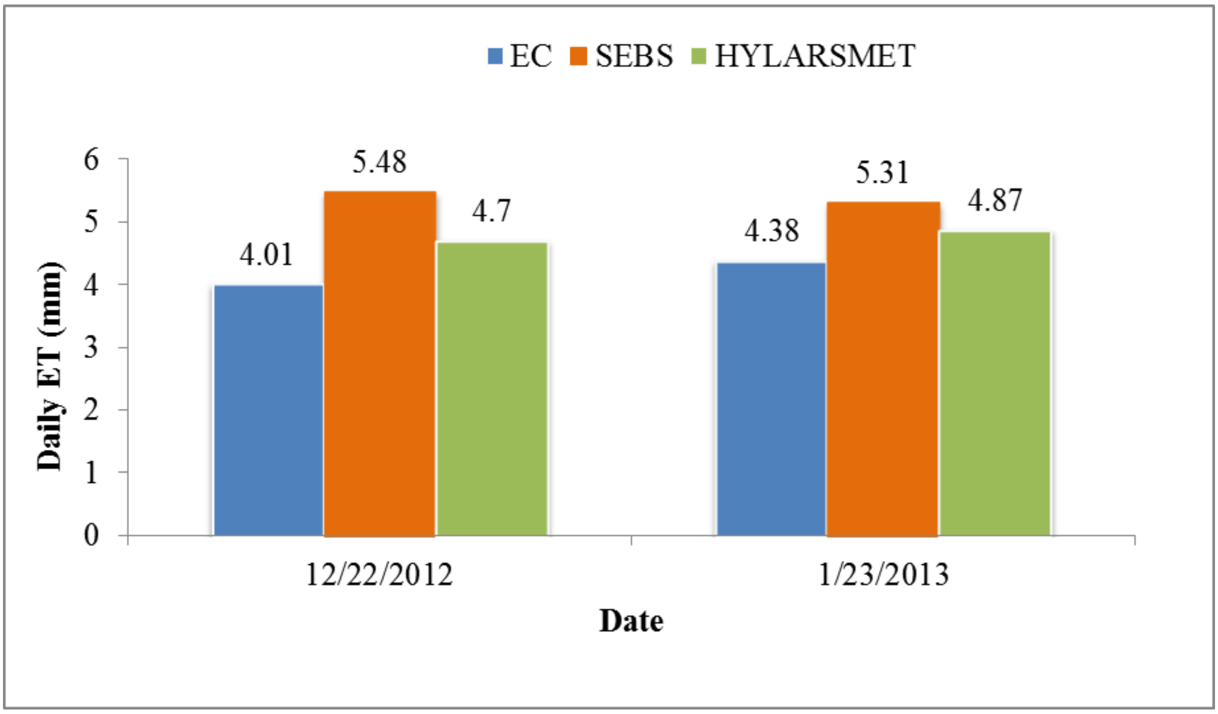

Figure 60. Comparison of the daily *ET* estimates for December 22, 2012 and 23 January 2013 at the maize site.

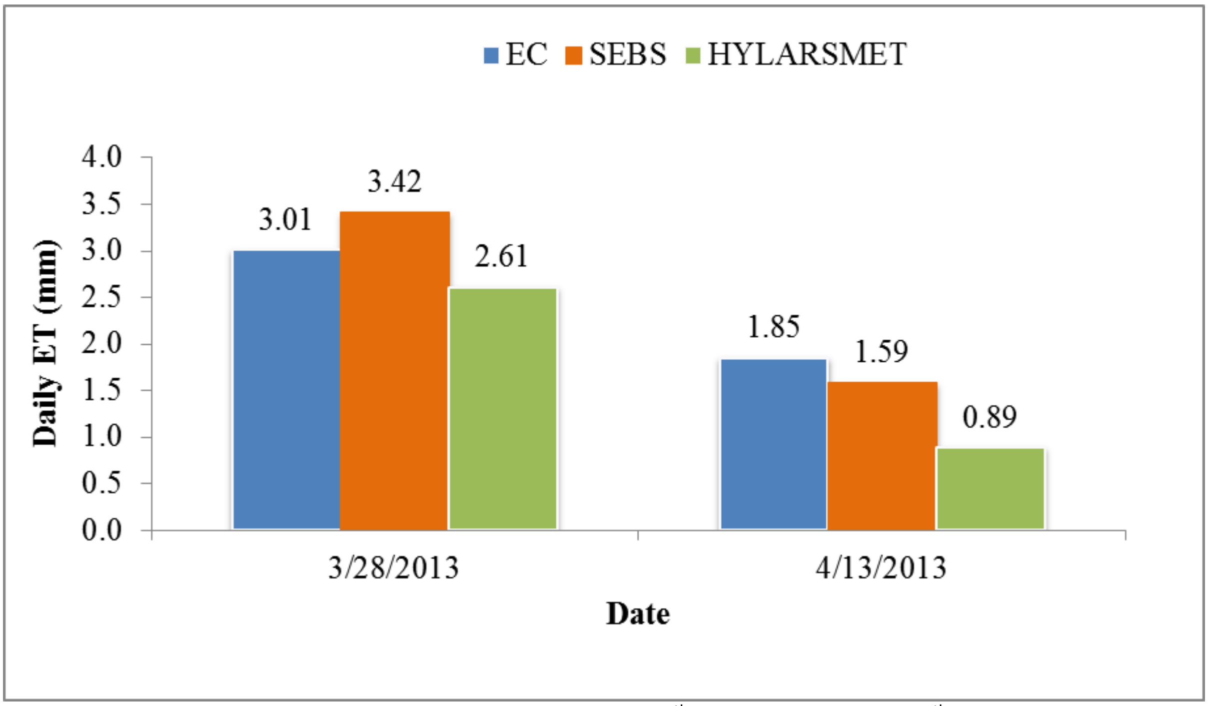

Figure 61. Comparison of the daily *ET* estimates for the 28th of March 2013 and 13th of April 2013 at the soybean site.

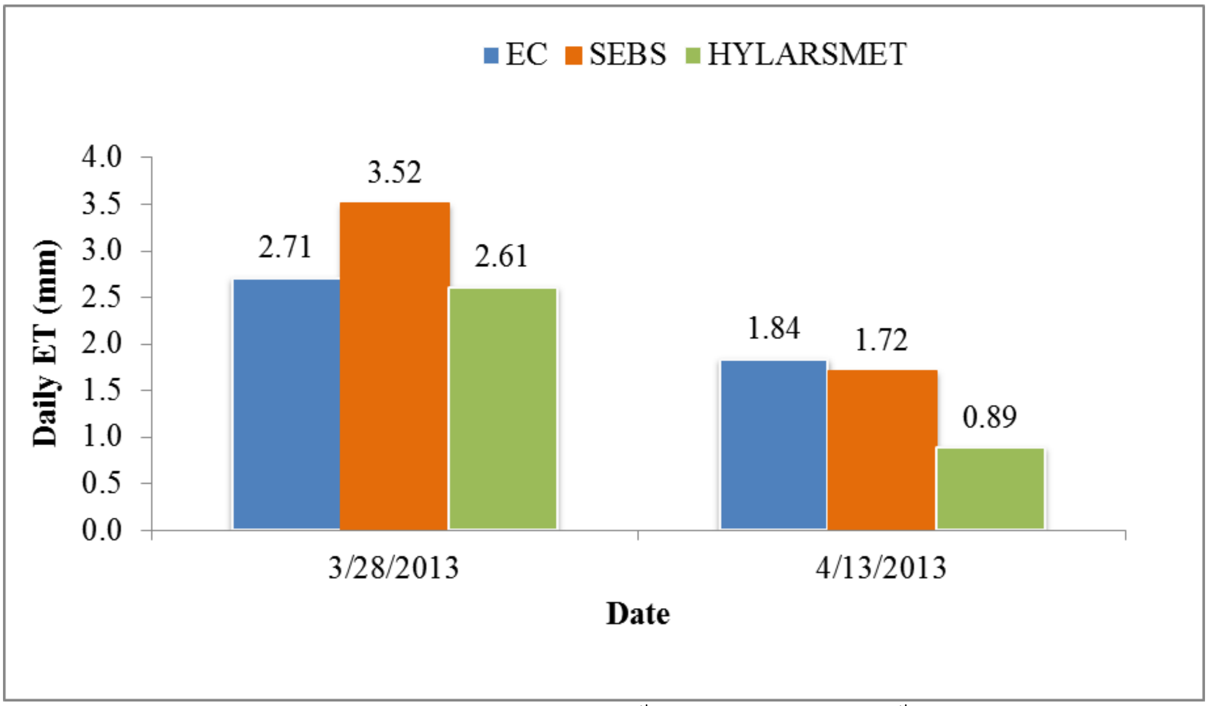

Figure 62. Comparison of the daily *ET* estimates for the 28th of March 2013 and 13th of April 2013 at the maize site.

Measured relative soil moisture (EC) and average relative soil moisture estimates using SEBS for 22 December 2012, 23 January 2013, 28 March 2013, and 13 April 2013 are presented in Figure 45. The HYLARSMET estimates of soil saturation index (SSI) are also depicted in Figure 63. The HYLARSMET SSI estimates followed the drying and wetting patterns of the SEBS relative soil moisture for the four validation days. SEBS relative soil moisture estimates and HYLARSMET's SSI estimates compared well, although they differ in the way they are computed and have different definitions.

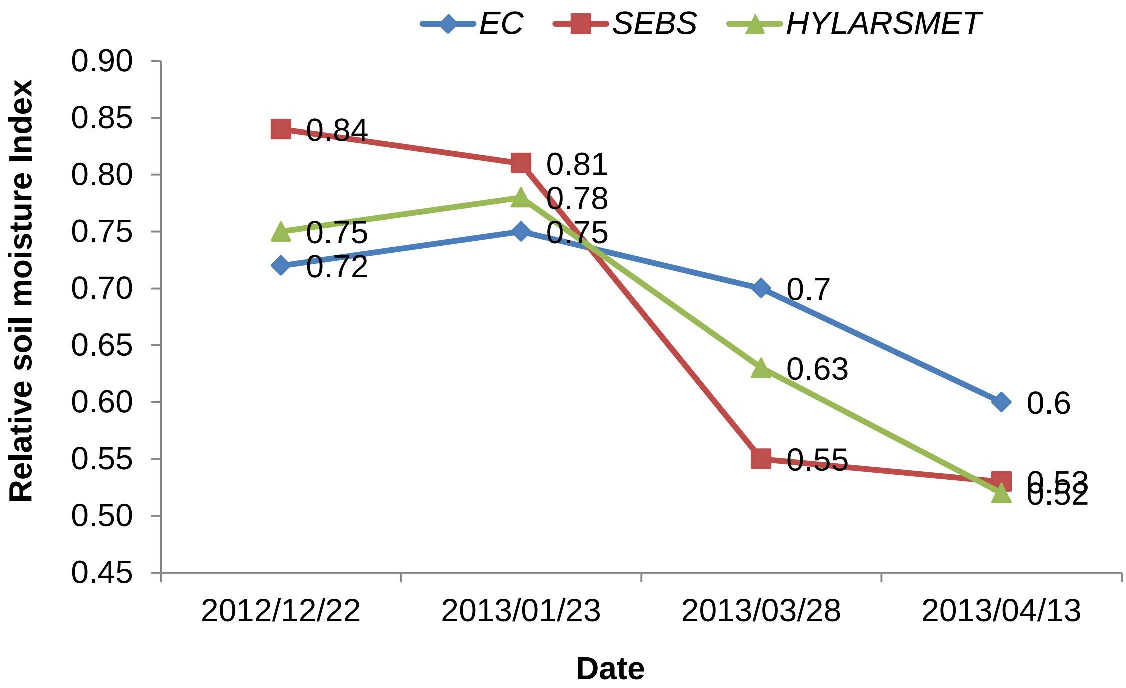

Figure 63. Relative soil moisture (EC and SEBS) and HYLARSMET soil saturation index (SSI) estimates at the maize site in Baynesfield.

7. CONCLUSIONS AND RECOMMENDATIONS

Spatial knowledge of land surface total evaporation (*ET*) and soil moisture (*SM*) is crucial for water resources management, crop modelling, optimizing irrigation water use, and flood forecasting. The purpose of this project was to provide a spatially explicit validation procedure for the 1 km grid of *SM* and *ET* produced by the SAHG UKZN and other hydrological models. The Flash Flood Guidance system (FFGS) requires near real time tracking of the current *SM* state and *ET* to provide alerts, based on current and predicted rainfall. Therefore, validating *ET* and *SM* estimates with better temporal and spatial resolution will make improvements to the SAFFG. In addition to spatial estimates of *ET*, the project was intended to use spatially distributed field based measurements of *SM* to verify *SM* sensors which were planned to be rolled out by SAWS at weather stations. The project team has made numerous attempts to encourage SAWS to provide their soil moisture probes for testing. All these attempts have failed and the project team therefore has abandoned these efforts. In this study, the SEBAL model was proposed for the estimation of *ET* and *SM*. However, SEBAL could not be easily applied by the project team due to intellectual property rights. Instead, the SEBS model was used for *ET* and *SM* estimates. The SEBS model is available in the Integrated Land and Water Information System ILWIS which is a free open-source software package.

Seven months of eddy covariance *ET* estimates and profile soil water content measurements at two sites within Baynesfield were used for the validation of the SEBS and HYLARSMET models. SEBS model was used to derive *ET* and the relative soil moisture maps using MODIS TERRA and Landsat 7 ETM+ images. Landsat images provided better *ET* estimates compared to MODIS images because of their higher spatial resolution (30 m).

The HYLARSMET daily *ET* estimates were lower than the EC and SEBS estimates. However, the HYLARSMET estimates followed the variation of the daily *ET* estimates for the different seasons. The HYLARSMET SSI estimates followed the drying and wetting patterns of the measured and SEBS relative soil moisture estimates. In general, the HYLARSMET estimates compared well with the measured and SEBS estimates. It would be valuable if more time series of spatially averaged HYLARSMET estimates were to be compared with the field measurements and SEBS estimates.

Landsat 7 malfunctioned in 2003 and no longer provides complete image information for all of its coverage due to the failure of the Scan Line Corrector. There was 22% data loss in each scene. However, Landsat 7 is still useful for those areas lying along the centre line of the flight path. The Landsat 8 satellite images the entire Earth every 16 days in an 8-day offset from Landsat 7. Two Landsat 8 images were used in SEBS to derive *ET* maps in this study. The Landsat 8 images provided *ET* maps without stripes and without any data loss. Landsat 8 carries a Thermal infrared (TIR) instrument with two thermal bands that can provide a more accurate estimate of the land surface temperature compared to Landsat 7 and 5. The use of TIR remote sensing and Landsat 8 images can provide valuable information for *ET* and *SM* estimation using surface energy balance models.

During the course of this reporting period a new technology (Cosmic ray probes) for measuring soil moisture at spatial scales of up to 660 m in diameter (34 Ha) has been investigated. The proposed method involves measuring low-energy cosmic-ray neutrons above the ground, whose intensity is inversely correlated with soil water content and with water in any form above ground level (Note: the contributions from subsurface and surface waters are distinguishable). The instrument, called a "cosmic-ray moisture probe," is brand new, but it is built on existing technologies that are put together in an innovative way. The use of such tried and tested technologies means the instrument and the technique are less likely to fail when deployed.

The recent advent of the cosmic-ray neutron probe (Zreda *et al*., 2008) has opened the door for accurate measurements of near surface soil moisture at the landscape scale (Franz *et al*., 2012). The project team submitted a PEER proposal and NRF RISP to cover the costs of these new probes. (approx. R250k each, six probes in total). Both proposals were successful and we propose to use the cosmic-ray moisture probe (Zreda *et al*., 2008) to derive key variables needed for monitoring of both agricultural and natural systems at a scale of a 34 ha circle (660 m diameter) to depth of 0.5 m . The South African network will become an important partner in the construction of the global COSMOS. The U.S. researchers have agreed to make available data processing and dissemination services that use COSMOS servers, will provide training and guidance with the cosmic-ray method that will be necessary for this project to succeed.

8. REFERENCES

Allen, R.G., Morse, A., Tasumi, M., Trezza, R., Bastiaanssen, W.G.M., Wright, J.L. and Kramber, W. (2002). Evapotranspiration from a satellite-based surface energy balance for the Snake River Plain Aquifer in Idaho. In *Proc. USCID/EWRI Conf. on Energy, Climate, Environment, and Water. San Luis Obisbo, CA*.

Allen, R.G., Pruitt, W.O., Businger, J.A., Fritschen, L.J., Jensen, M.E. and Quinn, F.H. (1996). Evaporation and Transpiration. Chap. 4, pp. 125-252. In *ASCE Handbook of Hydrology*, Wootton *et al*. (Ed.), New York, NY.

Allen, R.G., Tasumi, M. and Trezza, R. (2007). Satellite-based energy balance for mapping evapotranspiration with internalized calibration (METRIC)-Model. *ASCE J Irrigation Drainage Eng*., July/August, 395-406.

Allen, R.G., Tasumi, M., Morse, A. and Trezza, R. (2005). A Landsat-based energy balance and evapotranspiration model in Western US water rights regulation and planning. *Irrigat. Drain. Syst*. **19,** 251-268.

Arya, S.P., 2001. Introduction to Micrometeorology. Second edition. Academic Press. London, UK. 420 pp.

Bastiaanssen, W.G.M. and Bos, M.G. (1999). Irrigation performance indicators based on remotely sensed data: a review of literature. *Irrigation and Drainage Systems*. **13,** 291-311.

Bastiaanssen, W.G.M. and Harshadeep, N.R. (2005). Managing scarce water resources in Asia: The nature of the problem and can remote sensing help? *Irrigation and Drainage Systems*. **19,** 269-284.

Bastiaanssen, W.G.M., Pelgrum, H., Droogers, P., De Bruin, H.A.R., Menenti, M. (1997). Area-average estimates of evaporation, wetness indicators and top soil moisture during two golden days in EFEDA. *Agric Forest Meteorol*. **87**, 119-137.

Bastiaanssen, W.G.M., Menenti, M., Feddes, R.A. and Holtslang, A.A. (1998). A remote sensing surface energy balance algorithm for land (SEBAL): 1. Formulation. *Journal of Hydrology*. **212,** 198-212.

Bastiaanssen, W.G.M., Pelgrum, H., Wang, J., Ma, Y., Moreno, J., Roerink, G.J. and Van der Wal, T. (1998b). The Surface Energy Balance Algorithm for Land (SEBAL), Part 2: Validation. *Journal of Hydrology*. **212-213,** 213-229.

Carlson, T.N., Dodd, J.K., Benjamin, S.G. and Cooper, J.N. (1981). Satellite estimation of the surface-energy balance, moisture availability and thermal inertia. *J. Applied Meteorol*. **20(1),** 67-87.

Courault, D., Seguin, B. and Olioso, A. (2005). Review on evapotranspiration from remote sensing data: From empirical to numerical modelling approaches. *Irrigat. Drain. Syst*. **19,** 223-249.

De Bruin, H.A.R., Van den Hurk B.J.J.M. and Kohsiek W. (1995). The scintillation method tested over dry vine yard area. *Boundary-Layer Meteorol*. **76,** 25-40.

Drexler, J.Z., Snyder, R.L., Spano, D., Paw U, K.T., 2004. A review of models and micrometeorological methods used to estimate wetland evapotranspiration. Hydrol. Process. **18**, 2071-2101.

Finnigan, J.J., Clements, R., Malhi, Y., Leuning, R., Cleugh, H.A., 2003. A re-evaluation of long term flux measurement techniques: 1. Averaging and coordinate rotation. Boundary-Layer Meteorol. **107**, 1-48.

Franz, T. E., Zreda, M., King, E.G. (Draft paper). Cosmic-ray Soil Moisture Probe: A New technology to effectively manage African dryland ecosystems.

French, A.N., Jacob, F., Anderson, M.C., Kustas, W.P., Timmermans, W., Gieske, A., Su, Z., Su, H., McCabe, M.F., Li, F., Prueger, J. and Brunsell, N. (2005). Surface energy fluxes with the Advanced Spaceborne Thermal Emission and Reflection radiometer (ASTER) at the Iowa 2002 SMACEX site (USA). *Remote Sens. Environ*. **99,** 55-65.

Fritschen, L.J. and Simpson, J.R. (1989). Surface energy balance and radiation systems: general description and improvements. *J. Applied Meteorol*. **28,** 680-689.

Gowda, P.H., Chavez, J.L., Colaizzi, P.D., Evett, S.R., Terry A., Howell, T.A. and Tolk, J.A. (2007). ET mapping for agricultural water management: present status and challenges. *Irrigation Science*. DOI 10.1007/s00271-007-0088-6.

Green, W. and Ampt, G. (1911). Studies on soil physics, part 1, the flow of air and water through soils. *J. Agric. Sci.*, **4(1)**,1-24.

Gurney, R.J. and Camillo, P.J. (1984). Modelling daily evapotranspiration using remotely sensed data. *J. Hydrol*. **69,** 305-324.

Hafeez, M., Khan, S., Song, K., Rabbani, U. (2007). Spatial mapping of actual evapotranspiration and soil moisture in the Murrumbidgee Catchment: Examples from National Airborne Field Experimentation. *MODSIM 2007 International Congress on Modelling and Simulation, Modelling and Simulation Society of Australia and New Zealand.* Pp 74-80.

Hanson, R.L., (1991). Evapotranspiration and Droughts. In: Paulson, R.W., Chase, E.B., Roberts, R.S., and Moody, D.W., Compilers, National Water Summary 1988-89. *Hydrologic Events and Floods and Droughts*: U.S. Geological Survey Water-Supply Paper 2375, pp. 99-104.

Hemakumara, H. M., Chandrapala, L. and Moene, A. F. (2003). Evapotranspiration fluxes over mixed vegetation areas measured from large aperture scintillometer. *Agric. Water Manage*. **58(2),** 109-122.

Hill, R.J. (1992). Review of optical scintillation methods of measuring the refractive index spectrum, inner scale and surface fluxes. *Waves Random Media*. **2,** 179-201.

Jackson R.D., Reginato R.J. and Idso S.B. (1977). Wheat canopy temperature: a practical tool for evaluating water requirements. *Water Resour. Res*. **13,** 651-656.

Jackson, R.D., Idso, S.B., Reginato, R.J. and Pinter, P.J. Jr. (1981). Canopy temperature as a crop water stress indicator. *Water Resources Research*. **17(4),** 1133-1138.

Jackson, R.D., Kustas, W.P. and Choudhury, B.J. (1988). A re-examination of the Crop Water Stress Index. *Irrigation Science*. **9,** 309-317.

Kaimal, J.C., Finnigan, J.J., 1994. Atmospheric Boundary Layer Flows, Their Structure and Measurement. Oxford University Press, New York. 289 pp.

Koloskov, G., Mukhamejonav, K.H., Tanto, T.W. (2007). Monin-Obukhov length as a cornerstone of the SEBAL calculations of evapotranspiration. *J. Hydrol*. **335,** 170-179.

Kustas W.P. and Norman J.M. (1996). Use of remote sensing for evapotranspiration monitoring over land surfaces. *Hydrol Sci J*. **41(4),** 495-516.

Kustas, W.P. and Daughtry, C.S.T. (1989). Estimation of the soil heat flux/net radiation ratio from spectral data. *Agric Forest Meteorol*. **49,** 205-223.

Liu, Z., Todini, E. (2002). Towards a comprehensive physically-based rainfall-runoff model. *Hydrol. Earth Syst. Sci***. 6** (5) 859-881.

Martina MLV (2004). The distributed physically based modelling of the rainfall-runoff process. Ph.D. Thesis. University of Bologna, Italy.

Massman, W.J., 2000. A simple method for estimating frequency response corrections for eddy covariance systems. Agric. For. Meteorol. **104**, 185-198.

Massman, W.J., Lee, X., 2002. Eddy covariance flux corrections and uncertainties in long-term studies of carbon and energy exchanges. Agric. For. Meteorol. **113**, 121-144.

Menenti, M. and Choudhury, B.J. (1993). Parameterization of land surface evapotranspiration using a location dependent potential evapotranspiration and surface temperature range. In: Bolle HJ *et al* (eds). *Proceedings of exchange processes at the land surface for a range of space and time scales*. IAHS Publ. **212**, pp. 561-568.

Meyers, T.P. and Baldocchi, D.D. (2005). Current micrometeorological flux methodologies with applications in agriculture. In: Hatfield, J.L., Baker, J.M. (eds). *Micrometeorology in Agricultural Systems Agronomy Monograph*. no.**47**. pp. 381-396.

Moran M.S., Hymer D.C., Qi J., and Kerr Y. (2002). Comparison of ERS-2 SAR and Landsat TM imagery for monitoring agricultural crop and soil conditions. *Remote Sens. Environ* **79**, 243–252.

Moran, M.S. and Jackson, R.D. (1991). Assessing the spatial distribution of evapotranspiration using remotely sensed inputs. *J. Environ. Quality*. **20,** 725-737.

Moran, M.S., Rahman, A.F., Washburne, J.C., Goodrich, D.C., Weltz, M.A. and Kustas, W.P. (1996). Combining the Penman-Monteith equation with measurements of surface temperature and reflectance to estimate evaporation rates of semiarid grassland. *Agric Forest Meteorol*. **80,** 87-109.

Morse, A., Allen, R.G., Tasumi, M., Kramber, W.J., Trezza, R. and Wright, J.L. (2001). Application of the SEBAL methodology for estimating evapotranspiration and consumptive use of water through remote sensing. Final Report. *Idaho Department of Water Resources*, Idaho.

Paw U, K.T., Qui, J., Su, H.B., Watanabe, T. and Brunnet, Y. (1995). Surface renewal analysis: a new method to obtain scalar fluxes. *Agric Forest Meteorol*. **74,** 119-137.

Pegram GGS, Sinclair S, Parak M, Sakulski D and Nxumalo N (2007). National Flood Nowcasting System: Towards an integrated mitigation strategy. WRC Report No. 1429/1/06. Water Research Commission, Pretoria, South Africa.

Pegram G.G.S., Sinclair S., Vischel T. and Nxumalo N., (2010). "Soil Moisture from Satellites: Daily maps over RSA for Flash Flood Forecasting, Drought Monitoring, Catchment Management and Agriculture", *WRC Report No. 1683/1/10*, Water Research Commission, Pretoria, South Africa.

Price, J.C. (1982). On the use of satellite data to infer surface fluxes at meteorological scales. *J. Applied Meteorol*. **21(8),** 1111-1122.

Roerink, G.J., Su, B. and Menenti, M. (2000). S-SEBI: A simple remote sensing algorithm to estimate the surface energy balance. *Physics Chem. Earth* (B). **25(2),** 147-157.

Rosenberg, N.J., Blad, B.L., Verma, S.B., 1983. Microclimate: The Biological Environment. Second edition. John Wiley & Sons, New York. 495 pp.

Savage, M.J., Everson, C.S., Metelerkamp, B.R., 1997. Evaporation measurement above vegetated surfaces using micrometeorological techniques. Water Research Commission Report No. 349/1/97, p248, ISBN 1-86845 363 4.

Savage, M.J., McInnes, K.J., Heilman, J.L., 1995. Placement height of eddy correlation sensors above short turfgrass surface. Agric. For. Meteorol. **74**, 195-204.

Scott C.A, Bastiaanssen W.G.M. & Ahmad M.D. (2003). Mapping Spatio-Temporal Distributions of Soil Moisture Throughout Irrigated Watersheds using Optical and High Resolution Imagery. *ASCE Irrigat and Drain Eng*. **129, 5** (326).

Seguin, B. and Itier, B. (1983). Using midday surface temperature to estimate daily evaporation from satellite thermal IR data. *Int. J. Remote Sens*. **4,** 371-383.

Sellers, P.J., Randall, D.A., Collatz, G.J., Berry, J.A., Field, C.B., Dazlich, D.A. and Zhang, C. (1996). A revised land surface parameterization (SiB2) for atmospheric GCMS. Part 1: Model formulation. *J. Climate*. **9(4),** 676-705.

Sinclair S., Pegram G.G.S. (2012). Modelling soil moisture at national and catchment scale using a spatially distributed hydrological model forced by remote sensing and meteorological products. *16th SANCIAHS symposium*, Pretoria, South Africa.

Sinclair, Scott and Geoffrey Pegram (2013a). HYLARSMET: A Hydrologically Consistent Land Surface Model for Soil Moisture and Evapotranspiration Modelling over Southern Africa using Remote Sensing and Meteorological Data, Report to the Water Research Commission, WRC Report No. 2024/1/12, ISBN 978-1-4312-0392-5.

Sinclair S. and Pegram G.G.S., (2013b), "A sensitivity assessment of the TOPKAPI model with an added infiltration module", *J. Hydrol.*, 479, 100-112

Snyder, R.L., Spano, D. and Paw U, K.T. (1996). Surface renewal analysis for sensible heat and latent heat flux density. *Boundary-Layer Meteorol*. **77,** 249-266.

Su, Z. (2002). The surface energy balance system (SEBS) for estimation of turbulent heat fluxes. *Hydrol. Earth Sys. Sci*. **6(1),** 85-99.

Su, Z. (2002). The surface energy balance system (SEBS) for estimation of turbulent heat fluxes. *Hydrol. Earth Sys. Sci*. **6(1),** 85-99.

Su, Z., Li, X., Zhou, Y., Wan, L., Wen, J. and Sintonen, K. (2003). Estimating areal evaporation from remote sensing. In *International Geoscience and Remote Sensing Symposium*, *21-25 July 2003, Toulouse (PID20349.pdf)*.

Su, Z., Pelgrum, H. and Menenti, M. (1999). Aggregation effects of surface heterogeneity in land surface processes. *Hydrol. Earth Sys. Sci*. **3(4),** 549-563.

Su, Z., Pelgrum, H. and Menenti, M. (1999). Aggregation effects of surface heterogeneity in land surface processes. *Hydrol. Earth Sys. Sci*. **3(4),** 549-563.

Su, Z., Schmugge, T., Kustas, W.P. and Massman, W.J. (2001). An evaluation of two models for estimation of the roughness height for heat transfer between the land surface and the atmosphere. *J. Applied Meteorol*. **40(11),** 1933-1951.

Su, Z., Schmugge, T., Kustas, W.P. and Massman, W.J. (2001). An evaluation of two models for estimation of the roughness height for heat transfer between the land surface and the atmosphere. *J. Applied Meteorol*. **40(11),** 1933-1951.

Swinbank, W.C., 1951. Measurement of vertical transfer of heat and water vapour by eddies in the lower atmosphere. J. Meteorol. **8**, 135-145.

Tasumi, M., Allen, R.G., Trezza, R. and Wright, J.L. (2005). Satellite-based energy balance to assess within-population variance of crop coefficient curves. *Journal of Irrigation and Drainage*. **131(1),** 94-109.

Thiermann, V. and Grassl, H. (1992). The measurement of turbulent surface-layer fluxes by use of bichromatic scintillation. *Boundary-Layer Meteorol*. **58,** 367-389.

Timmermans, W.J., Kustas, W.P., Anderson, M.C. and French, A.N. (2007). An intercomparison of the Surface Energy Balance Algorithm for Land (SEBAL) and the Two-Source Energy Balance (TSEB) modelling schemes. *Remote Sens. Environ*. **108,** 369-384.

Van Atta CW. 1977. Effect of coherent structures on structure functions of temperature in the atmospheric boundary layer. Archives of Mechanics. **29**, 161–171.

Van den Hurk, B.J.J.M. (2001). Energy balance based surface flux estimation from satellite data, and its application for surface moisture assimilation. *Meteorology and Atmospheric Physics*. **76,** 43-52.

Verstraeten, W.W., Veroustraete, F., Heyns, W., Van Roey, T. and Feyen, J. (2008). On uncertainties in carbon flux modelling and remotely sensed data assimilation: The Brasschaat pixel case. *Advances in Space Research*. **41(1),** 20-35.

Vischel T., Pegram G.G.S., Sinclair S., and Parak M. (2008). Implementation of the TOPKAPI model in South Africa: Initial results from the Liebenbergsvlei catchment. *Water SA*. **34(3)**, 1–12.

Wieringa, J., 1993. Representative roughness parameters for homogeneous terrain. Boundary-Layer Meteorol. **63**, 323-363.

Zreda, M., Desilets, D., Ferre, T. P. A., Scott, R. L. (2008). Measuring soil moisture content noninvasively at intermediate spatial scale using cosmic-ray neutrons. *Geophysical Research Letters* 35:21: 5. doi:L21402.